STUTZMAN

NATIONAL ACADEMIES OF SCIENCE AND ENGINEERING

NATIONAL RESEARCH COUNCIL

of the

UNITED STATES OF AMERICA

UNITED STATES NATIONAL COMMITTEE

International Union of Radio Science

National Radio Science Meeting

5-8 January 1988

Sponsored by USNC/URSI
in cooperation with
Institute of Electrical and Electronics Engineers

University of Colorado
Boulder, Colorado
U.S.A.

National Radio Science Meeting
5-8 January 1988
Condensed Technical Program

MONDAY, 4 JANUARY

2000-2400

USNC-URSI Meeting		Broker Inn

TUESDAY, 5 JANUARY

0855-1200

A-1	Time Domain Measurements	CR1-40
B-1	Numerical Methods	CR2-28
D-1	Numerical Simulation of Solid State Devices	CR1-42
G-1	Ionospheric Modeling	CR2-26
H/G/B-1	Ionospheric Scintillation Theory	CR1-9
J-1	Radio Scattering From Icy Bodies	CR0-30

1115-1200

J-2	Radar Astronomy of the Inner Solar System	CR0-30

1355-1700

A-2	Microwave and Millimeter Wave Measurements	CR1-42
B-2	Scattering - I	CR2-28
B-3	Antennas	CR2-6
D-2	High Frequency Techniques	CR1-40
F/B-1	Random Media Theory/Measurements	CR1-46
G-2	Ionospheric Propagation	CR2-26
J-2	Radar Astronomy of the Inner Solar System (continued from Tuesday morning)	CR0-30

1700-1800

Commission A Business Meeting	CR1-42
Commission D Business Meeting	CR1-40
Commission G Business Meeting	CR2-26
Commission J Business Meeting	CR0-30

WEDNESDAY, 6 JANUARY

0830-1200

Plenary Session	Duane G0-30

1355-1700

A-3	Antenna and EM Fields Measurement	CR1-42
B-4	PDE-Based Methods for EM Problems in Open Regions	CR1-40
B-5	Guiding Structures	CR2-6
C-1	Signal Processing Theory	CR0-36
E-1	High Power Electromagnetics I. HEMP/EMP / II. Lightning	CR1-46
F-1	Satellite Remote Sensing A. Special Session on SSM/I / B. Satellites and Sea Floor	CR2-28
G-3	Ionospheric Modification	CR2-26
H-1	Waves in Space Plasmas	CR1-9
J-3	Image Processing in Astronomy	CR0-30

1535-1700

G/H-1	Ionospheric-Induced Errors in Ranging/Doppler Systems	CR1-9

United States National Committee

INTERNATIONAL UNION OF RADIO SCIENCE

PROGRAM AND ABSTRACTS

National Radio Science Meeting
5-8 January 1988

Sponsored by USNC/URSI in cooperation
with IEEE groups and societies:

Antennas and Propagation
Circuits and Systems
Communications
Electromagnetic Compatibility
Geoscience Electronics
Information Theory
Instrumentation and Measurement
Microwave Theory and Techniques
Nuclear and Plasma Sciences
Quantum Electronics and Applications

NOTE:

Programs and Abstracts of the USNC/URSI Meetings are available from:

USNC/URSI
National Academy of Sciences
2101 Constitution Avenue, N.W.
Washington, DC 20418

at $2 for meetings prior to 1970, $3 for 1971-1975, and $5 for 1976-1988 meetings.

The full papers are not published in any collected format; requests for them should be addressed to the authors who may have them published on their own initiative. Please note that these meetings are national. They are not organized by the International Union, nor are the programs available from the International Secretariat.

MEMBERSHIP

United States National Committee
INTERNATIONAL UNION OF RADIO SCIENCE

Chairman:	Sidney A. Bowhill*
Vice Chairman:	Chalmers M. Butler*
Secretary:	David C. Chang*
Immediate Past Chairman:	Robert K. Crane*

Members Representing Societies, Groups, and Institutes:

American Geophysical Union	Prof. Donald Gurnett
American Astronomical Society	Dr. A. Richard Thompson
IEEE Antennas & Propagation Society	Dr. W. Ross Stone
IEEE Microwave Theory and Techniques Society	Dr. A. A. Oliner
IEEE Geophysics and Remote Sensing Society	Dr. Robert E. McIntosh

Members-at-Large:	Dr. Gary Brown
	Dr. E.K. Smith
	Dr. Kenneth Davies
	Dr. Charles Rino
	Dr. Irene Peden
	Dr. Dave Hill

Liaison Representatives from Government Agencies:

National Telecommunications & Information Administration	Dr. Hans Liebe
National Science Foundation	Dr. Laura P. Bautz
Federal Communications Commission	Mr. William A. Daniel
Department of Defense	Mr. William J. Cook
Department of the Army	Mr. Earl J. Holliman
Department of the Air Force	Dr. Allan C. Schell

Chairmen of the USNC/URSI Commissions:

Commission A	Dr. Edmund K. Miller
Commission B	Dr. Robert S. Elliott
Commission C	Dr. Aaron D. Wyner
Commission D	Dr. Tatsuo Itoh
Commission E	Dr. John R. Herman
Commission F	Dr. Calvin T. Swift
Commission G	Dr. Charles M. Rush
Commission H	Dr. Mario Grossi
Commission J	Dr. J. Richard Fisher

Officers of URSI resident in the United States: (including Honorary Presidents)	
Honorary President	Prof. Henry G. Booker*
Chairmen and Vice Chairmen of Commissions of URSI resident in the United States:	
Chairman of Commission B	Prof. Thomas B.A. Senior
Chairman of Commission F	Dr. Robert K. Crane
Foreign Secretary of the U.S. National Academy of Sciences	Dr. William E. Gordon
Chairman, National Research Council, Commission on Physical Sciences, Mathematics, and Resources	Dr. Norman Hackerman
Chairman, National Research Council, Board on Physics and Astronomy	Prof. Norman F. Ramsey
Honorary Members	Dr. Harold H. Beverage Dr. Ernst Weber
NRC Staff Director	Mr. Donald C. Shapero
NRC Program Officer	Dr. Robert L. Riemer
NRC Administrative Specialist	Ms. Helene E. Patterson

* Member of USNC/URSI Executive Committee

DESCRIPTION OF THE INTERNATIONAL UNION OF RADIO SCIENCE

The International Union of Radio Science is one of 18 world scientific unions organized under the International Council of Scientific Unions (ICSU). It is commonly designated as URSI (from its French name, Union Radio Scientifique Internationale). Its aims are (1) to promote the scientific study of radio communications, (2) to aid and organize radio research requiring cooperation on an international scale and to encourage the discussion and publication of the results, (3) to facilitate agreement upon common methods of measurement and the standardization of measuring instruments, and (4) to stimulate and to coordinate studies of the scientific aspects of telecommunications using electromagnetic waves, guided and unguided. The International Union itself is an organizational framework to aid in promoting these objectives. The actual technical work is largely done by the National Committee in the various countries.

The officers of the International Union are:

President:	Prof. A.L. Cullen (U.K.)
Past President:	Dr. A.P. Mitra (India)
Vice Presidents:	Dr. Ing. H.J. Albrecht (F.R.G.) R.L. Dowden (New Zealand) E.D. Jull (Canada) Prof. V. Zima (Czechoslovakia)
Secretary-General	J. Van Bladel (Belgium)
Honorary Presidents:	G. Beynon (U.K.) H.G. Booker (U.S.A.) W. Dieminger (West Germany) I. Koga (Japan) J.A. Ratcliffe (U.K.)

The Secretary-General's office and the headquarters of the organization are located at Avenue Albert Lancaster, 32, B-1180 Brussels, Belgium. The Union is supported by contributions (dues) from 38 member countries. Additional funds for symposia and other scientific activities of the Union are provided by ICSU from contributions received for this purpose from UNESCO.

The International Union, as of the XXth General Assembly held in Washington, DC in August 1981, has nine bodies called Commissions for centralizing studies in the principal technical fields.

Every three years the International Union holds a meeting called the General Assembly. The next is the XXIIIrd, to be held in 1990. The Secretariat prepares and distributes the Proceedings of the General Assemblies. The International Union arranges international symposia on specific subjects pertaining to the work of one or several Commissions and also cooperates with other Unions in international symposia on subjects of joint interest.

Radio is unique among the fields of scientific work in having a specific adaptability to large-scale international research programs, since many of the phenomena that must be studied are worldwide in extent and yet are in a measure subject to control by experimenters. Exploration of space and the extension of scientific observations to the space environment are dependent on radio for their research. One branch, radio astronomy, involves cosmic phenomena. URSI thus has a distinct field of usefulness in furnishing a meeting ground for the numerous workers in the manifold aspects of radio research; its meetings and committee activities furnish valuable means of promoting research through exchange of ideas.

Steering Committee:

S.W. Maley, Chairman (303) 492-7004
D.C. Chang
D.S. Cook
P.L. Jensen
M.G. Kindgren

Technical Program Committee:

D.C. Chang, Chairman
K. Davies
R.S. Elliott
J.R. Fisher
M.D. Grossi
J.R. Herman
T. Itoh
M. Kanda
S.W. Maley
E.K. Miller
C.M. Rush
E.K. Smith
E. Soderberg
C.T. Swift
A.D. Wyner

Session A-1 0855-Tues. CR1-40
TIME DOMAIN MEASUREMENTS
Chairman: William L. Gans, Electromagnetic Fields Division, National Bureau of Standards, Boulder, CO 80303

A1-1
0900 **PULSE MEASUREMENTS IN THE PICOSECOND DOMAIN**

J.R. Andrews
Picosecond Pulse Labs, Inc.
Boulder, Colorado 80306

This is a tutorial lecture emphasizing the extremely broadband nature (DC-GHz) of picosecond pulse measurements and the many places in which significant errors can occur. The following subject areas are covered: oscilloscopes, calibration standards, coaxial cables, connectors and probes.

A1-2
0920

TWO LAYER DIELECTRIC MICROSTRIPLINE STRUCTURE: SiO2 ON Si AND GaAs ON Si MODELING AND MEASUREMENT

R.A. Lawton
Boulder Research Associates
Boulder, Colorado 80303

The two-layer dielectric microstripline structure is a structure that has found use in a number of applications. Two examples are in pulse waveform filtering to generate a pulse waveform standard and in the use of high quality silicon substrates in the manufacture of gallium arsenide devices.

This paper will describe the concept of reference waveform standards using the two-layer dielectric microstripline structure (R.A. Lawton, N.S. Nahman and J.M. Bigelow, IEEE Trans. I&M, IM-33, No. 3, 201-205, 1984) and the further modeling that has been recently completed. Scattering parameters are computed from the distributed element circuit model and compared with measured values over the frequency range from 90 MHz to 18 GHz for a microstripline made from a wafer with silicon dioxide on silicon. The sensitivity of the phase of S21 and the magnitude of the characteristic impedance to various parameters is also discussed.

The application of these techniques to the gallium arsenide on silicon system will be described and illustrative calculations will be given.

Note: This work was performed while Lawton was with the National Bureau of Standards.

A1-3
0940

PICOSECOND SILICON PHOTOCONDUCTIVE SWITCH BASED TIME-DOMAIN METROLOGY

W.R. Eisenstadt, Assistant Professor
Department of Electrical Engineering
University of Florida
Gainesville, Fl. 32611

The silicon photoconductive switch has been established as a picosecond time-domain measurement tool over the past five years. The photoconductive switch permits characterization of on-substrate integrated circuit signals with bandwidths above 75-GHz (W.R. Eisenstadt et al., Picosecond Electronics and Optoelectronics, Springer-Verlag, **21**, 66-69).

An overview of the experimental methodology used to perform picosecond photoconductor based time-domain measurements is presented. This overview discusses; 1) fabrication of photoconductors on the silicon substrate, 2) ion-implantation of photo-conductors to produce picosecond switches, 3) pulsed laser system for on-substrate photo-optic measurements, 4) cross-correlation measurements that characterize photoconductors, and 5) IC test structure measurements in a photoconductor based sampling system. Examples of current photoconductive switch research are reviewed.

The photomicrograph below displays the top-side of an IC test structure used to develop picosecond silicon photoconductive switches. The white areas are microstrip transmission lines and the black gaps between the lines are photoconductive switches.

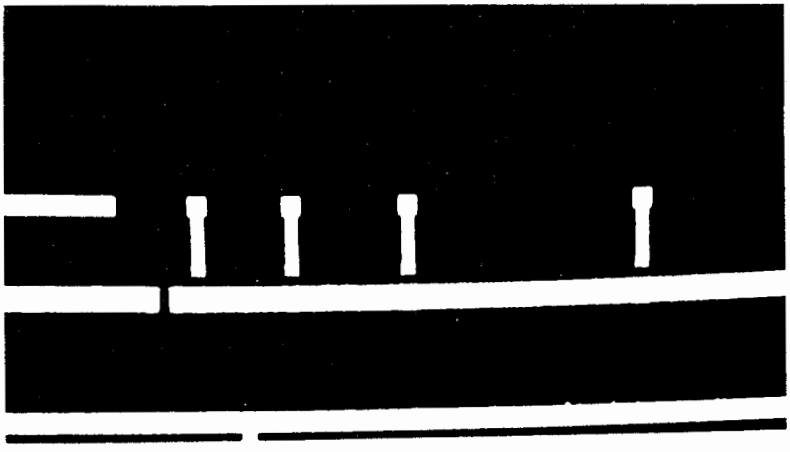

A1-4
1020

OPTIMIZATION AND APPLICATION OF ULTRA-HIGH-SPEED OPTOELECTRONIC TIME DOMAIN MEASUREMENTS

N.G. Paulter, Staff Member
Los Alamos National Laboratory
Los Alamos, NM 87544

Very high-frequency electronic devices and circuits have introduced the requirement of measurement capabilities that extend into the hundreds of GHz range. Optoelectronic and electrooptic techniques are under investigation to perform these measurements. The technique presented here is an optoelectronic one, based on photoexcitation and the subsequent relaxation of carriers in semiconductor photoconductive devices. (N.G. Paulter and R.B. Hammond, Proc. of the Critical Review of Technology 795, SPIE, Bay Point, FL, Mar. 1987.)

The optimization of the optoelectronic measurement test structure and applications of the measurement are given. The test structure optimization includes consideration of semiconductor substrate (SOI, SOS, GaAs), implant schedule, and transmission line structure (coplanar waveguide, coplanar strips, and microstrip). Modification of the chosen transmission line structure to enhance response magnitude without speed degradation and to minimize device area requirement without affecting temporal resolution are discussed. Novel applications of this measurement technique are presented.

The sketch below is of an arrangement used to characterize high-speed electronic devices. The PCEs (photoconductive circuit elements) are the active regions of a semiconductor.

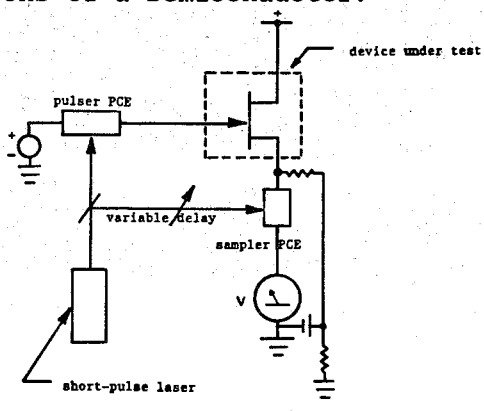

A1-5
1040

ELECTRO-OPTIC SAMPLING AND THE CHARACTERIZATION OF ULTRAFAST ELECTRONIC DEVICES

G. A. Mourou and J. F. Whitaker
Ultrafast Science Center, Laboratory for Laser Energetics
University of Rochester
250 East River Road
Rochester, NY 14623

With the extreme interest in subpicosecond phenomena and the operation of electronic devices in the single-picosecond regime has arisen the need for new measurement techniques. Beginning with the invention of the electro-optic sampling system at the University of Rochester, a revolution in the characterization of extremely short electrical events was triggered. The study of the propagation of signals with bandwidths exceeding one terahertz has been carried out for normal and superconducting transmission lines, and devices such as MESFETS, permeable base transistors, and resonant tunneling diodes have also been investigated.

The implementation of the electro-optic sampling technique involves the marriage of the fields of optics and electronics. An 80-fs pulse from a mode-locked dye laser provides an excitation beam which is used with a semiconductor to generate very short electrical transients. A probe beam split off from the same laser pulse, is used to sample the change in index of refraction induced by the electrical waveform in an electro-optic crystal.

In this manner, parameters such as the switching speed of a MIT Lincoln Laboratory resonant tunneling diode have been measured. This device, containing a single, double-barrier quantum well and displaying a prominent negative differential resistance characteristic, switches from a high to low current level in 2 ps (see Figure).

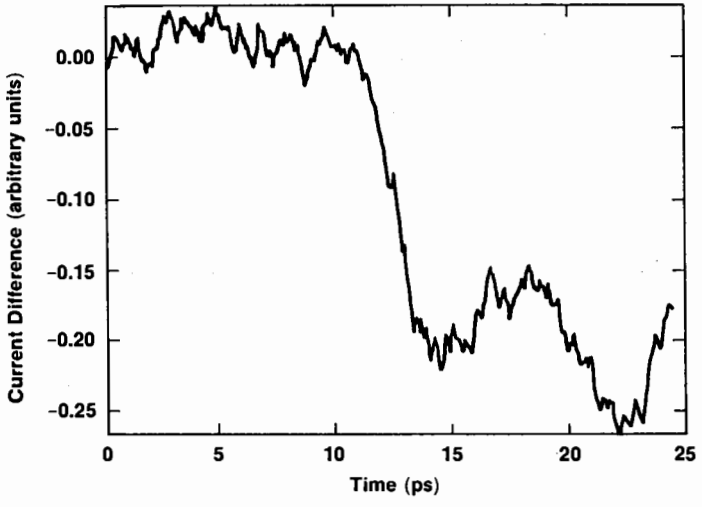

switching time of resonant tunneling diode

A1-6
1100

ULTRA-WIDE BANDWIDTH INSTRUMENT FOR TIME DOMAIN MEASUREMENTS BASED ON JOSEPHSON JUNCTIONS

E.R. Hanson, G.K.G. Hohenwarter,
S.R. Whiteley and S.M. Faris
HYPRES, Inc.
500 Executive Boulevard
Elmsford, NY 10523

The promises of the ultra-high performance properties of superconductivity and Josephson junction technologies have been known for quite some time. This presentation describes the integration of the first system to demonstrate those properties, as a 5 ps, 50 microvolt sensitivity sampling oscilloscope and time domain reflectometer instrument. In order to accomplish this, several technological hurdles had to be overcome including perfecting a manufacturing process for building Josephson junction IC chips, develop an innovative cooling technique, deal with interfaces and interconnections with bandwidths in excess of 70 GHz and develop the room temperature hardware and software necessary to make the instruments convenient, easy to use, and easy to learn, in addition to making available functions and features users have come to expect from sophisticated digital instruments. The presentation will cover the following topics:

* circuit design for both a fast rise time sampling oscilloscope and a time domain reflectometer;
* circuit fabrication and operation;
* operation of the unique cooling system;
* various aspects of system integration;
* circuit interconnections and packaging;
* unique problems associated with Josephson junction systems;
* examples of the technology's capabilities demonstrating the superior switching speed and sensitivity of superconducting integrated circuits as well as other unique features.

A1-7
1120

AN APPROACH TO REAL-TIME ESTIMATION OF THE DERIVATIVE OF DAMPED-EXPONENTIAL TIME-DOMAIN WAVEFORMS

W. Ross Stone
IRT Corporation
1446 Vista Claridad
La Jolla, CA 92037

Waveforms which are decaying exponential functions of time are often encountered in electromagnetic measurements. In some applications, the desired information is contained in the derivative of the data (which, of course, is also of exponential form), and it is desired to predict the value(s) of the function and its derivative in real time (as data is being collected). To be practical, a solution to this problem must remain robust in the presence of noise, and over the substantial dynamic ranges often encountered with such signals. Furthermore, in the applications considered in this paper, although the basic functional form of the waveform is known to be a decaying exponential, the decay constant is unknown and/or time varying. Least squares estimators (including polynomial and orthogonal function fitting) can tend to provide an overly "smooth" solution to such problems, with resultant errors in long-time estimation. Kalman-Bucy filters are often better suited to such estimation problems. However, they usually are formulated for problems in which the underlying model is known, or the unknown component can be "lumped" with the noise in the measurements.

This paper considers another approach to the problem, using recursive real-time Fourier analysis. A derivative theorem is used to recursively compute future-time estimates of the desired solution. The behavior of this approach as a function of measurement noise, decay rate, dynamic range, and length of time into the future for the estimate is examined, both analytically and numerically. Circumstances under which this approach should display substantially robust behavior in the presence of common noise distributions, and the reasons why, are explained. Examples using measured data are also presented.

Session B-1 0855-Tues. CR2-28
NUMERICAL METHODS
Chairman: Chalmers M. Butler, Dept. of Electrical and Computer Engineering, Clemson Univ., Clemson, SC 29634

B1-1
0900

THE USE OF SUBSECTIONAL UNIFORM DISTRIBUTIONS IN THE GALERKIN-MOMENT METHOD SOLUTION OF ELECTROMAGNETICS PROBLEMS

Bradley L. Brim and David C. Chang
Department of Electrical and Computer Engr.
University of Colorado
Boulder, CO 80309

When implementing a Galerkin Moment Method solution it may be advantageous to choose a subsectional expansion with very simple distributions. Ignoring delta functions (ie: point expansion/matching), uniform distributions are the most simple choice possible. However, the solution of integro-differential equations places certain constraints on the expansion/testing functions. For example, in an EFIE (electric field integral equation) formulation the existence of a second order differential operator implies that currents must be continuous in the direction they flow, but may be discontinuous normal to the direction of their flow. This means that "rooftop" expansions are the most simple distributions that may be used, which yield an expansion for current that is piecewise-linear in the direction of its flow and piecewise-constant in directions normal to its flow.

We will present three methods by which one may use constant distributions for both current and charge in Galerkin solutions for electromagnetics. Firstly, two EFIE formulations will be considered in which approximate rather than exact relationships are enforced to relate charges and currents. The first of these is based on an integrated form of charge conservation and yields charge cells that are not shifted with respect to current cells. The second is based on the spreading of concentrated charges and yields shifted charge cells. The exact variational nature of these two formulations is lost, but adequate numerical performance is maintained. Next, a true MPIE (mixed potential integral equation) formulation will be presented in which charges and currents are each treated as unknown trial expansions. The variational nature of this formulation is maintained throughout. These methods will be compared based on their physical interpretations, boundary conditions, numerical results, and numerical efficiency for a few select sample problems involving flat dipoles and microstrip structures. Recommendations will be made as to the use of these methods.

B1-2
0920

GUIDELINES FOR MODELING WITH THE ELECTRIC FIELD INTEGRAL EQUATION TRIANGULAR SURFACE PATCH CODE

W. A. Johnson*
Pulsed Power Theory Division
Sandia National Laboratories
Albuquerque, New Mexico 87185

R. M. Sharpe and D. R. Wilton
Department of Electrical Engineering
University of Houston
Houston, Texas 77004

Previous progress in the development of the Electric Field Integral Equation Triangular Surface Patch Code has been reported (W. A. Johnson, "Current Progress in the Development of and Modeling with the EFIF Surface Patch Code," IEEE-APS Meeting, Vancouver, British Columbia, June 1985). Since this time, new capabilities have been developed and modeling experience has been gained. In particular, the present version of this code has the following capabilities: an arbitrary number of triangles may be attached to an edge; multiple disjoint bodies may be modeled; non-orientable surfaces may be modeled; symmetry planes may be accounted for by placing perfect electric or perfect magnetic conductors in the x=0, y=0, and z=0 planes; the Thevenin circuit parameters for a pair of terminals defined at an edge may be computed; lumped and surface impedance loading may be added to an otherwise perfectly conducting body; excitation by plane waves, voltage sources or both may be used; far field patterns and radar cross sections may be computed; and field calculations at general observation points may be carried out. Modeling guidelines aimed at the intelligent use of these capabilities, understanding the limitations, and avoiding pitfalls will be discussed. Several realistic problems that have been solved with this code will be presented.

*This work supported by the U.S. Department of Energy under Contract No. DE-AC04-76-DP00789.

Extension time, fin patch
include

Kirchhoff current laws are not enforced explicitly.

B1-3
0940

NUMERICAL SOLUTION OF THE INTERIOR BOUNDARY VALUE PROBLEM OVER ROTATIONALLY SYMMETRIC INHOMOGENEOUS DOMAINS USING FINITE INTEGRATION TECHNIQUE

J. Lebaric, Campus Box 119, Rose-Hulman Institute of Technology, 5500 Wabash Av., Terre Haute, IN 47803
D. Kajfez, Electrical Engineering Dept., University of Mississippi, University, MS 38677

Numerical solution of the interior EM boundary value problem has been obtained using the Finite Integration Technique (FIT) (T. Weiland, URSI Int. Symp. on EM Theory, 537-542, Budapest 1986.). The technique involves simultaneous volume and field discretization by the virtue of "dual grids" and allows for a systematic discretization of the curl and divergence equations of Maxwell, the result being an equivalent standard algebraic eigenvalue problem involving large but sparse matrices.

Computer implementation of FIT, program package FITPAK capable of solving for the mode resonant frequencies, field distributions and Q-factors, has been applied to cylindrical cavities with arbitrary distributions of dielectric media. Comparisons of measured and numerical results confirm the abscence of non-physical ("spurious") modes in the numerical solution.

Electric field lines for the TM_{01} mode in a dielectric-rod-tuned tubular dielectric resonator resting on alumina substrate are shown in the figure below, to illustrate FITPAK versatility.

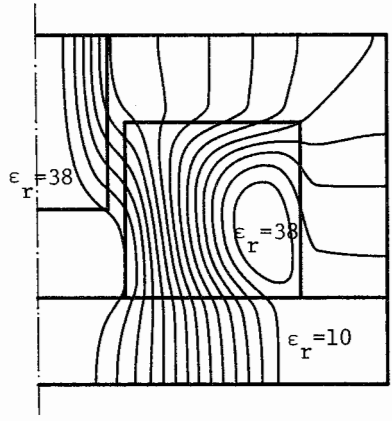

B1-4
1020

ALTERNATIVE FORMS OF THE MIXED-POTENTIAL ELECTRIC FIELD INTEGRAL EQUATION IN LAYERED MEDIA

K.A. Michalski and D. Zheng
Department of Electrical Engineering
Texas A&M University
College Station, TX 77843

The most general and efficient numerical procedures developed to date for solving the problems of radiaton and scattering by objects of arbitrary shape in free space are based on the so-called mixed-potential form of the electric field integral equation (EFIE) [Glisson and Wilton, *IEEE Trans. Antennas Propagat.*, AP-28, 593-603, 1980; Rao *et al.*, *ibid.*, AP-30, 409-418, 1982; Schaubert *et al.*, *ibid.*, AP-32, 77-85, 1984]. There has been a considerable interest in extending these procedures to the case of objects in layered media [Mosig and Gardiol, *Advances in Electronics and Electron Physics*, 59, 139-237, 1980; Johnson, *Radio Sci.*, 18, 1273-1281, 1983; Michalski, *Arch. Elektr. Übertrag.*, AEÜ-39, 317-322, 1985; Wilton and Singh, *AP-S Int. Symp.*, 229-272, 1985; Michalski and Zheng, *ICAP 87*, 507-511, 1987].

In this paper, three alternative forms of the mixed-potential EFIE in plane-stratified dielectric media are developed and their properties are discussed. It is shown that for objects that penetrate one or more interfaces, one of these forms enjoys a clear advantage over the others. The authors have applied this equation in conjunction with the triangular-patch code [Rao *et al.*, *op. cit.*] to compute the current distribution on a conductive surface of arbitrary shape penetrating the interface between contiguous half-spaces. Preliminary numerical results are presented.

B1-5
10:40

APPLICATION OF MAPPING FUNCTIONS FOR NUMERICAL SOLUTION OF SCATTERING FROM POLYGONS

L. Shafai and H. Moheb
Department of Electrical Engineering
University of Manitoba
Winnipeg, Manitoba, Canada R3T 2N2

In numerical solution of scattering from conducting objects integral equations are commonly used to formulate the problem for the surface current distributions. These current distributions are then determined by utilizing the moment methods to reduce the integral equations to a matrix equation. The process involves a segmentation of the scattering surface into a finite number of sub-surfaces, over which the induced currents are represented by appropriate basis functions. For three-dimensionl objects the segmentation is over the entire object and results in matrices of large dimensions. Consequently, the solution becomes limited to objects small in terms of the wavelength. The matrix dimension can be reduced by utilizing the symmetry of the geometry, or, when the induced currents can be expanded in terms of orthogonal sets such as Fourier series. The latter have been used in problems involving bodies of revolution to reduce the overall matrix to a number of small matrices of the azimuthal modes.

In the present study the method is extended to objects with polygonal cross-sections. A mapping function is used to express the induced currents in terms of an angular variable in the transformed domain. The process reduces the two-dimensional integral equations to a set of one-dimensional ones along the generating line of the object, similar to the case of bodies of revolution. The method is then used to study the scattering from a few geometries such as cubes, prisms, and plates. The method is general and can be used for any geometry, provided a mapping function is already available or can be determined.

B1-6
1100

COMPUTATIONAL METHODS IN THE DIAKOPTIC ANALYSIS OF A CYLINDRICAL ANTENNA

Chalmers M. Butler, William A. Walker, Robert G. Kaires
Department of Electrical and Computer Engineering
Clemson University, Clemson, SC 29634-0915
and
Felix Schwering
U. S. Army CENCOM
Fort Monmouth, NJ 07703

The modified diakoptic theory can be used to analyze cylindrical antennas to a high degree of accuracy. The basic point of view which one adopts in developing this theory is quite different from that of the method of moments but in several ways the computations involved in implementing the two solution methods are similar. Moreover, as is well known to be true of the method of moments, there are alternate procedures which one may employ in a modified diakoptic analysis of a given antenna problem. Using the cylindrical antenna as an example, the authors describe fundamentally different ways to carry out the analysis necessary to determine the current on the antenna by the diakoptic theory. An interesting feature of these alternate methods is that, in a single computation, one represents the antenna current in two distinct linear combinations of different basis functions. Also of interest is the fact that, in an iterative procedure used to achieve convergence of the current in the diakoptic analysis, the method of moments is employed in intermediate steps. Results obtained by means of the alternate procedures alluded to above are presented and are compared to one another and to data obtained via the method of moments. Convergence of the methods is discussed too.

B1-7 1120

ON REDUCING THE NUMBER OF FREQUENCY SAMPLES NEEDED TO RECONSTRUCT AN ELECTROMAGNETIC TRANSFER FUNCTION *

G. J. Burke, Lawrence Livermore National Laboratory
Livermore, CA 94550

E. K. Miller, Rockwell Science Center, Thousand Oaks, CA 91360

S. Chakrabarti and K. R. Demarest, U. of Kansas, Lawrence, KS 66045

A frequently encountered problem in electromagnetics is that of determining the response of an object over a frequency band. This transfer function is typically obtained by many successive evaluations of a numerical solution. In a method of moments solution for a large model this repetition can consume excessive computer time. One way of reducing the number of evaluations is by introducing *a priori* knowledge of the expected frequency behavior in the form of a pole series. Another approach is to compute frequency dervatives which can be evaluated recursively in significantly less time than for the initial solution. The derivatives can then be used in an expansion about the frequency or for interpolation between frequency points. Both of these approaches are discussed here.

Derivatives of the current can be obtained from a method of moments solution at any frequency f_0 by taking derivatives of the matrix equation at $f = f_0$ and solving recursively as

$$\begin{aligned} ZI &= V & I &= Z^{-1}V \\ Z'I + ZI' &= V' & I' &= Z^{-1}(V' - Z'I) \\ Z''I + 2Z'I' + ZI'' &= V'' & I'' &= Z^{-1}(V'' - Z''I - 2Z'I') \\ \cdots & & \cdots & \\ \cdots & & I^{(n)} &= Z^{-1}\left[V^{(n)} - \sum_{r=1}^{n} C_{n,r} Z^{(n)} I^{(n-r)}\right] \end{aligned}$$

where $C_{n,r}$ is the binomial coefficient. The derivative matrices can be evaluated without too much additional effort if they are done simultaneously so that terms can be shared. Also, each successive derivative requires on the order of N^2 operations as opposed to the N^3 operations for the initial matrix solution. The derivatives can be used in a Taylor series expansion about a frequency or for interpolation between frequencies. Rational approximations derived from the derivatives are more efficient for representing the resonances of the response, however. Use of a pole series can similarly reduce the overall time for evaluating a transfer function by limiting the number of frequency samples needed. Results of both of these approaches are compared.

* Work performed under the auspices of the U. S. Department of Energy by the Lawrence Livermore National Laboratory under Contract W-7405-Eng-48.

Session D-1 0855-Tues. CR1-42
NUMERICAL SIMULATION OF SOLID STATE DEVICES
Chairman: T. Itoh, The Univ. of Texas, Dept. of Electrical and Computer Engineering, Austin, TX 78712

D1-1 0900 **ENSEMBLE MONTE CARLO MODELING OF HEMTS**

D. K. Ferry
Center for Solid State Electronics Research
Arizona State University
Tempe, AZ 85287-6206

The high-electron-mobility transistor (HEMT) provides a cross between the Si MOSFET and the GaAs MESFET, in that the carriers are confined to a quantized channel, with an inversion density controlled by the metal gate, but the device is normally a depletion mode metal-gate transistor. The use of Ensemble Monte Carlo techniques to model this device allows one to avoid simplifying assumptions in the transport model and to concentrate on the details of the scattering processes themselves.

Transport in such devices is complicated by the transitions between two- and three-dimensional characteristics of the electrons themselves (U. Ravaioli and D. K. Ferry, Superlattices and Microstructures 2, 377-380, 1986). Quantization in the channel is another detail that must be considered. In this talk, these facets of the modeling will be discussed and several approaches used by various groups outlined.

D1-2
0920

MONTE CARLO SIMULATIONS OF HIGH ENERGY ELECTRON TRANSPORT IN SEMICONDUCTORS

K. Hess and U. Ravaioli
Coordinated Science Laboratory and
Department of Electrical and Computer Engineering
University of Illinois
1101 W. Springfield Ave.
Urbana, IL 61801

Recent developments of research on high energy transport in semiconductors are reviewed concentrating on results of Monte Carlo simulations. It is shown that large scale computation has resulted in considerable advances in the understanding of such diverse topics as impact ionization, high energy injection and ballistic transport as well as overshoot and nonlocal effects in field effect transistors.

This review concentrates on electron energy distributions above certain energy thresholds such as the impact ionization threshold and electron transport over barriers including the emission of electrons out of the semiconductor (cold cathodes). In the course of these discussions we also will present results related to new forms of devices such as hot electron transistors (HET's) and high mobility transistors (HEMT's).

D1-3 0940

SIMULATION OF BALLISTIC DEVICES ON A SUPERCOMPUTER

Michael Shur+ and Jingming Xu++
+Department of Electrical Engineering
University of Minnesota,Minneapolis, MN 55455
++Department of Electrical Engineering
University of Toronto, Toronto, Canada

We present the results of the simulation of ballistic hot electron transistors using Monte Carlo method. This simulation is based on the study of the transport of a large number of electrons in the base of hot electron transistors (i.e. in the region between the emitter and collector barrier). This study shows that the angular distribution of the electrons arriving to the collector barrier is more focused. This caused by the acceleration of electrons in the built-in electric field in the base region as well as by the fact that the electrons injected into the base under large angles are more likely to be scattered, hence more likely to loose energy and contribute to the base current. Hence, the distribution function of electrons arriving to the collector barrier is more suited for the effective launching of ballistic electrons. This leads to a concept of utilizing a doped and graded layer following a conventional emitter to accelerate and shape the electron beam for an efficient injection into the next stages. As an example of the concept, we proposed Double Base Hot Electron Transistors (DBHETs) where the first (doped and/or graded) base region acts as an "electron gun" accelerating electrons and as a "lens" providing a better focused ballistic electron beam that is injected into the second base where an input signal is applied. (No input signal is applied to the first base.) Using the Monte Carlo method, we calculate the energy and angular distributions of electrons at the collector and the barrier sandwiched in between the first and second bases. We also calculate the mean transit time, as a function of energy, across the base. The results of the calculation demonstrate potential advantages of Double base devices.

We also discuss applications of the Monte Carlo method to the studies of the electron transport in compensated material. These studies show that sharply increased impurity scattering in compensated compound semiconductors changes the conditions of intervalley transitions and affects the Ridley-Watins-Hilsum-Gunn effect causing (under certain conditions) the appearance of two maxima of the velocity vs. electric field curve.

D1-4
1020

ADVANCED DEVICE THEORY & CONCEPTS

H. L. Grubin
Scientific Research Associates, Inc.
Glastonbury, CT 06033

The issues of submicron high speed and high frequency semiconductor devices have focused on problems such as velocity overshoot and more recently, the breakdown of the Fermi golden rule, quantum phase-based transport and tunneling. Also high speed devices have concentrated mainly on the electronic component of transport. The questions that continually arise with respect to these devices focus on the question of the feasibility of extracting, experimentally, the relevant high speed parameters. The issues of hole as well as electron transport, high speed limitations and the role of experiment in extracting fundamental concepts will be addressed.

D1-5
1040

OPTIMIZATION OF THE P SUBSTRATE DOPING FOR THE N CHANNEL GaAs SUBMICRONIC-GATE MESFET'S

S. El-Ghazaly, T. Itoh and G. Salmer*
Department of Electrical and Computer Engineering,
The University of Texas at Austin,
Austin, Texas 78712, USA.

Microwave coplanar FET's are thin film devices since their active layers are just few tenths of a micron. The performance of these MESFET's is highly affected by the properties of the substrates as well as the properties of the active layer. Growing the active layer directly on the substrate results in a poor quality transistor due to the crystallographic defects and the diffusion of impurities to the active layer. To avoid these problems, an epitaxially grown undoped buffer layer is introduced between the active layer and the semi-insulating substrate. Considerable number of free carriers are injected into this buffer layer while they travel under the gate. This carrier injection produces a higher saturation current, a lower transconductance (g_m) and a higher drain output conductance (g_d) (G. Salmer *et al.* Proc. Int. Symp. GaAs and Related Compounds, 1984). To improve the MESFET performance, the authors proposed the use of a P substrate, or P buffer layer to increase the transconductance and reduce the drain output conductance (S. El-Ghazaly *et al.* XXIInd General Assembly of the Int. Union of Radio Science, 1987).

The P substrate problem is investigated using a two dimensional numerical model which solves Poisson's equ., continuity equ. and energy conservation equ. The mobility and the electron temperature are functions of the average electron energy. This model is capable of correctly simulating the submicronic gate MESFET taking into account the non-stationary effects such as velocity overshoot (S. El-Ghazaly *et al.* Proc. 13th European Solid State Devices Research Conf., 1983). Several MESFET structures of gate lengths equal to 0.5 μm were simulated. These structures include symmetrical MESFET's, which has no substrate effects, MESFET's on buffer layers and MESFET's on P substrates.

It was observed that MESFET's on P substrates demonstrate a considerably high transconductance compared to MESFET's on buffer layers. Due to the increase of the electrons confinement to the active layer, the gate-to-source capacitance is also high. However, MESFET's on P substrates demonstrate a higher current-gain cutoff frequency compared to the corresponding MESFET's on buffer layers. The doping of the P layer has a great influence on the MESFET parameters. The results of the optimized doping to obtain the best MESFET performance will be presented as well.

* Centre Hyperfrequences et Semiconducteurs,
Universite des Sciences et Techniques de Lille,
59655 Villeneuve d'Ascq Cedex, France.

D1-6 1100 SIMULATION AND MODELING OF PHYSICAL PHENOMENA IN MICROELECTRONIC DEVICES: G. Iafrate, Electronics Technology and Devices Lab, Ft. Monmouth, NJ 07703-5302

D1-7 1120 PANEL DISCUSSION ON DEVICE MODELING AND SIMULATION

G1-1
0900

MODELLING IONOSPHERIC DENSITY STRUCTURES

R. W. Schunk and J. J. Sojka
Center for Atmospheric and Space Sciences
Utah State University
Logan, Utah 84322-4405, U.S.A.

Large-scale density structures are a common feature in the high-latitude ionosphere. They have been observed in the dayside cusp, polar cap, and nocturnal auroral region over a range of altitudes, including the *E*-region, *F*-region and topside ionosphere. Relative to background densities, the perturbations associated with large-scale density structures vary from about 10% to a factor of 100. These structures can be created by a variety of mechanisms, including particle precipitation in the dayside cusp, in sun-aligned polar cap arcs, and in the nocturnal auroral oval; by structured electric fields which lead to structured enhanced loss rates; and by large-scale plasma convection which acts to separate and distort ionospheric density features. The origins, lifetimes and transport characteristics of large-scale density structures were studied with the aid of a three-dimensional, time-dependent ionospheric model. The study considered blob creation due to particle precipitation, the effect that structured electric fields have on the ionosphere, and the lifetimes and transport characteristics of density structures for different seasonal, solar cycle, and interplanetary magnetic field (IMF) conditions. The main conclusions drawn from the study are: (1) The observed precipitation energy fluxes are sufficient for blob creation if the plasma is exposed to the precipitation for 5–10 minutes; (2) Within 10–20 minutes after blob creation by precipitation, the *F*-layer recovers its shape, and hence, the source characteristics cannot be determined from the profile shape after this time period; (3) Structured electric fields produce structured electron densities, ion temperatures, and ion composition; (4) The lifetime of an *F*-region density structure depends on several factors, including the initial location where it was formed, the magnitude of the perturbation, season, solar cycle and IMF; and (5) Depending on the IMF, horizontal plasma convection can cause an initial structure to break up into multiple structures of various sizes, remain as a single distorted structure, or become stretched into elongated segments. These and other aspects of large-scale plasma density structures will be described.

G1-2
0940

URSI ACTIVITIES TO FOSTER IMPROVED IONOSPHERIC MODELS

Charles M. Rush
National Telecommunications and Information Administration
Institute for Telecommunication Sciences
Boulder, CO 80303

The International Radio Science Union has taken an active role in the development of improved ionospheric models that can aid in predicting the performance of telecommunication systems that rely on the ionosphere. The development of the International Reference Ionosphere (IRI) has been jointly sponsored by URSI and COSPAR for a number of years. In August 1986 an URSI-sponsored workshop brought together model builders and model users in an attempt to foster communication and appreciation of the needs of each for the other. This workshop identified a number of areas where further work is required in order to bring the results of ionospheric modeling into telecommunications applications. Commission G decided at the Tel Aviv General Assembly to form a new Working Group to look at the general topic of ionospheric models. This Working Group is currently defining its terms of reference and studies it will undertake.

In this paper we will review the status of these URSI activities and point out those areas where further URSI work is likely to be directed. Also, discussion will be given to studies that are needed to be addressed so that ionospheric model developments readily find their way into improvements in telecommunication system prediction and performance assessment.

G1-3
1000

Mapping of f_0F_2

By
Kenneth Davies
NOAA/ERL/SEL, Boulder, CO 80303

ABSTRACT

Working Group 5 of URSI has recently developed a new numerical map for a global representation of f_0F_2. The new maps are based on the Fox-McNamara (Australian) data base which includes both observed data and theoretical data obtained from a physical model of the ionosphere. Each map is described by 988 coefficients, which is consistent with those used by the CCIR. The new maps provide an improved description over ocean areas.

G1-4
1040

THE IONOSPHERIC RESPONSE TO A LARGE GEOMAGNETIC STORM: COMPARISON OF CALCULATED AND OBSERVED VALUES

D. N. Anderson
Air Force Geophysics Laboratory
Hanscom AFB, MA 01731-5000
M. Mendillo and K. Davies

The large geomagnetic storm on Feb. 8, 1986 produced dramatic increases in both TEC and NMAX values at a number of observing stations across the continental United States. Ionosonde data from Boulder indicated an order of magnitude increase in NMAX from 2 x 10^5 el/cm^3 to 1.8 x 10^6 el/cm^3 between 1400 and 1600 LT while at PT. Arguello, California the density increased from 4 x 10^5 to 3 x 10^6 el/cm^3. To better understand the mechanisms which brought about these dramatic increases, we calculate electron density distributions as a function of latitude and local time by solving the time-dependent plasma continuity equation including the effects of production, loss and transport of ionization. The separate and combined effects of both meridional neutral wind and zonal and meridional E x B drifts are studied to determine which transport mechanisms are responsible for the observed changes in NMAX, HMAX and TEC. The sudden increase in NMAX followed by a sharp decrease on the afternoon of the first day is a classic ionospheric-response signature to geomagnetic storms in the American sector. We discuss the implication of our findings to other longitude sectors.

G1-5 1100 The MUF(3000) as an F-region Variability Parameter

Adolf K. Paul
Naval Ocean Systems Center
Ocean and Atmospheric Science Division
Code 544
San Diego,California 92152-5000

Acoustic gravity waves continuously modify the F-region with a variable degree of intensity. The resulting deformations are visible as oscillatory variations of the virtual heights at fixed frequencies and to a lesser extent as variations of the maximum electron density. The virtual height oscillations are usually delayed in phase at lower frequencies (heights) compared with heigher frequencies (heights). The results are height dependant tilts which can have a variety of significant consequences ranging from errors in the computation of electron density profiles to large uncertainties in direction finding attempts.

The MUF(3000) is a standard parameter and is either directly or indirectly scaled for every ionogram. The height-frequency coordinates where the MUF is determined correspond to a point very close to the middle of the lower half of the F-region profile and temporal changes of the MUF usually reflect a combination of changes in the virtual heights and electron density in the vicinity of this point. For those reasons it appears that the temporal variations of the MUF could be a direct indicator for the reliability of ionospheric quantities. This can be verified by comparison of various F-region parameters with the time derivative of the MUF(3000).

G1-6
1120

EVALUATION OF A LONG WAVELENGTH PROPAGATION MODEL USING VLF DATA COLLECTED ABOARD A SHIP

Jerry A. Ferguson
Rita P. Brown
Ocean and Atmospheric Sciences Division (Code 544)
Naval Ocean Systems Center
San Diego, CA 92152-5000

VLF and LF signal strength data were collected aboard the MST Callaghan over the period between March 1985 and November 1985 while the ship made repeated crossing of the North Atlantic. the crossings were generally between ports on the east coast of the United States and Bremerhaven, West Germany. One crossing was from the east coast of the United States to Alexandria, Egypt. Good data were obtained from the US Navy transmitters at Annapolis, MD (21.4 KHz) and Cutler, ME (24.0 KHz) and from the British stations at Rugby (16.0 KHz) and Anthorne (19.0 KHz). These data provide the basis for statistical evaluation of signal strength variations and of the calculations of the long wavelength propagation capability (LWPC) being developed at the Naval Ocean Systems Center.

Results indicate a complete lack of solar zenith angle (seasonal) dependence on these paths. The calculations using the model of the daytime ionosphere in the LWPC shows excellent agreement with these measurements.

G1-7
1140

SSL RANGE ESTIMATION USING DIFFERENT IONOSPHERIC MODELS

Leo F McNamara
Andrew Antennas
Technology Park 5095
AUSTRALIA

Observations of the elevation angle and bearing of signals from distant HF transmitters, made with the single station location system SKYLOC, have been used to investigate the range accuracy obtainable with different models of the vertical distribution of electron density. Several N(h) profile shapes have been considered, all anchored at layer peaks defined by fairly standard procedures:-

1. A single 3-parabola profile for each hop

2. A variable 3-parabola profile which varies along the circuit

3. A variable Dudeney profile (JATP 40, 195, 1978)

4. A variable 3-layer Chapman profile

5. A variable International Reference Ionosphere profile (UAG-83)

Models (1) and (2) were converted into a set of quasi-parabolic profiles, for rapid no-field range estimation. Raytracing for models (3), (4) and (5) was three-dimensional, including the earth's magnetic field. The E layer was essentially the same for all profiles.

The five models have been scored according to how close their calculated ranges came to the correct range for F2 propagation. No significant differences were found for models (1) to (4), but model (4) usually gave the longest ranges and thus scored highest when all methods underestimated the range. The IRI profile fared badly, failing to support the observed propagation on many occasions, and scoring poorly on the other occasions.

Range estimates for F1 propagation present a confusing picture, indicating a generally unsatisfactory modelling of this region.

H/G/B1-1 0900

REVIEW OF PATH INTEGRAL TECHNIQUES AND SOLUTIONS OF THE FOURTH MOMENT OF WAVES PROPAGATING IN RANDOM MEDIA

R. G. Frehlich
Cooperative Institute for Research in the Environmental Sciences
University of Colorado
Boulder, CO 80309

Series solutions for the fourth moment of waves propagating through random media using path integral techniques are reviewed. The solution for the random phase screen is presented using Green's function techniques. Narrow angular scattering is assumed. The analogous result for extended random media is then derived using the path integral representation of the Green's function and the Markov approximation. The application of these results to extended incoherent sources is reviewed. The analogous result for space-time fourth moments of "frozen" random media is presented.

H/G/B1-2
0920

SCINTILLATION AND SCATTERING IN INHOMOGENEOUS MEDIA

Y. L. Li and C. H. Liu, Dept. of Electrical and Computer Engineering, University of Illinois, Urbana,IL 61801

This paper presents a method for studying scintillation and scattering of waves due to random irregularities embedded in a three-dimensional linearly inhomogeneous medium. In particular, the effects of the scattered fields on field distribution in the shadow zone will be investigated. The analysis is based on Green's function for such a medium derived from the path integral approach and expressed exactly by a onefold integral. The scattered waves which include the effects of random irregularities are computed using the Born approximation. The total field distribution in the shadow zone can be obtained by summing the incident wave and the contribution from the scattered waves. The method is quite general since source position and irregularity shapes are allowed to vary widely. A program for computing the field wherever the source and irregularities are distributed and the numerical techniques used to improve the program efficiency will be discussed. A technique used to generate random scatterers with prescribed spectral behavior will be presented. Numerical results for the various position of source and irregularities will be shown. These results demonstrate that, depending on the position of irregularities, the field distribution in the shadow zone can be drastically modified by scattered fields.

H/G/B1-3 0940 INTENSITY CORRELATION FUNCTION FOR WAVES OF DIFFERENT FREQUENCIES PROPAGATING THROUGH A RANDOM MEDIUM

A. Bhattacharyya[1] and K. C. Yeh
Department of Electrical and Computer Engineering
University of Illinois
Urbana, IL 61801

The fourth moment equation for waves of two different frequencies propagating through a two-dimensional extended random medium with a wavenumber-dependent refractive index is solved numerically. The numerical scheme is based on a split-step algorithm which approximates the solution by replacing the extended medium by a series of phase screens interspersed with diffraction layers. The phase screens give rise to different phase perturbations for the two waves. In addition to this, diffraction in the region between two phase screens also depends on the wave frequency. Therefore, in the calculation of intensity cross-correlation function for waves of different frequencies, propagation within the irregularity slab becomes increasingly important as the thickness of the slab is increased, unlike the case of monochromatic waves, where the intensity auto-correlation function for an extended medium is very well approximated by that for a single centrally located phase screen which produces the same mean square fluctuation of phase (H. G. Booker et al., J. atmos. terr. Phys., 47, 381-399, 1985).

Under multiple scattering conditions and with the assumption of "frozen flow", the intensity cross-spectrum shows increasingly steep decrease at high spatial frequencies as the ratio of the two wave frequencies deviates farther from unity. This feature is present for irregularities with either a Gaussian or a power-law power spectrum. The intensity cross-spectrum has the same behavior at high spatial frequencies when the refractive index of the medium is independent of wave frequency (S. J. Miller, Proc. R. Soc. Lond. A410, 229-249, 1987). However, at the low frequency end, the nature of the intensity cross-spectrum is determined by the wavenumber dependence of the refractive index fluctuations.

The effect of increasing the strength of the irregularities on the normalized correlation function of intensity fluctuations on waves of different frequencies is also investigated. In the weak scintillation limit, the decorrelation is independent of the strength of the irregularities. As the refractive index fluctuations increase in strength, at first only the lower frequency wave undergoes multiple scattering and this leads to rapid decorrelation of the intensities of the two waves, but when both waves undergo multiple scattering, there is little further loss of correlation.

The two-frequency space-time intensity correlation function is obtained for the "non frozen" situation where the irregularities have random velocity fluctuations with standard deviation σ_v superimposed on a uniform drift. The effects produced by the velocity fluctuations are similar to those in the monochromatic case (A. W. Wernik et al., Radio Sci., 18, 743-764, 1983; S. J. Franke and C. H. Liu, AGARD Conference Preprint, No. 419, 15-1, 1987). The peak value of the cross-correlation function for a non-zero spatial separation decreases as σ_v increases and the peak itself moves towards a smaller time lag and has a positive skewness. However, velocity fluctuations become increasingly ineffective in causing decorrelation as the ratio of the two frequencies deviates farther from unity.

[1] On leave from the Indian Institute of Geomagnetism, Bombay, India.

H/G/B1-4
1020

SPECTRAL DOMAIN METHODS FOR RADIOWAVE PROPAGATION IN CONTINUOUS RANDOMLY IRREGULAR MEDIA

Charles L. Rino
Mission Research Corporation
2300 Garden Road, Suite 2
Monterey, California 93940

The parabolic wave equation has been used extensively for propagation in continuous randomly irregular media. It assumes (1) small local perturbations (the Markov approximation), (2) narrow-angle scatter, and (3) negligible backscatter. More recently, the cumulative forward scatter single backscatter approximation has been used to improve backscatter computations. In this paper we describe a spectral-domain method for computing the first- and second-order moments of the wavefield that fully accommodates backscatter and makes minimal restrictions on angular extent. The forward and backward scattered wavefields are characterized by an exact spectral-domain formulation of the scalar Helmoltz equation. The interaction of the wavefields with the medium is characterized by incremental forward and backward scattering functions. Approximate forms are computed in terms of the spectral density function of the relative permittivity fluctuations. Solutions are obtained for incident plane and spherical waves, which yield the well-known results derived from the parabolic wave equation when the backscatter terms are neglected. The general results give new insights into backscatter enhancements by showing that they depend on the correlation between scattered waves in the strict forward and backward directions.

Computations are performed to illustrate the effects of backscatter on VHF transionospheric radiowaves.

H/G/B1-5
1040

THE MUTUAL COHERENCE FUNCTION IN REFRACTING MEDIA

L. J. Nickisch
Mission Research Corporation
2300 Garden Road, Suite 2
Monterey, California 93940

It has been recently shown (R. J. Hill, J.Acoust.Soc.Am, 77, 1742-1753, 1985) that a parabolic-type wave equation holds in refracting media provided that a particular coordinate system is used, the so called orthogonal trajectory coordinates. These coordinates are defined by path length along a deterministic ray and the surface of constant phase of the deterministic field at that path length. A stochastic equation for the two frequency mutual coherence function can be obtained from the parabolic wave equation. We show that this equation can be approximately solved by integration over the deterministic ray path corresponding to the mean refractive index.

The solution requires knowledge of the metric tensor for the surface of constant phase as well as information about deviated ray paths. We show that this information is given by integrating a set of differential equations describing deviated ray paths, obtained by varying the Hamilton equations for three-dimensional rays with respect to the independent variables.

H/G/B1-6
1100

ANALYSIS AND INTERPRETATION OF WIDEBAND SATELLITE DATA

Dennis L. Knepp
Mission Research Corporation
2300 Garden Road, Suite 2
Monterey, California 93940

Fifty satellite passes with the most severe scintillation data measured during the course of the DNA Wideband Satellite Experiment in the late 1970s are re-examined in order to test the two-component description of the in-situ electron density irregularity spectrum. Analytic results for the two-position, single-frequency mutual coherence function and the signal decorrelation time inferred from the two-component irregularity spectrum model are compared to measurements. A comparison of measurement and theory for the single-position, two-frequency mutual coherence function is presented using data from seven coherently related UHF tones. The theoretical ramifications of the two-component model will also be discussed.

Specific parameters including the signal decorrelation time, the decorrelation distance and the channel bandwidth are determined from the data. Through specific analysis procedures that apply coherent signal processing techniques to the Wideband measurements, it is shown that these parameters quantitatively determine many aspects of the performance of a radar that might operate through a disturbed propagation channel.

H/G/B1-7
1120

NUMERICAL FULL-WAVE SOLUTIONS TO THE MAXWELL EQUATIONS IN CONTINUOUSLY RANDOM MEDIA

L. J. Nickisch
Mission Research Corporation
2300 Garden Road
Monterey, CA 93940

Patricia Calvert
Naval Research Laboratory
4555 Overlook Ave. Code 8344
Washington, DC 20375

Full-wave solutions to the Maxwell equations have been implemented numerically using the time domain finite difference (TDFD) method [Yee, K. S., "Numerical Solution of Initial Boundary Value Problems Involving Maxwell's Equations in Isotropic Media,"IEEE Transactions on Antennas and Propagation, Vol. AP-14, No. 3 (1966)], but the physical extent of the regions one could consider were limited by computer speed and storage requirements. With the advent of specialized parallel processing machines such as the Connection Machine, it is now possible to perform such calculations much more efficiently. The Connection Machine in particular is designed to efficiently perform nearest neighbor calculations over a full array simultaneously, reducing the time required to obtain TDFD solutions to Maxwell's equations by several orders of magnitude. Because of the power of these computational resources the applicability of this method has now broadened to include areas such as wave propagation.

Current methods used to predict the behavior of waves travelling through the ionosphere use certain simplifying assumptions to the Maxwell equations. The first approximation generally made is to ignore the polarization coupling terms in the wave equation, reducing the equations to scalar Helmholtz form. This equation is typically further reduced to the parabolic wave equation, a transport-type, small angle scatter equation. Thus backscatter is ignored. The TDFD method requires no such simplifications, but is capable of solving the full vector problem with tensor dielectric. The method is based on the Maxwell curl equations, which are first order differential equations in time. Finite difference approximations are applied to the differential operators and the equations solved in small time steps. The evolution of an incident pulse on the dielctric structure of interest can thus be followed, and since the full content of the Maxwell equations is included in the calculation, all effects are properly accounted for (e.g., polarization coupling, backscatter, Faraday rotation, etc.), limited only by the accuracy inherent in the grid resolution and boundary effects.

Session J-1 0855-Tues. CR0-30
RADIO SCATTERING FROM ICY BODIES
Chairman: S.H. Zisk, MIT Haystack Observatory, Westford, MA 01886

J1-1
0900

RADAR STUDIES OF COMETS

J. K. Harmon
Arecibo Observatory
P.O. Box 995
Arecibo, PR 00613

Five comets have been detected with Earth-based radar: Encke, Grigg-Skjellerup, IRAS-Araki-Alcock (IAA), Sugano-Saigusa-Fujikawa (SSF), and Halley. In each case, with the probable exception of Halley, the dominant echo has come from the nucleus. Since all of the observations have been of the simple CW type, it has not been possible to determine simultaneously both the size and reflectivity of a comet nucleus from radar data alone. However, comparison of the radar results for IAA and Halley with other data suggests that the nuclei of these objects have relatively porous surfaces. The two closest-approaching objects (IAA, SSF) gave strong echoes from which it was possible to measure the shape and polarization of the nucleus Doppler spectrum. These echoes were similar in appearance to those obtained from many asteroids and were consistent with nucleus surfaces which are very rough on scales of a meter or larger. About 25% of the radar cross section of IAA was contained in a broadband component whose Doppler spectrum and polarization were consistent with scattering from cm-size grains in the inner coma. The most recent comet radar detection was that of Halley in November 1985. The broad Doppler spectrum and unusually high radar cross section (30 km^2) of the Halley echo are inconsistent with a nucleus echo given what we now know about the nucleus from the spacecraft encounters. Thus we conclude that the Halley echo most likely came from large grains such as those associated with Comet IAA. The high radar cross section could then be explained by the fact that Halley was a much more active comet than IAA.

The major goals of future radar work are 1) to resolve the nucleus of a comet with ranging-type observations, and 2) to observe additional bright active comets such as Halley, if possible at small heliocentric distances when nucleus activity is highest. Future comet observations at Arecibo will rely on new-comet apparitions, as the prospects for observing known periodic comets are poor for the next few years. Proposed upgrades to the Arecibo telescope and radar system could significantly improve both the frequency and scientific value of comet radar detections.

J1-2
0920

RADAR PROPERTIES OF THE ICY GALILEAN SATELLITES

S. J. Ostro
183-501, Jet Propulsion Laboratory
California Institute of Technology
Pasadena, CA 91109

Radar echoes from Europa, Ganymede, and Callisto are extremely strong and have bizarre polarization properties. At λ13 cm, these objects' average radar reflectivities dwarf values reported so far for other radar-detected planetary targets, including the Moon, the inner planets, a few comets, and several dozen asteroids. The satellites' radar albedoes increase logarithmically from Callisto to Ganymede to Europa, whose radar reflectivity is similar to that of a metal sphere. The satellites' average, total-power, angular scattering law is $\sigma_o(\theta) \sim (\cos \theta)^{1.5}$.

When the radar transmission is circularly polarized, most targets return echoes with the incident handedness reversed, but for the icy satellites the handedness is, quite remarkably, preserved. The circular polarization ratio, μ_c, of echo power in the same sense of circular polarization as transmitted (the SC sense) to that in the orthogonal (OC) sense, averages 1.2, 1.6, and 1.6 for Europa, Ganymede, and Callisto, compared to about 0.1 for the Moon and < 0.4 for most other targets. The linear polarization ratio, μ_L, of OL to SL power, is ~0.5 for all three satellites, or nearly 20 times the lunar value.

The available data indicate that the unusual radar signatures vanish for wavelengths much smaller than a centimeter or as large as one meter. Significant albedo and/or polarization features are common in the echo spectra and, in a few cases, the source of a radar scattering anomaly can be identified tentatively in Voyager images. (For a complete description of the radar dataset, see my review in *Satellites of Jupiter*, D. Morrison, ed., Univ. of Arizona Press, 1982, pp. 213-236.)

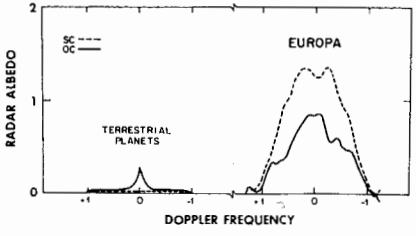

Typical λ13-cm echo spectra for the terrestrial planets and Europa. Radar albedo is radar cross section divided by the target's projected area. The abscissa has units of half the echo bandwidth.

J1-3
0940

INTERNAL REFRACTION AS A POSSIBLE CAUSE OF THE PECULIAR SCATTERING FROM THE GALILEAN SATELLITES.

T. Hagfors
National Astronomy and Ionosphere Center
Space Sciences Building
Cornell University
Ithaca, NY 14853

The radio wave scattering from the icy Galilean satellites is peculiar in that the cross section is larger than that of a metal sphere, yet the distribution of scattered power over the disk is relatively uniform, and lacking the quasispecular highlight characteristic of other bodies. Furthermore, the sense of circular polarization of most of the returned power is oppositely polarized to that of other solar system targets.

Several theoretical models have been deviced to explain this behavior involving hemispherical craters, randomly oriented surface cracks and voids, buried craters and refracting "lenses" of various types. The talk discusses details of the refracting lens model, elaborating on the original idea (T. Hagfors, Gold, T. and M. Ierkic, Nature, 315,637-640, 1985). It is shown that the model is capable of explaining the observed scattering properties. The physical mechanisms which can give rise to the structures postulated are discussed, as well as experiments which may be required to determine whether the postulated scattering mechanism is the correct one.

J1-4
1020

THE RADAR-GLORY THEORY OF ECHOES FROM THE ICY GALILEAN MOONS OF JUPITER

Von R. Eshleman
Stanford University
Stanford, CA 94305

The well-known electromagnetic phenomenon of total internal reflections (TIR) at a dielectric interface may be central to an explanation for the puzzling characteristics of radar echoes from Europa, Ganymede, and Callisto, giant ice-clad moons of Jupiter. A model in which TIR occurs in a geometry that favors the backscatter direction has the inherent properties needed to explain the exceptional strengths, surprising lack of specularity, and anomalous polarizations of the icy-moon echoes. Optical glory involves TIR in a spherical geometry (cloud water droplets) that favors backscatter (hence its appearance in the anti-solar direction). However, a roughly hemispherical geometry appears more appropriate for the icy-moon setting where cratering and flooding are known to occur. Hemispheres can be much superior to spheres as glory sources since they provide a break-out (and break-in) mechanism for the otherwise trapped TIR modes. To obtain radar glory from TIR in a hemispherical source, the hemisphere must have a higher refractive index than its curved surroundings. This leads to a proposed model of buried craters to explain the radar observations of the icy moons of Jupiter. The negative discontinuity in refractive index at the flood-crater interface could be due either to an overburden of higher density than the original surface material or to the formation of a thin low-density film on the old surface prior to flooding, due to ice sublimation or frost formation. More complete understanding of he icy-moon echoes, which are fundamentally different than the returns from rocky planets and Earth's moon, is important in basic studies of the icy bodies of the outer solar system and for planning radar mapping surveys of their surfaces.

J1-5 1040 GALILEAN SATELLITES, GEOLOGY: E.M. Shoemaker, Branch of Astrogeologic Studies, U.S. Geological Survey, Flagstaff, AZ 86001

J2-6 1100 OBSERVATIONS OF SATURN'S RINGS: D.O. Muhleman, California Institute of Technology, Pasadena, CA 91125

Session J-2 1115-Tues. CRO-30
RADAR ASTRONOMY OF THE INNER SOLAR SYSTEM
Chairman: S.H. Zisk, MIT Haystack Observatory, Westford, MA 01886

J2-1 1120 PROPOSED UPGRADE OF THE ARECIBO TELESCOPE: D.B. Campbell, Arecibo Observatory, Arecibo, PR 00612

GOLDSTONE SOLAR SYSTEM RADAR UPGRADE

J2-2
1140

N. A. Renzetti
Jet Propulsion Laboratory
4800 Oak Grove Drive
Pasadena, CA 91109

An extensive upgrade of the Jet Propulsion Laboratory's Goldstone Solar System Radar (GSSR) is planned for a 1993 operational date. The GSSR shares equipment and facilities with the Deep Space Network (DSN) and increase in performance will be accomplished by modifying the system components used uniquely by the GSSR, and by using the improvements planned for the overall DSN.

The major hardware upgrade will be to increase the GSSR X-band transmitter power output from 360kw at the feedhorn to 1 mw cw. This 4.4 db improvement coupled with a 2 db increased antenna performance will more than quadruple the effective radiated power from the GSSR X-band transmitter. Additional performance benefit will be realized with the upgrade of the exciter to provide sufficient drive for four Klystrons and to incorporate a phase correction loop necessary for the 1 mw combining. Using a new phase correction loop, the exciter design is expected to provide approximately 40 db in phase noise improvement over the current system.

The second major upgrade is to the DSN's Digital Data Acquisition hardware and software. Major modifications will accommodate complex, multi-channel dual circular polarization data acquisition. This will allow the GSSR to be used in gathering a much more extensive data base than is currently possible. In addition, the DAS bandwidth per channel will be increased to accommodate the enhanced resolution and wider spectral coverage which is being required in carrying out more detailed planetary radar measurements.

In addition to these major upgrades, improvements to the monitor and control system will be carried out. In particular, a new modularized distributed control system is being designed around Hewlett Packard's Vectra computer, an industrial equivalent of an IBM PC-AT. The plan is to have the various equipments, needed to support the 1 mw radar, connected with the control console via an IEEE-488 bus and fiber optic links. ADA will be the programming language and artificial intelligence techniques are currently being evaluated for transmitter maintenance augmentation. A prototype rule-based expert system is currently undergoing evaluation.

Session A-2 1355-Tues. CR1-42
MICROWAVE AND MILLIMETER WAVE MEASUREMENTS
Chairman: David F. Wait, Electromagnetic Fields Division, National Bureau of Standards, Boulder, CO 80303

A2-1
1400

A FIRST-ORDER FIELD CORRECTION TO THE CHARACTERISTIC ADMITTANCE OF A COAXIAL LINE

W.C.Daywitt Electromagnetic Fields Division
National Bureau of Standards
Boulder, Colorado 80303 USA

Since coaxial lines have been in heavy use for years it is an odd fact that a complete set of field equations correct to first order in the skin depth cannot be found it the literature, although Stratton does give a piece of this field in his book on electromagnetic theory (*Electromagnetic Theory*. New York: McGraw-Hill, p.552, 1941). In the process of correcting this situation for another application (W.C.Daywitt, *Metrologia* 24, 1987) the effect of the the first order field terms on the characteristic admittance and the distributed line parameters was calculated. The results are reported in this talk.

The coaxial line is treated as perfectly concentric with an infinitely thick outer conductor, and when the characteristic admittance $(2\pi a H_a / \int_a^b E_r\, dr)$ is calculated from the resulting field equations, the following expression for the admittance is obtained:

$$Y_0 = \hat{Y}_0 \left(1 + \frac{\delta Y_0}{Y_0} + a\mathcal{E}_a - \frac{\int_a^b \mathcal{E}_r\, dr}{ln(b/a)} \right)$$

where $\hat{Y}_0$ is the characteristic admittance for a lossless line, $\delta Y_0 / Y_0$ is the usual term accounting for finite conductivity, and the last two terms are the first order field corrections. The electric field corrections $\mathcal{E}_a$ and $\mathcal{E}_r$ are obtained from the equation

$$\mathcal{E}_r = \frac{rh^2}{2} \left(ln\frac{b}{r} + \frac{1}{2} - \frac{ln(b/a)}{1+b/a} \right)$$

where h^2 is the usual correction to the principal wave propagation constant.

The last two terms in Y_0 cause a 6.4% decrease in the distributed line resistance, while their effects on the other distributed line parameters are found to be negligible.

In addition to the results just presented, the investigation led to a first order correction $\Delta\gamma_m$ in the propagation constant for the symmetric TM_{0m} modes. For a positive harmonic time variation, this correction is

$$\Delta\gamma_m = \frac{jkz_s}{ab\gamma_m} \left[\frac{aJ_0(k_m a)N_0(k_m a) + bJ_0(k_m b)N_0(k_m b)}{J_0(k_m a)N_0(k_m a) - J_0(k_m b)N_0(k_m b)} \right]$$

where J_0 and N_0 are first and second kind Bessel functions, k is the free space wavenumber, and z_s is the normalized surface impedance of the conductors.

A2-2 INDUSTRY NOISE PARAMETER MEASUREMENTS
1420

W. C. Mueller, Sr. Applications Engineer, MSG
Avantek Inc. 3175 Bowers Avenue
Santa Clara, Ca 95054-3292

The following is a technique suitable for use between 2 and 18 GHz for determining the four noise parameters F_{min}, $|\Gamma_{opt}|$, $\angle \Gamma_{opt}$, R_n using standard production test equipment.

Measurement Technique (single sideband technique):

Ensure:ENR is set correctly (include correction for isolator if used); oscillator is stable to within ±1 MHz; choice of IF combined with rejection of filter provide at least 40 dB rejection. Connect (Noise Source) to (Second Stage). Set gain reading to 0.0 dB. Record F_2 in dB. Now connect (Input Tuner), (DUT), and (Output Tuner) as shown. Set tuners to 50Ω position. Record F_{50}, G_{50} in dB. Adjust (Input Tuner) for lowest noise, (Output Tuner) for highest gain. Record F_{meas}, G_{meas}, settings of tuners (slug and slide positions). Take tuners to a vector Network Analyzer, reproduce the tuning settings, record full s parameters for both (Input Tuner) and (Output Tuner).

Calculations:

F_{min}: F_{min} in dB = $10 \log_{10} [F_{meas(lin)} - (F_{2(lin)} - 1)/G_{meas(lin)}] - 10 \log_{10} [|s_{21}|^2 / (1-|s_{22}|^2)]$

where $x_{lin} = 10^{x/10}$ and $x = 10 \log_{10} (x_{lin})$

Γ_{opt} , (Noise Source) s par. are measured both with the noise diode on and with it off. An average s_{11} is taken. A model is made of the test fixture (50Ω line + capacitive fringing). These are combined with the measured s par of (Input Tuner) to yield Γ_{opt}.

R_n : $R_n = 12.5\Omega (10^{F_{50}/10} - 10^{F_{min}/10}) (1+|\Gamma_{opt}|^{-2} + 2\cos(\angle\Gamma_{opt})/|\Gamma_{opt}|$

Note:G_A = G_{meas} + loss(Input Tuner) + loss(Output Tuner); tuner loss = $10 \log_{10}[|s_{21}|^2 / (1-|s_{22}|^2)]$; G_A calculation provides noise parameter verification: check against predicted s par. gain at Γ_{opt}.

Concerns: s par of tuners (repeatability of settings and connections, significant figures, correcting for non-50Ω); temperature corrections; fixture model; diode s_{11}; R_n determination when Γ_{opt} is near 50Ω.

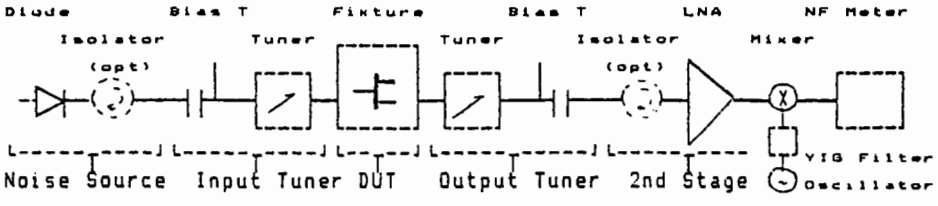

NOISE PARAMETER MEASUREMENT SETUP

A2-3
1440

MULTIVARIATE STATISTICAL CONTROL OF THE NBS AUTOMATED RADIOMETER

Dr. D. S. Friday, Electromagnetic Fields Division
National Bureau of Standards
Boulder, Colorado 80303

Each of the new NBS automated radiometers is designed to operate over a particular band of frequencies. A set of special check-standards will be maintained for each radiometer for the purpose of monitoring the stability of its measurements over time. In a band, checks will be made at several frequencies and it is desirable to have a single indicator of system stability for the entire band. The fluctuations in these measurements are a random process and it is important to efficiently detect real changes in the system while ignoring normal variation. Statistical methodology is proposed whereby the check-standard noise sources can be measured at several frequencies each time a radiometer is tested, and a single control chart is used to monitor the system performance. If the single chart exhibits an anomaly and suggests a more detailed investigation, then individual frequency charts can be studied.

The multiple frequency charts are based on a principal component transformation. Each data vector represents the measurements at the various frequencies on a specific check-standard at a particular point in time. The transformation is derived from prior measurements done over the history of the device. That is, all such vectors for which the radiometer was stable during past checks. The current observation vector is then compared statistically to the past data. The maximum eigenvalue and its distribution is then used for monitoring the entire frequency band. It has the appealing interpretation that this eigenvalue contains the most information, in a linear sense, on the joint variation at all the frequencies. Other relevant statistical control methodology for the radiometers is also discussed.

A2-4
1500

MEASURING CONNECTOR INSTABILITIES WITH HIGHLY REFLECTING LOADS

John R. Juroshek
National Radio Science Meeting
National Bureau of Standards
U.S. Department of Commerce
Boulder, CO 80302

Instabilities and inconsistencies in rf coaxial connectors are one of the basic mechanisms that are currently limiting the accuracy of coaxial impedance measurements at the National Bureau of Standards. Impedance changes that occur at the rf connector joint, during disconnection or reconnection, are often of the order of 1 part in 10^3 or greater. This fact coupled with the customers demands for better accuracy in impedance measurements has led to a significant effort to both improve the quality of the rf connectors and to measure and model its parameters. This talk describes the results of some of that effort.

The talk describes how the sensitivity of measuring connector parameters can be increased by using high VSWR and swept frequency measurement techniques. Subjecting the connector to a high VSWR and swept frequency means that at some frequencies the joint will be at a current maximum while at other frequencies it will be at a current null. The experimenter is therefore able to identify the resistive, capacitive, and inductive components of the joint as well as any changes that occur in these components. Experiments on some devices with 14-mm connectors are described. It is shown that the change in reflection coeficient, Γ, for a device with connector instabilities can be up to 4 times greater for the high VSWR environment as compared to the matched or VSWR=1 environment.

A2-5
1520

INTERCOMPARISON OF NBS NOISE STANDARDS

David F. Wait and George Counas
Electromagnetic Fields Division
National Bureau of Standards
Boulder CO 80303 USA

The National Bureau of Standards has constructed a primary noise standard (1 - 12.4 GHz) which operates at liquid nitrogen temperatures that overlaps the frequency coverage of two prior NBS primary noise standards; namely the WR284 (2 - 4 GHz) waveguide primary standard which operates at 419 C, and the WR90 (8 - 12 GHz) waveguide primary standard which operates at 1000 C. This has provided an opportunity to compare two independently developed primary noise standards.

The new coaxial noise standard was used to measure the noise temperature of two WR284 working noise standards at 3.0 GHz and 3.95 GHz (originally calibrated using the NBS WR284 primary noise standard); and four WR90 working standards at 8.2 GHz, 9.0 GHz, and 11.2 GHz (originally calibrated using the NBS WR90 noise standard). The agreement between the old and the new calibrations was within $\pm$ 0.35% for all frequencies.

The typical estimated errors in a calibration measurement, old or new, are similar. Sources of error and approximate estimated contribution to the measurement uncertainty of a working standard are; (a) uncertainty in the output of the standards ($\pm$0.5%), (b) uncertainty in measured power ratios ($\pm$0.5%), (c) mismatch uncertainty ($\pm$0.2% for calibrations of waveguide standards using the old manual comparison radiometers, negligeable with the coaxial standard using the new automated noise comparison radiometer), (d) radiometer nonlinearity ($\pm$0.01%), (e) switch asymmetry in the new automated comparison radiometer ($\pm$0.2%), (f) connector non-repeatability ($\pm$0.8% for the coaxial connectors at the higher frequency, negligeable for the waveguide flange connectors), (g) i.f. offset error ($\pm$0.2%), and (h) random error ($\pm$0.3%).

Interestingly, the difference between the old and the new calibrations is less than the estimated uncertainty caused by either the old or the new primary standard alone. It is on the order of the random uncertainties in the measurement procedures. It is about one third of the connector loss for the coaxial standard operating at the upper frequencies. In other words, the agreement is better than one might expect. Comments on the significance of the close agreement in the intercomparison of NBS primary noise standards will be discussed in this paper.

A2-6
1540

TEST SYSTEM FOR WR-22 BAND NOISE SOURCES

P. E. Nolan, Staff Engineer
Lockheed Missiles and Space Co.
Primary Standards Laboratory
Orgn. 48-75, Bldg. 195A
P. O. Box 3504
Sunnyvale,CA 94088

This facility has recently developed a test system that can accurately determine excess noise ratio for both solid-state and gas-discharge type sources in WR-22 Band at 33 to 50 GHz. Estimated accuracy is +-0.15 dB. Key component in the system is a commercial hot-cold load combination that was adapted for this application. Several aspects of the hot and cold references will be considered.

The ability to make accurate measurements is dependent on various factors associated with the mixer and local oscillator used to down-convert millimeter-wave signals to the IF range. Three methods of reducing the mismatch error caused by mixer input impedance are covered. Characteristics of the local oscillator can also adversely affect measurement results so that consideration should be given to the selection.

The measurements are preferably made in some type of room that is free of interfering sources. Effects on the measurements caused by radiation from an instrument controller and leakage from an RF bridge are discussed.

Verification of system performance was accomplished as part of a measurement assurance program involving other defense contractors and two equipment suppliers.

A2-7
1600

HIGH FREQUENCY TEST METHODS FOR GaAs MMICs: T.H. Miers, D. Williams, V. Hirsch, and M. Brunsman, Ball Aerospace Systems Division, P.O. Box 1062, Boulder, Colorado 80306

Testing strategy and methodology is extremely important for successful realization of GaAs MMICs (Monolithic Microwave Integrated Circuits). Since this is so closely coupled and is invaluable to the design activity and data base generation, it is important that standardized testing with automatic reduction and rapid feedback be integrated with the entire MMIC activity. Accurate and reliable standards and deembedding techniques are required for the data to be useful from a design standpoint. Standard methods and test structures are needed to track and characterize process and material behavior. Well known and accurate testing and deembedding techniques are necessary for device and circuit performance evalution.

Standard Process Control Monitor (PCM) structures compatible with in-process wafer level microwave/millimeter wave parameter evaluation are extremely valuable. These structures must allow testing without the use of through substrate via holes. Therefore coplanar waveguide transmission media is a natural for this application. GaAs devices embedded in coplanar waveguide (CPW) transmission media are useful test structures to determine the high frequency effects of material and process variables upon device behavior. Correlations between material/process parameters and device performance are not well known and these structures are designed for in-process automated testing for generating such a data base. Device modeling and circuit performance predictions are also possible from analysis of CPW FETs or components. This also gives circuit designers a wealth of information for statistical design purposes. Large amounts of high frequency statistical data can be generated from these in-process wafer level test devices.

Wafer level probe and testing techniques for measurement of GaAs devices and circuits at frequencies up to 26.5 Ghz will be presented. Additionally, measurement and deembedding techniques for in-fixture evaluation of GaAS devices and MMIC's for noise parameters up to 26.5 Ghz and S parameters up to 50 Ghz will also be presented.

A2-8
1620

MILLIMETER WAVE NOISE CALIBRATION AND MEASUREMENTS

Peter Tong
Stanford Park Division
Hewlett Packard
1501 Page Mill Rd., 5M
Palo Alto, CA 94304

This paper is separated into 2 parts. The first part is on the theory, methods and accuracies of the calibration of millimeter wave noise sources. The second part describes accurate and automated noise figure measurements at millimeter wave frequencies.

The introduction of two new millimeter wave noise sources, one at 26.5-40 GHz and the other at 33-50 GHz, relies on accurate noise calibration. The computer controlled calibration procedure is based on room temperature and liquid nitrogen loads. It will be described and its accuracy will be elaborated.

The noise sources allow accurate noise measurements. The methods discussed include a simple method which eliminates noise figure contributions of the measurement system and a second method which eliminates errore due to impedance mismatches and the effect of the measurement system noise. This paper also contains techniques and examples of double sideband(DSB) and single sideband(SSB) measurements of passive and active devices.

The figure below shows a typical DSB measurement system with maximum DSB system noise figure of 7.5dB across the whole waveguide band.

Double Side Band Measurement System:

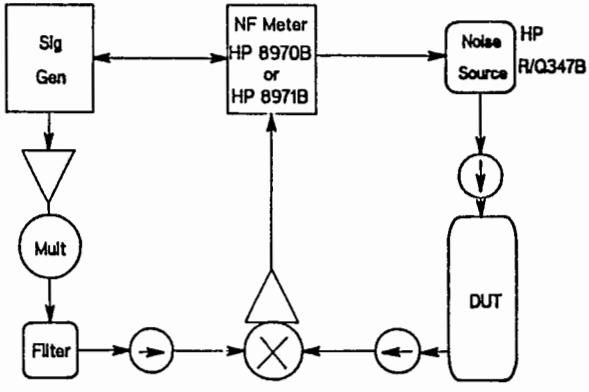

Session B-2 1355-Tues. CR2-28
SCATTERING—I
Chairman: P.L.E. Uslenghi, Dept. of Electrical Engineering and Computer Science, Univ. of Illinois, Chicago, IL 60680

B2-1
1400

SCATTERING FROM PARTIAL SURFACES OF REVOLUTION

M. P. Hurst and L. N. Medgyesi-Mitschang
McDonnell Douglas Research Laboratories
P.O. Box 516
St. Louis, MO 63166

Electromagnetic problems dealing with bodies of revolution (BORs) have been the subject of extensive investigations using a variety of classical, analytical, and more recently, numerical methods. When the Galerkin technique is used with a harmonic circumferential expansion along ϕ, there is modal decoupling in the integral operators. (J. R. Mautz and R. F. Harrington, AEU 32, 159-164, 1978; P. L. Huddleston et al. AP-34, 510-520, 1986.) This coupling is true for conducting as well as for penetrable surfaces or bodies. This highly desirable mathematical property is lost if the problem lacks rotational symmetry.

This paper examines classes of partial surfaces of revolution in the presence of perfectly electrically or magnetically conducting (p.e.c. or p.m.c.) image planes where modal decoupling is preserved by a judicious choice of circumferential basis functions. As an application of the general formulation, a class of surfaces is examined in the context of reflectors in a compact range. The effect of edges on the near-field behavior of these reflectors is discussed.

B2-2
1420

SCATTERING BY A COMPOSITE AND ANISOTROPIC CIRCULAR CYLINDRICAL STRUCTURE: EXACT SOLUTION

H. Massoudi, N.J. Damaskos
Damaskos, Inc., P.O. Box 469,
Concordville, PA 19331
and
P.L.E. Uslenghi
Department of Electrical Engineering and Computer Science
University of Illinois, Chicago, IL 60680

Exact analytical solution for the two-dimentional problem of electromagnetic (EM) scattering by a composite and anisotropic circular cylindrical structure is presented in this paper. The scatterer consists of a metallic cylinder coated by a lossy anisotropic layer and by an impedance sheet. In the anisotropic layer both permittivity and permeability tensors, when referred to principal axes (ρ,φ,z), are biaxial and diagonal. The impedance sheet is also anisotropic and is characterized by a surface admittance tensor $\bar{\bar{\eta}}$. The primary EM sources are either an arbitrarily polarized plane wave, normally incident on the cylinder, or line sources parallel to the axis of the cylinder.

Closed form expressions are derived for the EM fields in the biaxial layer, induced currents on the conducting core and on the impedance sheet, and also the scattered fields in the exterior region. The axial components of the EM fields are expressed in terms of Fourier Series whose terms are products of radial eigenfunctions and azimutal harmonic functions. It is shown that, in the anisotropic region, the radial eigenfunctions satisfy the Bessel differential equation with complex orders.

Curves showing the bistatic scattering cross-section as a function of the scattering angle, for a variety of composite anisotropic geometries, are presented. In addition, the extension of this analysis to EM scattering by a multilayered anisotropic cylinder, for oblique incident, is discussed.

B2-3
1440

ELECTROMAGNETIC SCATTERING FROM NONLINEAR ANISOTROPIC CYLINDERS

M.A. Hasan
Systems Engineering, RCA/ESD
Moorestown, N.J. 08057

P.L.E. Uslenghi
Dept. of Electrical Engineering and Computer Science
University of Illinois at Chicago
Chicago, IL 60680

The solution of the electromagnetic scattering of obliquely incident plane waves from homogeneous, nonlinear anisotropic cylindrical structures is obtained. The medium of the scatterer is characterized by Volterra-type integrals for the electric and magnetic flux density vectors. For the particular case of a nondispersive dielectric medium, the displacement vector $\underline{D}$ reduces to a Taylor series expansion near zero.

The nonlinear problem is solved using both the iteration method and the perturbation method, and the results are compared.

The effect of nonlinearities on the field properties both inside and outside the scatterer, together with the effect on the radar cross section are investigated. A numerically efficient computer code is developed and tested on a variety of scattering media for solid and hollow cylindrical bodies.

It is concluded that the two methods give nearly identical results for small nonlinearities, or if the characteristic dimension of the scatterer is small compared to the wavelength. However, the results obtained using the iteration method diverge from the linear results, with distortion, faster than those obtained by the perturbation method.

B2-4
1500

A UNIFORM GTD TYPE ANALYSIS OF ELECTROMAGNETIC PLANE WAVE SCATTERING BY A FULLY ILLUMINATED PERFECTLY CONDUCTING SEMI-INFINITE CONE

Keith D. Trott
RADC/EECT
Target Characterization Branch
Applied Electromagnetics Division
Hanscom AFB, MA 01731, USA

Prabhakar H. Pathak
The Ohio State University
ElectroScience Laboratory
1320 Kinnear Rd
Columbus, OH 43212, USA

Fredric A. Molinet
Societe Mothesim
Centre de la Boursidiere
92357 Le Plessis-Robinson, France

A uniform high frequency asymptotic solution, based upon the physical optics (PO) approximation, is obtained in the format of the uniform geometrical theory of diffraction (UTD) to describe the fields diffracted by the tip of a semi-infinite perfectly conducting cone when it is fully illuminated by an electromagnetic plane wave. The PO approximation is based upon the use of the geometrical optics (GO) currents on the cone. The solution is expressed in terms of an integral, over finite limits, which can be numerically integrated without difficulty. Previous solutions based upon PO are valid only on the deep shadow side of the reflection shadow boundary (RSB) and become singular at the RSB; however, the present solution is uniform in the sense that it remains bounded and continuous within the transition region adjacent to the RSB. Outside the transition region, the various terms in the integral form of the solution can be interpreted in terms of the geometrical theory of diffraction (GTD) as being associated with the incident, surface reflected, and tip diffracted ray fields. The results from the uniform asymptotic PO solution compare well with previously published results for narrow angle semi-infinite cones (L.B. Felsen, IRE Trans. Antennas and Propagat., AP-5, 121-129, 1957). In addition, the results compare well with measurements and an independent moment method (MM) solution for scattering by a finite flat-backed cone. For the finite cone, several higher order wave interactions are found to be significant; one such interaction is between the tip and the base of the cone. It appears that until now, there were no expressions in the open literature to calculate this tip-base wave interaction even though it was suspected to be important (W.D. Burnside, L. Peters, Radio Sci, Vol 7, No.10, 943-948, 1972). The present work provides the expressions necessary to calculate this interaction and also to confirm its relative importance.

B2-5
1540

ON THE INVERSE SCATTERING BY A PARABOLIC REFLECTOR ANTENNA

A.Z.Elsherbeni, Electrical Engineering Department, University of Mississippi, University, MS 38677
Z.Y.Chen, The Institute of Electronics Academia Sinica, Beijing, China
M.Hamid, Electrical Engineering Department, University of Manitoba, Winnipeg, Canada R3T 2N2
(On leave at the University of Central Florida, Orlando,Florida 32816)

Approximate relations for retrieving the aperture diameter and focal distance of a parabolic reflector antenna are derived from out of band inverse scattering procedure. A detection system consisting of four probes is proposed which could be fixed in position or mounted on a moving platform (e.g. ship or aircraft). The first probe (sending probe) is responsible for transmitting the test plane wave signal, whereas the second probe (sensing probe) is used to correct the orientation of the incident plane wave on the reflector in order to maintain normal incidence by maximizing the back scattered signal at a specific wavelength. At frequencies much lower than the operating frequency of the reflector feed, the main re-radiation lobe from the reflector due to the test plane wave signal, is found to be broad, therefore the remaining two receiving probes should be highly directive. An incident plane wave with a low frequency relative to the operating frequency of the feed horn is employed. Numerical results are presented to illustrate the method and to show that while it does not require any time domain or phase measurements, highly accurate scattering data are necessary, especially if the observation angles of the receiving probes are close to each other. The method is yet to be extended to arbitrary polarization, wave type and direction of incidence as well as to other types of antennas.

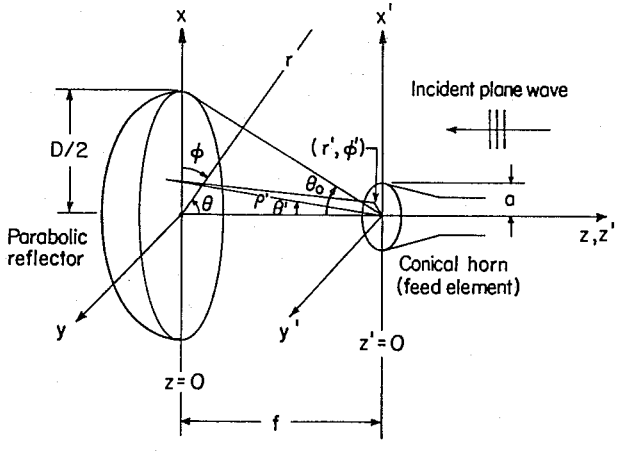

B2-6
1600

Response of a Souce in a Composite Medium

W.C. Chew
Department of Electrical and Computer Engineering
University of Illinois
Urbana, IL 61801

We will discuss the solution to the problem of the radiation of a source on top of a composite half space where the inhomogeneity is varying in two dimensions, and the field is varying in three dimensions. This represents a two-and-one-half dimensions problem.

To solve this problem, we divide the inhomegeneity into layers, whose whose electromagnetic parameters are varying in one dimension. The eigenmodes in each layer is found by a one dimensional finite element method. Then boundary conditions at the interface between the layers are matched. From the boundary conditions, we define transmission and reflection operators at each interface. With the available of these reflection and transmission operators, we can gain a physical feel for the scattering process at each interface. Because of this, we can write down the propagation of waves through many layers of the medium easily, and also the solution of a source in such a medium.

We will illustrate the applications of this solution in geophysical sensing and integrated optics.

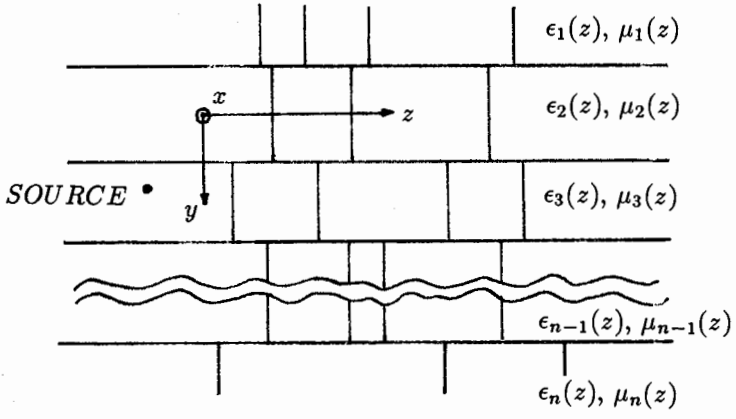

B2-7
1620

CURRENT INDUCED ON AN INFINITELY LONG CONDUCTING CYLINDER RESIDING ON A GROUND PLANE DUE TO AN INCIDENT PLANE WAVE

T.C.K.Rao,Electrical Engineering Department,University of Lowell
Lowell,MA 01854.
R.Barakat,Division of Applied Sciences,Harvard University
Cambridge,MA 02138.

An exact solution for the problem of plane wave scattering by an infinitely long conducting cylinder that is situated on the surface of a perfectly conducting ground plane is presented.The total field consists of contributions from the incident field,the reflected field and the scattered fields from the cylinder and the image cylinder.By employing the addition theorem for the cylindrical waves,a set of two coupled infinite system of equations for the even and odd expansion coefficients is obtained.These coefficients are numerically evaluated by a matrix inversion procedure.The induced current is calculated from the coefficients for the case of an obliquely incident plane wave of the TM type.The magnitude of the current is plotted as a function of the angle of incidence and the electrical radius of the cylinder as shown in the Figure.

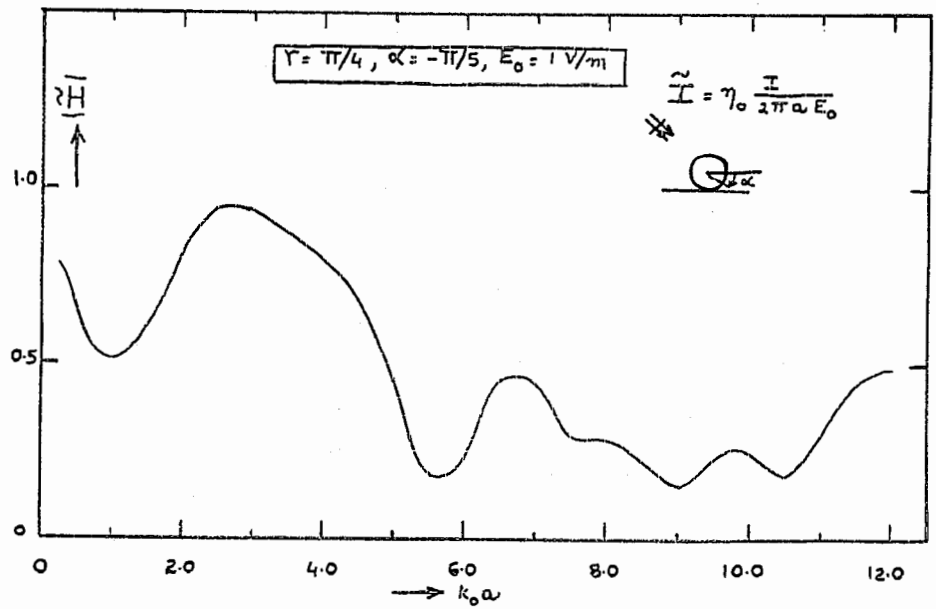

B2-8
1640

EM SCATTERING BY BURIED OBJECTS OF LOW CONTRAST

David A. Hill
Electromagnetic Fields Division
National Bureau of Standards
Boulder, Colorado 80303

The plane-wave, scattering-matrix formulation provides a convenient means for combining antenna, scattering, and interface effects that arise in detection of buried objects [D.A. Hill and K.H. Cavcey, IEEE Trans., GE-25, 422-431, 1987] However, it requires the full plane-wave scattering matrix [D.M. Kerns, Plane-Wave Scattering-Matrix Theory of Antennas and Antenna-Antenna Interactions, National Bureau of Standards Monograph 162, 1981] for the buried object for all incident and scattered plane waves. For scatterers of arbitrary shape where numerical methods are generally required to determine the scattering characteristics, this requires a large amount of computation.

In this paper we use the Born approximation to obtain an approximate expression for the scattering matrix of the buried object in terms of an integral over the volume of the object. For simple shapes (such as a sphere, a circular cylinder, or a rectangular box), the volume integral can be evaluated analytically to obtain a closed-form expression for the scattering matrix. The Born approximation requires small contrast between the electrical properties of the buried object and the earth. This requirement is restrictive, but the low-contrast case is important because it represents a difficult detection situation.

We present numerical results for scattering by buried spheres, cylinders, and boxes for plane-wave incidence. Far field results are obtained by asymptotic methods, and near field results are obtained from two-dimensional fast Fourier transform (2D FFT). The advantages of 2D FFT are speed and simplicity, and Sommerfeld integrals are avoided. Only a portion of the scattering matrix is used for plane-wave incidence, but the total scattering matrix will be useful when the buried scatterer is illuminated by a realistic near-field source.

B3-1
1400

COUPLED LINE MODEL FOR MULTIRESONATOR WIDEBAND MICROSTRIP ANTENNAS

K.C. Gupta and Brian Bandhauer
Dept. of Electrical and Computer Engineering
University of Colorado
Boulder, CO 80309-0425

Various multi-patch configurations of rectangular shaped microstrip antennas have demonstrated [Kumar and Gupta, IEEE-APS International Antenna Propagat. Symp., Houston, 1983] considerably larger bandwidth than that obtained from single patch configurations commonly used. Out of the various configurations proposed, a multipatch arrangement with the patches coupled along the non-radiating edges [Kumar and Gupta, IEEE Trans. AP-33, 1985] is attractive as its size can be made very compact by reducing the widths of the individual patches. When the widths of these patches become small, the capacitive coupling alone (as considered in the previous work) is not sufficient to provide an accurate analysis.

This paper proposes a coupled line model for multiple patch microstrip antenna configurations wherein the adjacent patches are gap-coupled along the non-radiating edges. The case of a two-patch configuration is considered in detail. A four-port network model for a coupled microstirp section is taken as the basic building block of the equivalent network model. When the two patches are of unequal length, the extra length of one of the patches is accounted for by an additional capacitance at the corresponding end of the coupled line section.

Detailed computed results for two-patch antennas based on the proposed model will be presented. Current experiments performed to verify the proposed model will be reported.

B3-2
1420

AN INVESTIGATION OF THE IMPEDANCE OF REACTIVELY LOADED MICROSTRIP ANTENNAS

Stuart A. Long and Ajaz Ali Khan
Department of Electrical Engineering
University of Houston
Houston, Texas 77004

In the past, printed-circuit or microstrip antennas have proven to be quite versatile and have been used in a wide variety of applications. Their main advantages include structural simplicity, ease of construction, ruggedness, conformability, low profile, and low cost. In some applications, however, it would be quite desirable to be able to exert some control over the impedance of the element without affecting the pattern or the resonant frequency. This feature would be most valuable for use in a scanned phased array to alter the active array impedance of the elements to compensate to some degree for scan blindness. This investigation has shown that such an element can be designed through the use of suitably placed reactive loads.

Using previous theoretical work (W.F.Richards and Y.T.Lo, Electromagnetics, 3, 371-385, 1983), it is seen that the input impedance can be varied with a single short-circuit load without altering the resonant frequency. This impedance can be varied for a fixed feed location by the movement of the nodal line of the loaded resonant mode as the position of a short-circuit load is varied. The results indicate that a single short circuit placed on the proper locus can provide the required modification. Movement of the short circuit along this path can then be used to adjust the resonant resistance over a wide range of values. Unfortunately this rather simple structure tends to produce levels of cross polarization that can be undesirable in some applications. The use of a pair of symmetrically located loads can be used instead to eliminate this cross polarized component and, as an added advantage, allows even further flexibility in impedance control.

The proper loci for load positions have been calculated and plotted, and several configurations have been fabricated and tested. In each case good agreement was found between theory and experiment.

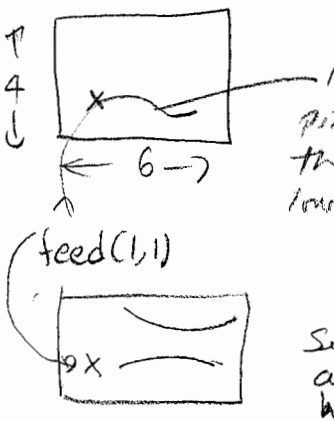

B3-3
1440

ANALYSIS OF COMPOUND SLOTS

Sembiam R. Rengarajan
Department of Electrical and Computer Engr.
California State University, Northridge
Northridge, CA 91330

This paper presents a mathematical model to analyze broad wall compound slots, having an offset from the center line and a tilt angle with respect to the longitudinal axis of rectangular waveguides. Figure shows the geometry of the problem. The slot is imbedded in an infinite planar conductor. The electric field in the slot is expanded in terms of entire domain sinusoidal functions in the longitudinal direction with a constant transverse distribution. The internal fields are in terms of Stevenson's Green's functions and the external terms are those of half space. Wall thickness is rigorously accounted for by considering a waveguide between inner and outer apertures.

400,000 terms!

Compound slots are used in antenna array applications as radiating elements or coupling slots between main line and branch line guides. Their analysis has been complicated by the mathematical and computational work involved and hence antenna designs are presently relying on experimentally measured data. Numerical results presented in this work have considerable practical application.

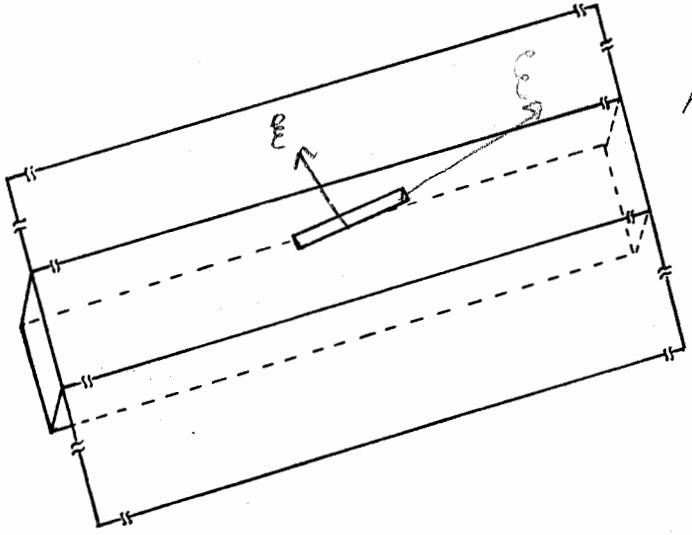

Can ignore E_ϕ
Match only H_{long}

Compound ≡ offset and inclined

Elliott says this is very important result and experimental approaches are very lengthy

B3-4
1500

PLANAR ARRAY EXCITATIONS TO PRODUCE FLAT-TOPPED BEAMS

R.S. Elliott and Y.U. Kim
Department of Electrical Engineering
University of California
Los Angeles, CA 90024

The advent of satellites has spawned the growth of antennas whose patterns can cover a portion of the earth's surface (e.g., the U.S.) more or less uniformly. Conventionally, this is done with a cluster of horns feeding a parabolic dish, with the pencil beams due to the individual horns forming an overlapping two-dimensional mosaic on the targeted area. Disadvantages of this approach are a ripple in the coverage of about 3 dB, no control over the side lobes, and a modest aperture efficiency.

Potentially, a properly excited planar array can overcome all of these shortcomings. This paper addresses the question of pattern synthesis for such arrays. A modification of Orchard's technique (H.J. Orchard, et al, IEE, Part H, 132, 63-68, 1985) is used to generate a pattern with a flat-topped beam, controlled ripple, and controlled side lobes, due to an equispaced linear array. The requisite excitation is used as the collapsed distribution for the planar array. With the aid of a Baklanov transformation one can then deduce the two-dimensional excitation. An example will illustrate the procedure.

Overlap of pencil beams (from feeds in a reflector) gives about 3 dB ripple

Can reduce planar array array factor to that of the form of a linear array to one pattern cut,

To extend to other pcuts consider rect. array 2N x 2N let $W = \cos u \cdot \cos v$ (Baklanov) gives a one variable polynomial (cw).

Yahya cautioned that multiple beam design is different from contoured beam design which Elliott is attacking.

B3-5
1520

ANALYSIS OF A CYLINDRICAL ANTENNA INSIDE A HOLLOW, INFINITELY LONG, CONDUCTING CYLINDER – WITH EXPERIMENTAL VERIFICATION

Anthony Q. Martin and Chalmers M. Butler
Department of Electrical and Computer Engineering
Clemson University, Clemson, SC 29634-0915

A solution technique is presented for the current induced on a cylindrical antenna residing coaxially within a hollow, infinitely long, conducting cylinder of circular cross section. The analysis begins with an integral equation formulated in terms of the magnetic vector potential Green's function for an axially-directed dipole inside the cylindrical tube. This Green's function consists of an infinite series of Sommerfeld-type integrals whose integrands comprise combinations of Bessel functions. With circularly symmetric excitation and when the antenna and cylinder axes coincide, the series simplifies to a single term (a Sommerfeld integral). When the antenna is not too long electrically, the integral equation can be solved by standard numerical methods. These methods employ either real-axis integration or integration along an alternate contour when the integrand possesses real-axis singularities.

The accuracy of the integral equation solution is verified through comparisons with measured data. Measurements are performed below the cutoff frequency of the (empty) cylindrical tube, allowing substitution of the infinite-length tube by one of finite length. Measured and computed data are presented for the current and charge induced on the inner wall of the conducting cylinder. Data for the driving point-admittance of thin-wire and sleeve-fed antennas are presented. Preliminary results reveal that the integral equation solutions are very accurate.

B3-6
1540

COMPUTATION OF THE FIELD DUE TO A CYLINDRICAL ANTENNA INSIDE A CONDUCTING CYLINDRICAL TUBE

Anthony Q. Martin and Chalmers M. Butler
Department of Electrical and Computer Engineering
Clemson University, Clemson, SC 29634-0915

For a cylindrical antenna residing coaxially within a hollow, infinitely long, conducting cylinder, we present a comparison of techniques for computing interior fields. The field components are expressible in terms of a direct contribution due to the antenna and a reflected contribution due to the cylinder. While the reflected contribution is computed from a Sommerfeld-type integral, the direct contribution can be expressed either as a Sommerfeld integral or as an integral over the antenna current. The disadvantages of numerically evaluating the former is that the integrand is oscillatory and that the convergence can be slow. Also, the presence of a factor containing Bessel functions makes difficult the application of techniques to address the oscillations. The disadvantage of numerically evaluating the latter integral is that the integrand can be unbounded or highly peaked at various locations within the range of integration. The findings of an investigation of the relative merits of the two computational methods are presented. The results of these computations are supported by measured data.

B3-7
1600

IMPLEMENTATION OF A HYBRID METHOD FOR COMBINING FULL WAVE AND QUASI-STATIC METHODS IN ANTENNA PROBLEMS Bob

P. D. Mannikko and R. G. Olsen
Electrical and Computer Engineering Department
Washington State University
Pullman, WA 99164-2752

Recently, a hybrid method for the analysis of electromagnetic problems involving electrically small but geometrically complex sub-regions was presented (R. G. Olsen and G. L. Hower, "On the Use of Quasi-Static Techniques in Electrically Small Regions of Electromagnetic Problems", 1987 National Radio Science Meeting Digest, p 127) . The method provides a detailed electrical description of the electromagnetic fields in the complex sub-region. This information is useful for analyzing the breakdown properties of antenna loads and is not available from codes which treat these sub-regions as lumped elements. The analysis involves the simultaneous solution of integral equations for both the quasi-static and full wave regions while accounting for the mutual coupling between the different regions.

The method has since been numerically implemented using moment method techniques for axially symmetric wire antennas with "capacitive like", electrically small loads which may consist of conductors and dielectrics. Results are given for several geometries including capacitor loaded and top hat loaded antenna configurations. Wherever possible, input impedance and current distributions are compared with results from existing wire antenna codes.

Can correct MINIMEC using an effective length of h+a (monopole over perfect ground plane).

Nat. Rad. Sci. Meet. Jan. 1988

B3-8
1620

EFFECTS OF RANDOM ERRORS ON REFLECTOR SURFACE COMPENSATION USING ARRAY FEEDS

Y. Rahmat-Samii
Jet Propulsion Laboratory
California Institute of Technology
Pasadena , CA 91109

To overcome the deteriorating effects of thermally (or gravitationally) slowly varying reflector surface distortions, arrays in the focal plane of reflectors can be used. The complex excitation coefficients of the array are typically obtained using a focal plane conjugate field match concept. This is achieved by utilizing a vector diffraction analysis approach which results in the determination of the complex excitation coefficients by requiring both the gain and sidelobe control and by incorporating the knowledge of the surface distortion.

Once the complex excitation coefficients are determined they are then used to set the attenuators and phase shifters for each element. The reflector is subsequently illuminated by the array with the adjusted excitation coefficients to result in the improved performance. In practice, however, the array excitation coefficients may not be set exactly and there will be random and systematic errors in setting the attenuators and phase shifters.

In this paper, the effects of random errors on the reflector performance are studied by using numerical simulations in generating random errors for both the amplitude and phase excitation coefficients of the array. It is shown that for specified thermal distortions of an offset reflector antenna how much random errors can be tolerated. Results of many simulations will be presented for different antenna configurations, array geometries and random error specifications. The results of this investigation will be useful in defining practical error bounds for the application of the surface compensation techniques and in performing meaningful measurements.

D2-1
1400

ADVANCES IN QUASI-OPTICAL MILLIMETER-WAVE INTEGRATED CIRCUITS

Tatsuo Itoh
Dept. of Electrical and Computer Engineering
The University of Texas
Austin, TX 78712

Traditionally, microwave and millineter-wave components have consisted of distinctly separate components such as antennas, mixers, diplexers, amplifiers and oscillators. Recently, these compnents are built in an increasing degree in a planar form in preference to a waveguide format. Many of these planar components constructed in hybrid or monolithic forms are more cost effective and more flexible in design than their waveguide counterparts. However, the RF front ends such as the mixers and transmitters are usually connected to external antennas. As the frequency of operation is increased, the loss caused by transmission medium between the antenna and the front end increases significantly. An alternative approach is to fabricate an antenna directly integrated onto the planar substrate. In this scheme, it is possible to create a mixer and an antenna integrated into a single element. These mixers are called the quasi-optical mixers. The output port of the antenna and the RF input port of the mixer are indistinguishable and usually not accessible.

In addition to the quasi-optical mixers, there is an emerging technology to create planar quasi-optical structures that perform othere "active' functions such as frequency-multiplying, control and amplification. Technology for quasi-optical planar components is still not matured and a number of trials and new concepts are experimented. This talk summarizes some of the recent development in this area of research. The technology summarized here is not only useful at higher frequencies but also is believed to be available for low cost component development.

D2-2
1440

NOVEL INTEGRATION OF A COPLANAR WAVEGUIDE FED MICROSTRIP ANTENNA WITH AMPLIFIER*

P. Aoyagi, J. Brenneman, S.L. Chuang and Y.T. Lo
Department of Electrical and Computer Engineering
University of Illinois at Urbana-Champaign
Urbana, IL 61801

Microwave integrated circuits using coplanar waveguides with microstrip antennas are investigated experimentally. We consider a hybrid integration of microwave amplifiers, and matching networks using coplanar structures and coplanar-fed microstrip antennas. In particular, the possiblity of integrating microwave amplifiers (realized entirely with coplanar line) electromagnetically with microstrip antennas is demonstrated. This novel configuration should prove useful for MMIC phased array integration.

As a preliminary test of the integration between a microstrip antennas and coplanar line structures, a 4.0 GHz single element microstrip antenna array was interfaced via proximity feed to a microwave amplifier realized on coplanar line. The diagram below shows a successful integration scheme with the amplifier. Our results show that the amplifier adds approximately 13 dB gain in the radiation pattern over that without the amplifier.

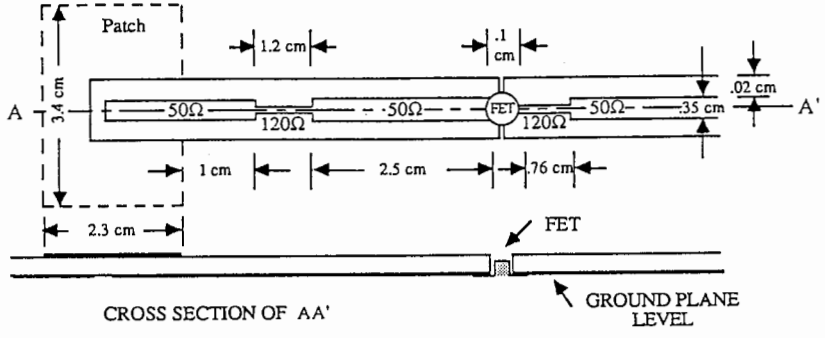

D2-3
1500

INTEGRATED OPTICAL DEVICES*

S. L. Chuang
Department of Electrical and Computer Engineering
University of Illinois at Urbana-Champaign
1406 W. Green Street
Urbana, IL 61801-2991

Integrated optical devices and their applications to microwave modulation will be discussed. These include semiconductor lasers, optical directional couplers, quantum-well electro-optical modulators and superlattice photodetectors.

Based on an improved coupled-mode theory derived from a generalized Lorentz reciprocity theorem (S. L. Chuang, J. Lightwave Technol., LT-5, 5-15 and 174-183, 1987), optical directional couplers and optical filters have been investigated theoretically and the results agree very well with those for the experiment.

New designs of electro-optical modulators using intersubband optical transitions in quantum-well structures have been proposed. The optical absorption properties of a quantum-well structure are controlled by an external bias field. The optical power output is thus modulated by the applied electric field. Our theoretical prediction (D. Ahn and S. L. Chuang, Phys. Rev. B, 35, 4149-51, 1987) was recently confirmed by experiment (K. Bajema et al, Phys. Rev. B, 36, 1300, 1987).

A novel design of superlattice photodetectors has also been proposed (S. L. Chuang and K. Hess, J. Appl. Phys. 59, 2885-94, 1986). Some recent experiments also confirm our early prediction of the physical mechanisms of the device.

A general overview of these integrated optical devices especially novel devices using quantum-well structures and their microwave modulation will be presented. Possible future research in this area will be discussed.

Session F/B-1 1335-Tues. CR1-46
RANDOM MEDIA THEORY/MEASUREMENT
Chairman: Gary S. Brown, Bradley Dept. of Electrical Engineering, Virginia Polytechnic Institute and State Univ., Blacksburg, VA 24061

F/B1-1
1340

AN ASYMPTOTIC FORM OF THE FLAT SURFACE IMPULSE RESPONSE FOR LARGE OFF-NADIR POINTING ANGLES

Gary S. Brown
Bradley Department of Electrical Engineering
Virginia Polytechnic Institute and State University
Blacksburg, Virginia 24061

The flat surface impulse response is an important ingredient in describing how a short pulse radar altimeter responds, in the mean, to a rough surface. It includes all effects except those due to the radar pulse shape, tracking loop jitter, and the range spread of the surface roughness. One of the most important included characteristics is the pointing angle of the radar antenna relative to nadir. In a previous paper [G.S. Brown, IEEE Trans. Antennas & Propag., AP-25, 67-74, 1977] an analytic expression for the flat surface impulse response involving an infinite series of Bessel functions was derived to describe the effects of a nonzero pointing angle. This series reduces to essentially one term when the pointing angle is less than one antenna beamwidth. However, when the pointing angle becomes large. such as the case with a multiple beam altimeter, a very large number of terms in the full Bessel function series must be retained. Although this can be done via downward recurrence, it is time consuming process. In this paper, the integral giving rise to this series is reexamined and the large angle problem is identified and explained. By expanding this integral about a point of maximum contribution, we are able to derive a much more compact (closed form) result. We compare this result with conventional radar formulas based on an illuminated area established by the antenna beamwidth and the slant range cell size due to the radar pulsewidth. We emphasize the approximations that must be satisfied in order for this approximation to give essentially the same result as the Bessel series.

F/B1-2
1400

BACKSCATTER ENHANCEMENT FROM SPARSELY DISTRIBUTED LARGE PARTICLES WITH ROUGH SURFACES

Ezekiel Bahar and Mary Ann Fitzwater
Electrical Engineering Department
University of Nebraska-Lincoln
Lincoln, NE 68588-0511

The incoherent diffuse specific intensities (modified Stokes parameters) backscattered from a parallel layer consisting of sparse random distributuions of finitely conducting particles with smooth and rough surfaces are evaluated. The normally and obliquely incident excitations at infrared and optical frequencies are vertically or horizontally polarized. The particle surface roughness, which is characterized by its joint probability density function, is assumed to be sufficiently rough in order to significantly effect the diffuse specific intensities. Thus, the full wave approach is used to determine the phase matrix as well as the extinction coefficient that appears in the equation of radiative transfer. The enhanced backscattered intensities that depend upon the particle surface roughness are compared with the enhanced backscatter that is associated with Mie scattering from smooth spherical particles. The enhanced backscattered diffuse specific intensities are evaluated for different particles sizes, complex permittivities, roughness parameters and excitations. The effects of varying the optical thickness of the layer are also considered. Since the enhanced backscatter phenomenon reported here is primarily due to the particle surface roughness it appears in both the first order and the multiple scatter solutions of the radiative transfer equations.

F/B1-3 PROPAGATION OVER IRREGULAR INHOMOGENEOUS TERRAIN*
1420

R. M. Bevensee
Lawrence Livermore National Laboratory
Livermore, California 94550

Recently an article entitled "Propagation Over an Inhomogeneous Irregular Surface," (Z. Wu, T. S. M. Maclean, D. J. Bagwell, and M. J. Mehler) was submitted to Radio Science. In it the authors show how to compute the surface field launched by a vertical current source with one Volterra integral equation derived from the Compensation Theorem. Furthermore, they compute the total ground wave (space wave and surface wave) in a manner which allows for cliff-type surface discontinuities. The assumptions, including the usual neglect of backscatter, appear not to be serious. Computations of field over homogeneous surfaces with cliff-type discontinuities show very good agreement with measurements over long distances from the discontinuities.

We will compare this work with the Compensation-Theorem formulation of the writer, which presently treats TM_ρ surface wave propagation over irregular inhomogeneous terrain and requires the solution of three Volterra integral equations to obtain the surface field at a distant point. In particular, we will consider the possibility of modifying this formulation to describe the total ground wave (space wave and surface wave) and also cliff-type discontinuities.

We will also describe the modified formulation for TE_ρ surface wave propagation due to a horizontal current source.

F/B1-4
1440

SOME NEW RESULTS IN RANDOM-MEDIUM BACKSCATTERING

David A.de Wolf
Bradley Dept.of Electrical Engineering
Virginia Polytechnic Inst. and State U.
Blacksburg, VA 24060

Inspired by the phase-screen approach of C.L.Rino (J. of Wave-Mat. Int., 1, 181-204, 1986), we have re-examined the problem of wave propagation and scattering in a random medium with weak extended fluctuations of refractive index. As in Rino's work, we include backscatter effects by working with the scalar wave equation rather than its parabolic approximation. We employ Bremmer's forward- and backward-wave operator formalism to recast the wave equation into two pseudo one-dimensional equations, and then solve for first and second moments (average field and mutual coherence).

The results for the mutual coherence are of particular interest. Four first-order differential equations are obtained for the four squared flux quantities that can be formed from the forwards and backwards fields. These are solved for zero and for nonzero transverse separation of observation points, and in the former case they incorporate energy conservation and reduce to the usual result when backscatter is ignored. The connection with backscatter enhancement is discussed. The interpretation appears to differ from previous results.

F/B1-5
1500

A SPATIAL FILTERING TECHNIQUE FOR REMOVING PHASE ERRORS IN AUTOMATED BISTATIC SCATTERING MEASUREMENTS

Marc G. Cote
Rome Air Development Center
Applied Electromagnetics Division
Target Characterization Branch
Hanscom AFB, MA 01731

A spatial filtering scheme for removing phase errors in electromagnetic scattering data is examined experimentally and theoretically. Measuring the coherent narrowband plane-wave scattering pattern of an object (target) as a continuous function of bistatic angle is problematic because the direct coupling between the transmit and receive antennas may dominate the total field. This problem can be alleviated in many cases by using a background subtraction technique. The technique requires measuring the amplitude and phase of the total electric field with and without the target. Subtracting the background field, i.e. the field without the target, from the total field with the target leaves the scattered field of the target, provided multiple interactions between the target and its surrounding are negligible. Gross uncertainties in the resultant data can arise from small errors in the phase of the background data if the target scattered field is small relative to the background. We will show that, for a -10 dB target-to-background ratio, a 0.5 degree phase error produces a 10% uncertainty in the amplitude of the electric field scattered by the target. This uncertainty shows up as high frequency variations in the target scattering pattern. To remove this uncertainty we filter the data applying the natural $k(a + \lambda)$ spatial frequency band limit common to ordinary radiating objects (L. J. Chu, J. Appl. Phys., vol. 19, pp. 1163-1175, Dec. 1948). This bandlimited filtering scheme allows us to make accurate automated bistatic scattering measurements of targets with regions of low scattering. Scattering measurements with and without filtering will be compared to theoretically predicted scattering for a number of targets.

National Radio Science Meeting
Jan 1988

F/B1-6
1540

MEASURED SIGNAL DEGRADATION EFFECTS BY ROADSIDE TREES AT UHF AND L-BAND FOR MOBILE SATELLITE SYSTEMS

Julius Goldhirsh
The Johns Hopkins University/Applied Physics Laboratory, Johns Hopkins Road, Laurel, Maryland 20707
Wolfhard J. Vogel
The University of Texas at Austin,
10100 Burnet Road, Austin, Texas 78758

During June 1987, the Applied Physics Laboratory of the Johns Hopkins University and the Electrical Engineering Research Laboratory of the University of Texas at Austin performed a fifth in a series of propagation measurements related to planned Mobile Satellite Systems (MSS). The previous four experiments involved transmitter platforms represented by remotely piloted aircraft (static measurements) and helicopters (static and dynamic measurements), and the receiver and data acquisition systems were located on a van operated by the University of Texas [W.J. Vogel and J. Goldhirsh, IEEE Trans. Antennas and Prop., AP-34, 1460-1464, 1986; J. Goldhirsh and W.J. Vogel, IEEE Trans. Antennas and Prop., AP-35, 598-596, 1987]. Fundamental aims of these previous helicopter measurements were to assess the cumulative fade distributions at UHF for a geometry in which the van was in motion and roadside trees contributed shadowing effects. They were made in Central Maryland only at UHF (870 MHz) and during the October 1985 and March 1986 periods. The former periods represented a time in which the deciduous trees contained small moisture contents as the leaves were in the process of falling (approximately 80% of full blossom) in October and the trees were bare in March.

The June 1987 measurements, which are the subject of this paper, were also implemented in Central Maryland and replicated the geometries and road configurations of the previous two helicopter-van tests. The major differences were: (1) Both UHF (870 MHz) and L-Band (1.5 GHz) were simultaneously transmitted, and (2) deciduous trees were in full blossom having larger moisture contents than during previous tests. Measurements at the L-band frequency were a result of the recent FCC ruling that this band (in the vicinity of 1.5 GHz) be used for the planned MSS system. In this paper, cumulative fade distributions at L-band and UHF are described for typical roads and for various fixed elevation angles and distances between the van and the helicopter. These distributions are compared to previous roadside fade results made in the absence of leaves and the effects of foliage are described. Enhanced attenuations at L-band relative to the UHF measurements are also characterized.

F/B1-7
1600

UHF FADING IN FACTORIES

Theodore S. Rappaport and Clare D. McGillem
Engineering Research Center for Intelligent Manufacturing Systems
School of Electrical Engineering
Purdue University
West Lafayette, IN 47907

There has been much interest recently in characterizing UHF propagation in and around houses and office buildings (S.E. Alexander, Elec. Letters, 19;20,860,1983; D.C. Cox, R.R. Murray, A.W. Norris, BSTJ,62;9,2695-2717,1983 and BSTJ,63;6, 921-954,1984; D.M.J. Devasirvatham, IEEE Trans. A.&P., AP-34;11,1300-1308,1986; R.J.C. Bultitude, IEEE Comm. Mag.,25,6,5-12,1987). Rappaport and McGillem have recently reported propagation measurements at 1300 MHz in factories (T.S. Rappaport, C.D. McGillem,Elec. Letters,23;19,1015-1017,1987).

In this paper, we detail the measurement apparatus and the experiments performed to characterize narrow band fading within five large and fully opeational factories. It is believed that such propagation measurements have not been available previously in the literature. The propagation experiments are designed to determine path loss, shadowing, small scale spatial fading, and temporal fading of the factory radio channel. It is found that most line of sight (LOS) paths exhibit gain over free space path loss whereas obstructed (OBS) paths have power fall off as distance to the 2.8 power. Local area fading is found to be primarily Rayleigh, although Rician and Log-normal distirbutions fit some of the data well. Temporal fading appears to be Rician with K=10 dB.

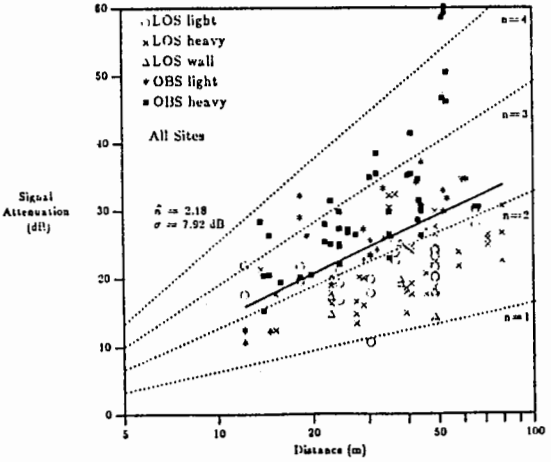

Large scale path loss at all sites.

F/B1-8
1620

SECOND MOMENT ESTIMATES FROM A METEOROLOGICAL RADAR

Janet S. Gibson
Michael J. Carpenter
National Oceanic and Atmospheric Adminstration/ERL
Wave Propagation Laboratory
Boulder, CO 80303
and
National Center for Atmospheric Research
Boulder, CO 80307

ABSTRACT

Spectral moment estimation is of importance to radar meteorologists for several reasons. Zero moment estimates measure average power received by the radar. This can be related to total liquid water content within the pulse volume by an assumed drop size distribution. First moments are estimates of Doppler mean velocity and thus can give the meteorologist information on particle speed, and direction from which wind is inferred. Second moment estimates lead to information on turbulent dissipation rates and wind shear.

This paper describes and compares the results of two signal processing techniques used to compute spectral moments in a meteorological pulsed Doppler radar system operated by the Wave Propagation Laboratory, Environment Research Laboratories, NOAA, in Boulder, Colorado.

Signal transmission, data acquisition, real time processing of the returned echo from the analog-to-digital converter through a pulse pair processor, and the current post spectral analysis techniques used are reviewed briefly. Post spectral analysis techniques included are a pulse pair algorithm and a discrete fast Fourier transform method. These two methods are used to estimate mean Doppler velocity, average power received, power spectral density, and spectral width. The results of processing simulated by the two methods are compared for various ranges of spectral widths and various signal to noise ratios. The resulting biases are explored.

F/B1-9
1640

CALCULATION BY NUMERICAL INTEGRATION OF DIFFRACTION ATTENUATION AT VHF AND UHF

J. H. Whitteker
Communications Research Centre
3071 Carling Avenue
P.O. Box 11490, Station H
Ottawa, Canada
K2H 8S2

The Communications Research Centre has a computer program (J.H. Whitteker, IEEE Int. Conf. Communications, 44-48, 1983) that predicts propagation attenuation at VHF and UHF over terrestrial paths, using a topographic data base. For the calculation of diffraction attenuation, the terrain is modelled as a small number of circular hills to which known solutions are applied. While the results are usually good, they are sometimes inaccurate because the terrain has been over-simplified, and because the theory available for more than one obstruction has limited validity.

A new method of calculation has been worked out which applies approximate diffraction theory (Fresnel approximation) to a terrain model that retains most of the complexity of the real terrain. (A preliminary version was reported on at this conference two years ago.) The terrain is modelled along the propagation path simply by connecting the given terrain points with straight lines. The earth may be imperfectly reflecting, and may also be assigned a roughness. The classical solutions of the diffraction problem are not used. Instead, a new solution is found for each path profile starting from elementary principles, making the calculation a kind of numerical simulation. The method is to find the radiowave field as a function of height above each terrain point by integrating over the field above the preceding terrain point, using Huygens' principle for both direct and reflected waves.

The method of calculation has been tested against rigorous diffraction theory (residue series) in the special case of a smooth spherical earth, on paths up to 100 km, with agreement to 2 dB. It has also been tested for up to 40 collinear equally spaced knife edges (no reflection) and the results agree with a result by Lee (J. Math. Physics, 19, 1414-1422, 1978) and Vogler (Radio Sci. 17,1541-1546, 1982) to well within 2 dB. Verification of reciprocity has been also made for simple asymmetrical paths, with agreement to a few decibels. Finally, comparisons have been made with measurements on real paths, with mixed results. The accuracy seems to be limited by uncertainties in the terrain.

Since the field must be found at many points, the algorithm requires much more computer time that the one mentioned in the first paragraph. However, efforts to eliminate unnecessary steps in the calculation are expected to result in a program with acceptable speed.

Session G-2 1355-Tues. CR2-26
IONOSPHERIC PROPAGATION
Chairman: Gary Sales, Univ. of Lowell, Center for Atmospheric Research, Lowell, MA 01854

G2-1
1400

MODELING OF HIGHLY IRREGULAR PROPAGATION PATHS AT VLF AND LF

F. Perry Snyder
Ocean and Atmospheric Sciences Division (Code 544)
Naval Ocean Systems Center
San Diego, CA 92152-5000

Global longwave propagation is often modeled using a waveguide model formulation wherein a naturally or artificially produced irregular earth-ionosphere waveguide is accommodated by modeling the propagation path as discrete homogeneous segments of some appropriate definition. The mode summation is found by matching the mode fields across the discontinuities between the various consecutive slabs - a procedure commonly called mode conversion. Reported computational procedures usually employ one of two possible mode conversion formulations. Although both formulations use full wave modal solutions, one matches electromagnetic field components (numerically obtained) throughout the entire height range of the guide, resulting in an orthogonal set of modal height gain functions. The other matches electromagnetic field components (analytically defined) only throughout the height region below ionospheric elevations, resulting in an "almost orthogonal" set of modal height gain functions. The use of numerically obtained field components provides an exact formulation but is very computer run-time intensive. The analytic forms, although resulting in an approximate formulation, are very fast on the computer.

Apparently quite accurate under most conditions, the bounds of the validity of the approximate mode conversion formulation has never been clearly shown. Also, the approximate formulation has been recently found to exhibit numerical instabilities, resulting in sharp discontinuities in the computer field strength. These instabilities appear most frequently associated with the higher frequencies into the LF band and with naturally or artificially stressed ionospheres.

The validity bounds as well as the occurrence of instabilities in the approximate formulation has been investigated and the results are reported. A controlling factor is found to be the departure of the analytic forms for the height gains from the numerically obtained full-wave forms near ionospheric evaluations. Some potential procedures to circumvent the failure of the approximate procedure while maintaining good computer efficiencies is discussed. Longwave propagation modeling based on a mixed application of the two mode conversion forms is also described.

G2-2
1420

ALFAN2: A SECOND EXPERIMENT TO MEASURE TE & TM RADIO NOISE IN THE EARTH-IONOSPHERE WAVEGUIDE

A.C. Fraser-Smith[1], J.P. Turtle[2], P.R. McGill[1], and R.A. Helliwell[1]

[1]Space, Telecommunications and Radioscience Laboratory
Stanford University
Stanford, CA 94305
[2]Radio Propagation Branch
Rome Air Development Center
Hanscom Air Force Base, MA 01731

Last year at this meeting we reported some of the results of a first experiment to measure TE and TM noise in the earth-ionosphere waveguide. Called ALFAN (for Airborne Low Frequency Atmospheric Noise), the experiment involved the flight of a specially-designed instrumentation package on a free-floating balloon. The flight took place on August 4, 1986, in New Mexico: the balloon was launched soon after dawn from a location near Roswell, it flew at an altitude of 18–21 km for roughly five hours, and the flight was terminated near White Sands.

The ALFAN measurement system consists of three identical low frequency receivers and an octahedron-shaped loop antenna arrangement consisting of two orthogonal vertical loops and one horizontal loop suspended below the instrumentation package. In level flight the two vertical loops respond to time variations of the horizontal magnetic field and the horizontal loop responds to variations of the vertical magnetic field. Thus, for low frequencies, measurements can be made simultaneously on electromagnetic waves propagating in the Transverse Magnetic (TM) and Transverse Electric (TE) modes.

The TE-to-TM noise ratios at 42.5 kHz that were obtained during the ALFAN flight were appreciably larger (by approximately 10 dB) than those reported during earlier theoretical and experimental studies. To confirm these ratios and to obtain new information about the ratios during the night, a second ALFAN experiment, designated ALFAN2, was conducted on May 16, 1987, once again in New Mexico. The instrumentation package and antennas for the second experiment were essentially the same as for the first, with some improvements; the balloon was launched at Holloman AFB near White Sands at 0336 LT and the flight was terminated around 0859 LT near Deming. Once again the instrumentation package was recovered without damage.

During the daylight portion of the ALFAN2 flight, the measured TE-to-TM noise ratios at 42.5 kHz were comparable to those obtained during the ALFAN flight, thus confirming the earlier result. During the nightime portion of the flight the measured ratios were even higher, with the measured TE noise levels being roughly the same or even greater than the TM noise levels. There was an interesting large decrease (by roughly 20 dB) in the strength of the TE signal from an LF station (55.5 kHz) in the San Francisco area during the transition from night to day.

G2-3
1440

AN HISTORICAL REVIEW OF MINIMUF - A MUF PREDICTION ALGORITHM

D.B. Sailors
Ocean and Atmospheric Sciences Division
Naval Ocean Systems Center
San Diego, CA 92152-5000

The development of MINIMUF is reviewed beginning with MINIMUF-1.0 concluding with the current version under development MINIMUF-7.0. MINIMUF was developed for predicting the MUF on small mobile propagation forecast terminals. The parameter foF2 is modeled as a response of a dynamic system "driven" by a function of cos χ (the cosine of the instantaneous solar zenith angle) and based on the analogy to a signal-lag linear system (e.g., an RC circuit).

The versions differ mainly in how the solutions to the differential equation for cos χ were implemented. The foF2 in Version 1.0 was given by a linear relationship between cos χ_{eff} and sunspot number; its M-factor had only a range dependence. Version 2.0 introduced a sunspot number dependency in the foF2 and a latitude dependence at the equator in the M-factor. In version 3.0 the form of the fit of cos χ to foF2 was non-linear and correction factors were added to the M-factor for high-latitude paths. In MINIMUF-3.5, the M-factor was changed to make it applicable beyond 8000 km. In these versions a fit was made to 36 path-months of data measured on three paths.

Subsequent modifications to MINIMUF were made to represent phenomena not previously considered. In MINIMUF-4.0 there was an attempt to include the E-layer in the determination of the MUF. MINIMUF-5.0 was developed for ray-tracing applications where h_mF2 and foF2 are needed. MINIMUF-85 (Version 6.0) included sunspot dependence in both the foF2 and M-factor calculations, seasonal and time dependence in the M-factor, and a special polar model for high-latitude paths.

A more accurate MINIMUF algorithm for use in a sounder updating is being developed. Both improved foF2 and M-factor models are being developed. The basis for the foF2 model is a data base of foF2 data measured at 175 sites. For the mid-latitudes supplementary data produced using model data from Rush et al. (Radio Science, 19, 1083-1097, 1984; Radio Science, 18, 95-107, 1983) is being used in ocean areas to fill gaps. For low-latitudes a semi-empirical model due to Anderson et al. (Radio Science, 22, 292-306, 1987) is being used to fill in gaps. The MINIMUF parameters for the diurnal variation of foF2 will be determined as a function of sunspot number, season and geographic location. The M-factor model is based on a calculation proposed by Sailors et. al. (Naval Ocean Systems Center TR 1121, July 1986) which uses the distance factor M(D)F2 developed by Lockwood (IEE Proc., 130, pt. F, no. 4, June 1983).

G2-4
1500

THE VERTICAL IONOGRAMS AND DISPERSIVE BANDWIDTH FOR AN OBLIQUE PATH

K. C. Yeh, Department of Electrical and Computer Engineering, University of Illinois, Urbana, IL 61801
Haim Soicher, Center for C^3 Systems, US Army Communications-Electronics Command, Fort Monmouth, NJ 07703

The propagation geometry and dispersiveness of the ionospheric medium will both give rise to dispersion of an electromagnetic pulse. In this connection, a useful measure of the propagation channel is the dispersive bandwidth. There are many ways to define dispersive bandwidth, but they all lead to very similar results. For several model ionospheres, the dispersive bandwidth has been computed. These curves will be shown. A simple analytical relation has been obtained that enables us to compute the dispersive bandwidth for a given oblique path, frequency and vertical ionogram. This relation is used to compute the dispersive bandwidths for a typical day by using real ionograms.

G2-5
1540

IONOSPHERIC LIMITATIONS TO THE ACCURACY OF SSL RANGE ESTIMATION

Leo F McNamara
Andrew Antennas
Technology Park 5095
AUSTRALIA

The single station location (SSL) technique for the determination of the position of an HF transmitter overcomes several of the difficulties inherent in the use of a traditional bearing-only DF network, such as the transmitter being audible at only one station of the network. The SSL technique combines observations of the elevation angle and bearing of signals from the transmitter with procedures for raytracing through a model of the ionosphere, to produce an estimate of the position of the transmitter.

The SSL technique also has its limitations, mostly imposed by the ionosphere and by our inability to model it successfully on all occasions. This paper will describe some of these limitations, and discuss procedures for their elimination, or at least for their minimization.

The diagram illustrates one of the more interesting cases encountered during a trial of the Andrew SSL system SKYLOC. The transmitter was at North West Cape, 2783km from the SSL site, and on a bearing of 294.6 degrees. However ray-retracing placed the transmitter in the middle of the extremely inhospitable Great Victoria Desert. This case will be discussed in some detail.

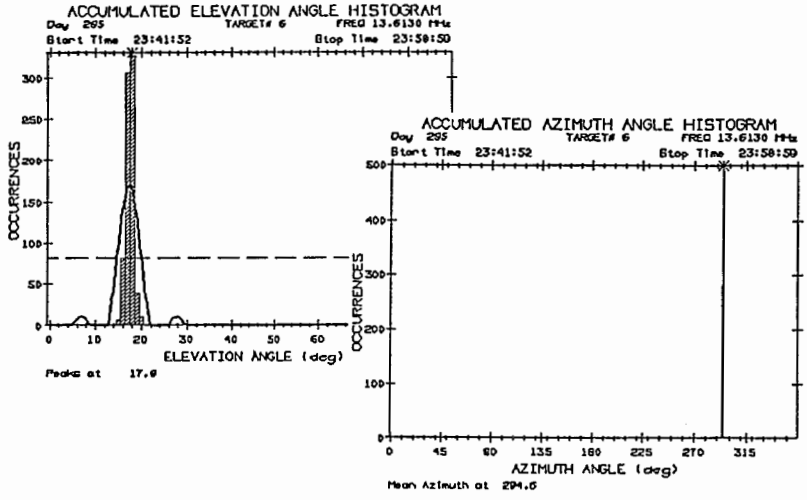

G2-6
1600

PERFORMANCE OF METEOR BURST COMMUNICATION SYSTEMS IN THE PRESENCE OF ENHANCED D-LAYER IONIZATION

Thaddeus Kaliszewski

The MITRE Corporation
Burlington Road
Bedford, Massachusetts 01730

Meteor Burst Communication (MBC) is supported by radio waves scattered by ionized trails that are formed by small particles upon their entry into the earth's atmosphere. The ionization of the meteor trails varies depending on the energy of the entering particles and on their angle of entry. Typically, the ionization is high enough to support communications at very high frequencies (VHF).

A normal, undisturbed D-layer is rather innocuous at VHF, even though the layer is interposed between most of the trails and the ground terminals. The D-layer screening becomes a concern when its ionization is enhanced by the influx of ionizing particles or radiation. The origins of such enhancement can be either natural or man-made.

The D-layer screening has the effect of reducing the radio visibility of the meteor trails. More importantly, it reduces also the performance of the meteor burst communication systems. The two indices of performance, the throughput and the packet delay, are greatly affected by the increase in absorption of the layer. In certain extreme cases, the absorption can be high enough to cause a total blackout.

In the present paper, the effect of D-layer screening is modeled in the context of a reference meteor burst communications circuit. Performance indices are computed as a function of both frequency and absorption. A critical absorption, at which a total blackout occurs, is also identified for the particular circuit under consideration.

G2-7
1620

DETERMINATION OF UPPER ATMOSPHERIC TIDES FROM RANDOMLY SPACED METEOR ECHOES

C. A. Whitmore
S. K. Avery
Department of Electrical and Computer Engineering
University of Colorado, Boulder
Campus Box 425
Boulder, CO 80309

ABSTRACT

Radar echoes from ionized meteor trails have proven useful in estimating tidal components in upper atmosphere winds. Previous signal processing methods have used the pulse pair processor to determine the mean velocity of the neutral wind from the echo doppler shifts. From these velocity points (which are randomly spaced in time) and an a priori estimate of the tidal components, amplitudes and phases of the tides are then estimated. A new technique, however, does not assume a priori knowledge of the frequency components, but instead interpolates the randomly spaced data into a uniformly spaced representation, and then performs standard spectrum analysis to determine more accurate tides.

A minimum-energy, reduced rank interpolator has been derived. This interpolator has been tested through simulations, with the results comparing favorably with well-known estimators acting on evenly-spaced data. A new study on this topic involves deriving an analytic relationship between the resulting mean squared error of the interpolator and several factors: the average sampling density of the random sampler, the noise variance in each sample, and the bandwidth of the desired signal. In my talk I will discuss this interpolator and its performance characteristics.

Session J-2 1355-Tues. CR0-30
(continued from Tues. AM)
RADAR ASTRONOMY OF THE INNER SOLAR SYSTEM
Chairman: S.H. Zisk, MIT Haystack Observatory, Westford, MA 01886

J2-3
1400

MARS: RECENT RADAR RESULTS

T. W. Thompson and L. Roth
Jet Propulsion Laboratory
California Institute of Technology
Pasadena, CA 91109

We report on three topics; radar altimetry of the Martian cratered highlands from 1971-1973 observations, Mars reflectivities from the 1986 observation, and possibilities for Mars observation for the next few oppositions. The radar altimetry of crater highlands is a new reduction of old data, while the Mars reflectivities and dielectric constants are preliminary results from the new 1986 data. Finally, the consequences of Mars and earth orbital configuration on earth-based radar observations of Mars through the next two decades will be discussed.

Topography in the -14^{o} to -22^{o} latitude strip of the martian cratered highlands was measured by the Goldstone Solar System Radar during the 1971/1973 perihelic oppositions. Overall, the landscape is flat. Most of the local relief is provided by the structural elements of large impact craters. Low or non-existent exterior relief, rather than overall shallowness, is the distinguishing characteristic of large martian craters.

Radar echoes from the planet Mars were obtained on 26 S-band (wavelength = 12.5 cm) and 2 X-band (wavelength = 3.5 cm) tracks using the Goldstone Radar in 1986. These observations took advantage of the favorable 1986 opposition since the earth-Mars distance in July was 0.40 AU, the smallest earth-Mars distance since the 1971 and 1973 oppositions. The observations were conducted via the cw-spectra techniques like those of Harmon et al. (1982 and 1985). A continuous tone was transmitted at Mars and the radar echo was sampled to obtain a Doppler-spread spectrum. Each received cycle was separated into polarized (opposite sense circular, OC) and depolarized (same sense circular, SC) periods. Also, a minute or two of noise was recorded in each transmit-receive cycle.

Coverage on Mars started at -8^{o} in June, travelled north toward the equator to -3^{o} during August, and then migrated south to -14^{o} for the last run in October. These are new areas for earth-based radars. Longitudes 180^{o} to 90^{o} have low polarized (OC) reflectivities, high depolarized (SC) reflectivities and inferred bulk dielectric constants of 3.0-4.0. These values in general agree with those observed by Harmon et al. (1985) for areas north of the equator. In contrast, longitudes 75^{o} to 0^{o}, the Valles Marineris, have high polarized (OC) reflectivities, low depolarized reflectivities and inferred bulk dielectric constants near 5.0. Longitudes 360^{o} to 180^{o} have intermediate values with inferred bulk dielectric constants of 3.5-4.5.

J2-4
1420 RECENT OBSERVATIONS AND IDENTIFICATION OF FEATURES ON THE MOON AND VENUS: D.B. Cambell, Arecibo Observatory, Arecibo, PR 00612

J2-5
1440

VENUS: REGIONS OF HIGH SURFACE PERMITTIVITY

G. H. Pettengill, Center for Space Research, Rm 37-241
Massachusetts Institute of Technology
Cambridge, MA 02139

Regions on the surface of Venus, generally located at high altitude, have been determined to possess high values of dielectric permittivity. Values as high as 39 (in the Maxwell Montes area) have been inferred from both radar scattering and radio emission observations at wavelengths between 5 and 20 cm. In the absence of liquid water, the most likely explanation for this behavior. appears to be a "loading" of surface rock with small, electrically conducting inclusions.

Laboratory measurements of artificially produced material (J. M. Kelly *et al*, J. Appl. Phys., **24**, 258-262, 1953), as well as of natural pyrite-containing minerals (S. D. Nozette, Ph.D. Thesis, M.I.T. Dept. of Earth, Atmosphere and Planetary Sci., Nov. 1982) show that a volume fraction of about 13% conducting inclusions embedded in a host rock having an intrinsic permittivity of 5 will yield an effective bulk dielectric permittivity of 39.

J2-6
1520

A VENUS TOPOGRAPHY MODEL

P.G. Ford
Center for Space Research, 37-491
MIT, Cambridge, MA 02139
and
E. Eliason
U.S. Geological Survey
2255 Gemini Drive,
Flagstaff, AZ 86001

Sources of systematic error contributing to the Pioneer Venus topography model (Pettengill *et al.* J. Geophys. Res. 85, 8261–8270, 1980) have been studied. The chief factors are spacecraft timing uncertainties and inaccuracies in orbit determination. These errors have been estimated, and the planetary radius values corrected, by two methods: a) adjusting the Keplerian elements of the orbit, and b) imposing a "smoothness" constraint on local variations in planetary radius.

The resulting topographic model and error estimates agree well with available earth-based measurements, and will provide the basis for the automatic mapping system under development for the Magellan project.

J2-7
1540

RADAR STUDIES OF ASTEROIDS

S. J. Ostro
183-501, Jet Propulsion Laboratory
California Institute of Technology
Pasadena, CA 91109

Echoes from 30 mainbelt asteroids (MBA's) and 17 near-Earth asteroids (NEA's) have provided a wealth of unique information about these objects' sizes, shapes, spin vectors, and such surface characteristics as decimeter-scale morphology, topographic relief, regolith porosity, and metal concentration. On average, small NEA's are much rougher at decimeter scales than MBA's, comets, or the terrestrial planets. Some of the largest MBA's (e.g., 1 Ceres and 2 Pallas) are smoother than the Moon at decimeter scales but much rougher than the Moon at some much larger scale. There is at least a five-fold variation in the radar albedoes of MBA's, implying substantial variations in these objects' surface porosities or metal concentrations. The highest MBA albedo estimate, for 16 Psyche, is consistent with a metal concentration near unity and lunar porosities.

The diversity of NEA radar signatures is extreme. The radar albedo of 1986 DA is twice that of Psyche and strongly suggests that this Earth-approacher is a ~2-km metallic fragment with hardly any regolith; it might be the source of some of our iron meteorites. The radar polarization signature of 2101 Adonis is most unusual, resembling that of Jupiter's icy satellite Callisto more than that of any other radar-detected planetary target. NEA polar silhouettes range from slightly non-circular to highly elongated and distinctly non-elliptical. Delay-Doppler resolution of 1627 Ivar has yielded the first two-dimensional images of an asteroid; they show this ~7-km object to be elongated, irregular, non-convex, and bifurcated. The radar signatures of NEA's often seem extraordinarily complex compared to those of large MBA's, and suggest an abundance of exotically shaped objects in the near-Earth population.

Echoes from 1986 JK, detected at 11 lunar distances from Earth three weeks after its discovery, yield Doppler-frequency measurements that will help to ensure optical recovery of this asteroid. "Radar astrometry" of NEA's is important even for asteroids with an extensive optical-astrometric history, because a handful of radar measurements can shrink the positional error ellipsoid of the prediction ephemeris by a factor ≥ 2 for decades.

J2-8
1600

EARTH - RADAR STOKES PARAMETER MEASUREMENTS AND INTERPRETATIONS.

Jakob J van Zyl and Howard A. Zebker
Jet Propulsion Laboratory
California Institute of Technology
4800 Oak Grove Drive
Pasadena, CA 91109

We have converted a conventional synthetic aperture radar system into an imaging radar polarimeter by by employing two orthogonally polarized antennas and recording both the amplitude and phase measurements of the received electric fields. This enables us to measure the complete complex scattering matrix for each individual resolution element in the radar image. This sytem was used to measure the scattering matrices of a number of lava flows in the Snake River Plain, Idaho.

Knowledge of the scattering and Stokes matrices allows one to decompose the scattered waves into polarized and unpolarized parts. Images of the polarized and unpolarized energy shows that the return from the rougher lava flows contain more unpolarized energy than the returns from the smoother areas. We interpret this behavior as indicative of the increased role of multiple scattering as the surface gets rougher.

The polarization signatures measured with the JPL imaging polarimeter allow us to determine the dominant scattering mechanism for each flow. We find that the signatures are similar to those predicted by models of scattering by slightly rough dielectric surfaces. Specifically, the smoothest lava flows are modeled quite well by even the first order rough surface model, while at least a second order model is required to interpret the signatures of the rougher flows. At present we do not have complete, quantitative measurements of the actual surface roughness, however, we do have photographs and crude surface-height template measurements that indeed indicate a qualitative agreement between the radar observations and the ground-truth measurements of r.m.s. height.

J2-9
1620

LUNAR RADAR IMAGES AT 15-M RESOLUTION

S.H. Zisk
MIT Haystack Observatory
Westford, MA 01886

New 5-m-resolution radar measurements of the lunar surface have yielded range-doppler images with a projected surface resolution (pixel size) of 30 to 60 meters. About 6 areas were mapped between June and October, 1987. Each map covers a rectangular area of about 30 by 400 km. These data are being used to further our understanding of the present geologic properties and past history of the lunar surface, specfically regarding volcanism and impact as major formative processes. They will be used as well to investigate the details of radar backscattering from planetary surfaces, which is of particular interest for the interpretation of the imminent Magellan mission to Venus.

J2-10
1640

MULTI-STATION RADAR IMAGES OF VENUS AT MODERATE AND HIGH RESOLUTION

R. F. Jurgens and M. A. Slade
Communications Systems Research Section
Jet Propulsion Laboratory
Pasadena, CA 91109

During the past three years, the Goldstone radar system has undergone a significant upgrade such that radar ranging data can have a time resolution as fine as 0.3us. The first radar observations of Venus with this system show that interferometric fringes can be obtained without serious degradation, and that images can be formed with resolutions near 1 km. The new images cover the region from 280 to 5 degrees longitude and are near the equator. Resolutions vary from 1 to 4 km depending upon the distance to the planet.

We have also processed several of the observations from the 1980 and 1982 series and have reprocessed some of the 1978 series. Some earlier observations that were defective due to one of the interferometer stations being bad have been processed with a new generalized multistation algorithm that allows selecting the number of operation stations. The first images have been selected to provide multiple coverage with our earlier images. Distinct features found in these series of images have been used to calculate a new and much more accurate pole position and spin rate for Venus.

Several of the images made from the older data have shown some remarkable features that possess either very high or very low effective cross sections. These features have little topography associated with them, so that the scattering anomalies cannot be associated with the usual quasispecular scattering from slopes in the kilometer scale size. Preferentially aligned slopes in the 10 to 100 meter size cannot be ruled out; however, we believe these anomalies may be due to changes in the Fresnel reflection coefficient. Enhancements as much as 500% have been observed on one feature and would indicate Fresnel reflection coefficients in the order of 80 to 90%. Metallic material could also cause such reflections. Pioneer Venus data show no large anomalies in this region except for a slight increase in the Fresnel reflection coefficient, thus ruling out large variations in effective rms roughness. A temperature anomaly should be expected, however, the resolution of the PV radiometer may be inadequate to show the anomaly. Further studies of these regions will be required, especially the low reflection areas which have not received much attention.

Wednesday Morning, 6 January, 0830-1200

Plenary Session 0830-Weds. Duane G0-30

Session A-3 1355-Weds. CR1-42
ANTENNA AND EM FIELDS MEASUREMENT
Chairman: Motohisa Kanda, Electromagnetic Fields Division, National Bureau of Standards, Boulder, CO 80303

A3-1 1400 **AN OPTICALLY LINKED ELECTRIC AND MAGNETIC FIELD SENSOR FOR POYNTING VECTOR MEASUREMENTS IN THE NEAR FIELDS OF RADIATIING SOURCES**

L. D. Driver and M. Kanda
Electromagnetic Fields Division - 723.03
National Bureau of Standards
325 Broadway, CO 80303

A unique, single-element antenna sensing scheme is described which can simultaneously measure the electic, magnetic, and time-dependent Poynting vectors of electromagnetic (EM) fields. The electric and magnetic responses are separated by a 0/180 degree hybrid junction; these rf voltages along with relative phase and frequency information are transmitted to a remotely located vector analyzer by a pair of well-matched fiber optic downlinks; and the remote receiver displays (1) the electric dipole response, (2) the magnetic loop response, and (3) the time phase difference between the two, which can be used to determine the time-dependent Poynting vector. Both a theoretical analysis and a discussion of experimental measurements performed are presented which describe the capabilities and performance of a working prototype of the antenna measurement scheme. The results indicate that a properly characterized isotropic version of this system can function properly in the near-fields of EM sources to thoroughly characterize such fields and to describe the resulting energy flow.

A3-2
1420

NUMERICAL CALCULATION AND EXPERIMENTAL VERIFICATION OF NEAR FIELDS FROM HORNS

Don W. Metzger
Kaman Sciences Corporation
P.O. Box 7463
Colorado Springs, CO 80933
Ronald M. Sega, John D. Norgard
University of Colorado
Department of Electrical Engineering
Colorado Springs, CO 80933-7150

The testing of system response and vulnerabilty to high power microwaves necessarily involves the creation of the highest possible power microwaves. In order to simulate actual threats, testing should be performed in the far-field region where the propagating waves are plane waves. However, to maximize the power density at the test aperture, the system is often located in the near-field. Additionally, it is often impossible to locate the test object in the far-field due to size constraints of the anechoic chamber. Thus, an accurate prediction of the near-field region is necessary.

An extension of Silver's solution for the fields produced by a distribution of currents provides the basis for this method of calculating near fields. The horn is treated as a distribution of source currents which can be determined from a generalized distribution of E and H fields. The currents lie on a planar surface from which the wave is launched with a phase correction to account for the horn flare.

Experimental verification of the near-field calculations was accomplished through the infrared imaging method currently in use at the University of Colorado at Colorado Springs. In this method, when a lossy dielectric sheet is illuminated by the microwave source, it heats. The sheet can then be viewed using an infrared camera and the electric field pattern is determined. The agreement between theory an experiment is very good and will be presented.

A3-3
1440

NBS EFFORTS ON ELECTRIC FIELD PROBES FOR MILLIMETER WAVES

J. Randa, M. Kanda, and D. Melquist
Electromagnetic Fields Division - 723.03
National Bureau of Standards
325 Broadway
Boulder, CO 80303

The National Bureau of Standards is pursuing research aimed at developing electric-field probes to operate in the frequency range 18 - 110 GHz. Work thus far has concentrated on two particular efforts: extension of the resistively tapered dipole design to higher frequencies and a new design based on a fiber-optically sensed temperature probe.

The resistively tapered dipole with Schottky diode detector is the basis of a previously developed probe which operates up to 18 GHz using dipoles of length 8 mm. This same design with shorter dipoles is being developed for a probe to cover the lower end of the frequency range of interest (up to about 40 GHz). Preliminary measurements of both frequency response and antenna pattern are encouraging up to at least 30 GHz.

The second design is intended to cover frequencies up to 110 GHz (and down to about 20 GHz). It consists of a thin resistive film deposited on the tip of a fiber-optically sensed thermometer. The optimal thickness and conductivity of the resistive film have been calculated, and measurements have been made on thin nichrome strips deposited on glass to test the feasibility of this probe configuration. The test results indicate that the heating of the strip can be detected, but that very high fields are required. This is due in part to the large ambient thermal fluctuations (of order $1\ ^{0}C$) in the test environment. The effect of thermal isolation is estimated, as are the effect on the field due to the substrate and the effect of different input impedances for different resistive strip geometries.

A3-4
1520

THREE-DIMENSIONAL THEORETICAL AND EXPERIMENTAL ANALYSIS OF INTERNAL CYLINDRICAL FIELDS COUPLED THROUGH A SLOT APERTURE

Paul E. Bussey, John D. Norgard, and Ronald M. Sega
University of Colorado at Colorado Springs
Department of Electrical Engineering
Colorado Springs, CO 80933-7150

A modal expansion technique is used to predict the fields inside of a closed circular cylinder due to coupling through an axial slot aperture. The main interest is to determine which modes are excited in the cylindrical cavity, and the relative strengths of these modes. These results are then compared to experimental measurements made using an infrared technique developed at UCCS. The measurements are made so that the electric field vector can be determined, and the mode strengths calculated. The field distributions are obtained from heating of lossy dielectric sheets in a particular cylinder cross-section of interest. The lossy material is also cut so as to measure the amplitude of the given spatial electric field components. A comparison of theory and experiment is presented.

A3-5
1540

DEVELOPMENT OF PHOTONIC PROBES FOR THE MEASUREMENT OF ELECTROMAGNETIC FIELDS

K. D. Masterson and L. D. Driver
Electromagnetic Fields Division, MS/723.03
National Bureau of Standards
325 Broadway
Boulder, CO 80303

Fiber optic, all dielectric light guides provide wide bandwidth, EMI immune, and unperturbing links over which information characterizing electromagnetic fields can be transmitted. This philosophy has been extended to include the design of the field-sensing probe itself.

We have developed passive, all dielectric probes that utilize electric-field-induced birefringence in certain crystals (esp. $LiNO_3$) to measure field strengths down to 5 V/m at frequencies to 1.5 GHz(K.D. Masterson, High Bandwidth Analog Applications of Photonics, SPIE Vol. 720, 100-104, 1986). The physical and electrical characteristics of the probe are described in detail, with particular emphasis on results obtained for increased bandwidths obtained with the most recent version of the probe.

A3-6
1600

MUTUAL COUPLING BETWEEN MICROSTRIP ANTENNAS

S.R. Bhadra Chaudhuri, A.K. Bhattacharjee,
D.R. Poddar & S.K. Chowdhury
Department of Electronics & Tele-communication Engineering
Jadavpur University,Calcutta 700 032, West Bengal, INDIA.

In the design of Microstrip Antenna Array the mutual coupling between microstrip elements have a marked effect on array performance. Rectangular microstrip antenna arrays have been used for various application e.g. in space vehicles, aircrafts etc. Generally, when a properly matched individual element is placed in an array, its terminal properties change due to mutual coupling effect. The properties such as side lobe level may increase, nulls may be shifted and grating lobes may appear. The antenna when scanned may show a degraded pattern which is also a function of scan angle.

Penard et.al. (E. Penard, J.P. Daniel, Electronics letters, 8th July, 1982, Vol - 18; No : 14; pp. 605-607) used the cavity method and the equivalence theorem to determine the mutual coupling between H-plane coupled rectangular microstrip antennas. Jedlicka et.al. (R.P. Jedlicka, M.T. Poe, K.R. Carver; IEEE Trans. on A.P. Vol. A P : 29, no : 1, January, 1982,pp. 147-149) reported measured data on the mutual coupling between microstrip antennas. The theory presented by Penard et.al. above involves the computation of a number of numerical double integrations and computation time is quite large.

A thorough investigation has been made by the present authors on the mutual coupling between rectangular half wave length microstrip antennas fed by a co-axial line at the centre of one of the radiating edges for a frequency ranging from 1 GHz to 8 GHz on various thickness of the substrate ranging from .1 to .305 cm. with the spacing between adjacent edges from .005λ to λ and di-electric constant chosen 2.5 to 2.55. The values of λ_g for the antennas (the mutual coupling properties of which were investigated) were calculated from schneider's formula (M.V.Schneider, G.Bernard and W.F.Bodtman, The Bell System Tech. Journal,1969) [Fig. 1] Sij (i=j and i$\neq$j) of the above antennas were measured by an HP 8410 B Network Analyser.

A3-7
1620

LOW-FREQUENCY REFLECTION FROM AN ARRAY OF PYRAMID-CONE ABSORBERS

Edward F. Kuester and Christopher L. Holloway
Dept. of Electrical and Computer Engineering
University of Colorado - Campus Box 425
Boulder, CO 80309

Pyramid-cone absorbers made from graphite-impregnated plastic foam are typically used to line the walls of anechoic measurement chambers. These cones operate on the principle of repeated plane-wave reflection between faces of neighboring cones, which results in an overall low reflection coefficient from a wall lined with such cones. When this physical picture is valid (i.e., when cone dimensions are at least a wavelength) then good suppression of reflected waves results.

For some purposes, it may be desirable to oprate a measurement chamber at frequencies where this "geometrical optics" picture does not apply. We present an analysis of plane-wave reflection from a periodic array of cone absorbers when the wavelength is large compared to the transverse spacing between cones. We show, using a method called homogenization, that the array of cones is equivalent, in the low-frequency limit, to a one-dimensionally inhomogeneous, anisotropic layer, whose permittivity is easily calculated from the bulk permittivity and geometrical dimensions of the cones themselves. The plane-wave reflection coefficient is then found rather easily.

Computed results show some interesting features of the reflection coefficient, apparently due to damped standing waves within the equivalent layer. A certain amount of experimental data is also available, which shows good comparison to the theory.

Session B-4 1355-Weds. CR1-40
PDE-BASED METHODS FOR EM PROBLEMS IN OPEN REGIONS
Co-Chairmen: M.A. Morgan, Electrical and Computer Engineering Dept., Naval Postgraduate School, Monterey, CA 93943; and L.W. Pearson, McDonnell Douglas Research Labs, St. Louis, MO 63166

B4-1
1400

REVIEW OF PROGRESS IN FINITE-DIFFERENCE EQUATION SOLUTION METHODS FOR ELECTROMAGNETIC WAVE INTERACTIONS

Allen Taflove
EECS Department
Technological Institute
Northwestern University
Evanston, IL 60201

Korada R. Umashankar
EECS Department
Communications Laboratory
University of Illinois at Chicago
Chicago, IL 60680

Contemporary high-frequency electromagnetics problems can involve wave interactions with complex, electrically large, three-dimensional structures. These structures can have shapes, material compositions, apertures, or cavities which produce near fields that cannot be resolved into finite sets of modes or rays. Proper numerical modeling of such near fields requires sampling at sub-wavelength resolution to avoid aliasing of magnitude and phase information. The goal is to provide a self-consistent model of the mutual coupling of the electrically small cells comprising the structure.

Two recent numerical modeling approaches for this purpose involve finite-difference equation solution methods. The first, which we denote as finite-difference frequency-domain (FD-FD) methods, involves either a direct solution of the Helmholtz equation on a space grid containing the structure, or a solution of a transformed problem involving Debye potentials. FD-FD methods generate a potentially large system matrix. To date, published applications principally involve two-dimensional wave interactions.

The second approach, which we denote as the finite-difference time-domain (FD-TD) method, is a direct marching-in-time solution of Maxwell's time dependent curl equations, applying simple, second-order accurate, central-difference approximations for the space and time derivatives. This achieves a sampled-data reduction of the continuous electromagnetic field in a volume of space over a period of time, simulating the actual waves by numerical analogs propagating in a computer's data space. The resulting system of equations for the fields is fully explicit, so that there is no need to set up or solve a set of linear equations, and the required computer storage and running time is proportional to the electrical size of the volume modeled. Recent FD-TD research progress includes: 1. Scattering models for three-dimensional reentrant structures spanning up to $9\lambda_o$; 2. Conformal models of curved surfaces; 3. Scattering models for two-dimensional, anisotropic structures; 4. Penetration models for narrow slots and lapped joints in thick screens; 5. Coupling models for wires and wire bundles in free space and in arbitrary metal cavities; 6. Penetration models for the electromagnetic fields within detailed, inhomogeneous tissue approximations of the complete human body (at UHF frequencies); 7. Microstrip / waveguide models; 8. Scattering models for relativistically vibrating mirrors; 9. Inverse scattering reconstruction of one-dimensional, spatially coincident profiles of ε and σ; 10. Inverse scattering reconstruction of two-dimensional conducting, homogeneous, and inhomogeneous dielectric targets from minimal TM scattered field pulse response data; and 11. Large-scale computer software.

B4-2
1420 A FINITE-DIFFERENCE FREQUENCY-DOMAIN APPROACH TO ELECTROMAGNETIC SCATTERING PROBLEMS

R. T. Ling
Mail Code 3812/82
Northrop Aircraft Division
One Northrop Avenue
Hawthorne, California 90250

A finite-difference, frequency-domain (FD-FD) approach to electromagnetic wave scattering is presented. This approach evolved from recent progress [R. T. Ling, AIAA Journal, Vol. 25, pp. 560-566 (1987), AIAA Papers 87-0487 and 88-0180] that features the concept of generalized scattering amplitudes, the application of boundary-fitted curvilinear coordinate systems, and the use of Debye potentials for 3-D obstacle scatterings. The introduction of the radially non-oscillatory generalized scattering amplitudes circumvents the difficulties in dealing with oscillatory field quantities in the infinite exterior scattering region and allows the finite-difference method to be applied to scattering problems in an effective manner. The radiation condition in terms of the generalized scattering amplitude is very simple in form and can be enforced exactly in the far field. For a 3-D scattering problem the formulation in terms of Debye potentials, expressed as functions of body-fitted coordinates, not only decouples the vector scattering problem into a combination of two independent scalar scattering problems but also makes the exact enforcement of obstacle surface condition simple. Specific examples with numerical results validated by the eigenfunction expansion method and the moment method are given to illustrate the salient features of the FD-FD approach.

B4-3
1440

A TIME DOMAIN DIFFERENTIAL SOLVER FOR ELECTROMAGNETIC SCATTERING PROBLEMS

Vijaya Shankar and William Hall
Rockwell International Science Center
Thousand Oaks, California 91360

Abstract

The transverse magnetic (TM) wave form of the Maxwell equations written in conservation form is solved using a hyperbolic, finite–volume, upwind based multizone scheme originally developed for solving the Euler/Navier–Stokes equations of Computational Fluid Dynamics (CFD). The Maxwell equations are shown to represent a linearly degenerate set of hyperbolic equations with real characteristics with values $\pm c$, where c is the speed of light. The electric and magnetic fluxes at a finite volume cell interface are computed using a characteristic subpath integration referred to as the Riemann Solver. A multistep Lax–Weindroff scheme which is second order accurate in both space and time is applied to solve the TM equations. At a material interface, the boundary condition requiring continuity of tangential total electric and magnetic field is satisfied, while at a perfectly conducting surface the total electric field is set to zero. At the far field, a first order accurate no–radiation boundary condition derived from the characteristic theory is applied. A near field–to–far field transformation is applied to the computed electric and magnetic fields to obtain the bistatic radar cross section (RCS). Results are presented for both time harmonic and transient electromagnetic scattering problems involving layered material mediums.

B4-4
1500

THE TLM METHOD AND ITS APPLICATION TO OPEN AND BOUNDED FIELD PROBLEMS

Michel M. Ney and Wolfgang J.R. Hoefer
Laboratory for Electromagnetics and Microwaves
Dept. of Electrical Engineering
University of Ottawa
Ottawa, Ontario, Canada K1N 6N5

Inspired by earlier network simulation techniques, Johns and Beurle introduced in 1971 a novel numerical method for solving general electromagnetic field problems. They modelled the propagation of fields in space by computing the progress of voltage and current impulses in a network of interconnected transmission lines. They showed that both fields and network variables obey the same differential equations as long as the mesh size is small compared with the wavelength.

The basic TLM algorithm describes the scattering of Dirac impulses at series and shunt nodes, a phenomenon which is equivalent to Huygens's principle in discretized form. The impulse response of the TLM network is computed in time steps equal to the transit time between nodes, and the frequency response is obtained therefrom via Fourier transform.

Lossless and lossy boundaries can be modeled by introducing suitable reflection coefficients in the TLM mesh. Since the mesh is discretized, boundaries are approximated by piecewise straight walls deployed halfways between nodes to preserve synchronism of scattering events. Open problems can be modeled as structures with absorbing boundaries. Dielecric and magnetic materials are simulated by loading shunt nodes with shunt stubs, and series nodes with series stubs, respectively. The simulated ϵ_r or μ_r values depend on the characteristic immittances of these stubs. Losses and anisotropy can be properly accounted for as well. Since the procedure is executed in the time domain, non-linear problems as well as situations involving time-variant material parameters can be treated with the TLM method.

In this paper, the TLM algorithm and the modeling of various boundary and material properties will be described briefly. Recent advances such as condensed nodes, graded mesh techniques, and error correction techniques will be discussed. Computational expenditures will be analyzed and compared with those of other numerical techniques. Finally, two applications of the method, one to an open problem (EMP response of an airplane), and one to a bounded problem (modeling of a finline T-junction) will be presented to illustrate the potential of the TLM method.

B4-5
1540

GENERALIZED COUPLED AZIMUTHAL POTENTIALS FOR ELECTROMAGNETIC FIELDS IN INHOMOGENEOUS MEDIA

Michael A. Morgan
Electrical and Computer Engineering Department
Naval Postgraduate School, Monterey, CA 93943

The original coupled azimuthal potential (CAP) formulation (Morgan, Chang & Mei, *IEEE Trans. Ant. & Prop.*, AP-25, pp. 413-417, 1977), has the advantage of using only two continuous potentials to represent all field components in "arbitrary", but axially symmetric, inhomogeneous material media. It has been used as the basis for several finite element numerical efforts involving radiation, scattering and penetration problems.

A generalization of the original formulation is presented, whereby the restriction to axisymmetric media is removed. This new methodology retains the advantage of vector field generation in terms of only two scalar potentials. Alternate forms for solving the generalized CAP equations are considered, including eigenfunction decomposition and circumferential natural basis functions. Numerical examples are presented for boundary value problem solutions in 3-D using finite elements. Finally, the procedures for solving scattering problems using this theory are discussed.

B4-6
1600

RELATIVE ACCURACY OF FREQUENCY-DOMAIN INTEGRAL AND DIFFERENTIAL EQUATION FORMULATIONS FOR OPEN-REGION ELECTROMAGNETIC SCATTERING PROBLEMS

Andrew F. Peterson
Electromagnetic Communication Laboratory
1406 W. Green St.
University of Illinois
Urbana, IL 61801

Steven P. Castillo
Department of Electrical Engineering
New Mexico State University
Las Cruces, NM 88001

Open-region electromagnetic scattering problems can be formulated as integral or differential equations. The integral equation approach has been widely used, possibly because the Green's function appearing in the kernel of the integral operator implicitly accounts for infinite space and incorporates the radiation condition. Techniques for the numerical solution of integral equations usually involve fully-populated matrices. In contrast, differential equation formulations must explicitly enforce the radiation condition a finite distance from the scatterer. These methods generally require more unknowns than the integral formulations, but typically involve sparse matrices.

To evaluate the relative advantages of the integral and differential equation formulations in the context of numerical solutions, systematic comparisons have been carried out for several two-dimensional, open-region geometries. Numerical results indicate that both formulations provide similar accuracy when applied to identical scatterer models. However, the differential equation methods can have significant computational advantages because of the efficiency in treating sparse matrices. This suggests that differential equation methods may be better alternatives for numerical solution than the integral equation formulations currently in widespread use.

Examples illustrating the relative accuracy of integral and differential equation methods will be presented. The accuracy of the Bayliss-Turkel type of "near-field" radiation condition as a function of distance from the scatterer will be examined. Finally, efficient algorithms for treating sparse systems will be surveyed.

B4-7
1620

TO BE OR NOT TO BE IN THE TIME DOMAIN

Kenneth K. Mei
Department of Electrical Engineering and Computer Sciences
University of California
Berkeley, CA 94720

Maxwell's differential equations in the frequency domain are elliptical, which results in classical boundary value problems. In the time domain they are hyperbolic, the solutions of which march in time. Numerically, the frequency domain differential equations require solutions of matrices; the time domain differential equations, if explicit, are spared from such endeavor. Before the coming of super computers, almost all electromagnetic problems were solved in the frequency domain. Now, there is a choice. This talk enumerates the pros and cons of computations in either domain. Depending on the objectives of the computation, one can make a rational decision in the computational domain. However, individual familiarity and personal beliefs often are the dominant factors of to be or not to be in one particular domain.

B4-8
1640

A FINITE-DIFFERENCE INTERPRETATION OF THE TRANSMISSION-LINE-MATRIX METHOD

Richard C. Booton, Jr., Chief Scientist
TRW Electronic Systems Group
TRW E2/3080
One Space Park
Redondo Beach, CA 90278

The finite-difference (FD) method and the transmission-line-matrix (TLM) method are recognized to be alternate approaches to the calculation of transient electromagnetic response. This paper demonstrates the equivalence of the two methods, provided two conditions are met. Initial conditions and boundary conditions must be assigned consistently. The ratio of time interval to space interval must have a certain value, namely the maximum value for which FD is a stable computational process. This value is $1/c\sqrt{2}$ for two dimensions and $1/c\sqrt{3}$ for three dimensions. The fact that the TLM solution satisfies the FD equations is demonstrated in detail for the two-dimensional case, and extension to three dimensions is summarized.

Equivalence of the methods is demonstrated by beginning with a single TLM pulse and utilizing the TLM rules to calculate pulse and nodal values for several time intervals. Direct comparison of the nodal values shows that the FD version of the scalar wave equation is satisfied for the ratio of time interval to space interval specified above. Superposition then shows that beginning with an arbitrary set of pulses, the same conclusion follows.

Nodal values for initial conditions for FD that correspond to the TLM pulses are determined from the TLM rules, as described above. Consistent boundary conditions for FD and TLM for Dirichlet and Neumann conditions are demonstrated. The TLM rules at boundary nodes are similar to one-dimensional transmission-line reflection at shorted and open terminations, respectively. Conditions for a boundary between two dielectrics present severe problems for TLM, which are not completely resolved herein, even though FD can handle the situation directly.

Another approach to the comparison starts with the discrete form of Maxwell's equations. If the nodal values correspond to the electric field, the magnetic field values can be shown to be proportional to the difference between the values of the pulses travelling in opposite directions.

B5-1
1400

A BIVARIATIONAL APPROXIMATION FOR THE SCATTERING PARAMETERS OF A 90° MICROSTRIP-SLOTLINE CROSSOVER

Edward F. Kuester and Alexander Anger
Dept. of Electrical and Computer Engineering
University of Colroado - Campus Box 425
Boulder, CO 80309

One of the most challenging problems in the modeling of planar transmission lines is the characterization of the 90° microstrip-slotline crossover. Here the microstrip rests on the top side of a dielectric substrate, while the slotline is cut into the ground plane on the bottom side of the substrate, at 90° to the microstrip axis. A rough equivalent circuit model for this crossover has been known for some time [J.B. Knorr, IEEE Trans. MTT. 22, 548-554 (1974)], but this has been found to be insufficiently accurate for some close tolerance applications.

We present here a bivariational approximation to calculate the S-matrix of this junction. A pair of coupled integro-differential equations is found for the unknown surface current density on the microstrip and aperture electric field in the slot. A suitable formulation then results in a variational formula for any of the scattering parameters we desire. The trial functions are the scattered currents and slot fields of the junction. A simple choice of trial function involves the fundamental microstrip and slotline modes with adjustable amplitudes. Substitution of this trial function into the variational principle yields terms which involve double Sommerfeld integrals and must be carefully handled numerically. Results obtained in this way will be compared with others available in the literature.

B5-2
1420

SIMPLE TRIAL CURRENT DENSITIES FOR THE BIVARIATIONAL ANALYSIS OF AN AIR-LOADED, SYMMETRIC STEP-IN-WIDTH MICROSTRIP JUNCTION

Robert T. Johnk and David C. Chang
Electromagnetics Laboratory
Campus Box 425
University of Colorado
Boulder, Colorado 80309-0425

One method for extracting the frequency-dependent S-parameters of an air-loaded symmetric step-in-width microstrip junction is the so-called bivariational technique. This approach involves the application of a simple trial current density to a bivariational functional in order to obtain a more accurate total current. The frequency-dependent S-parameters accounting for the junction radiation and reactance can be extracted from this corrected total current. This talk deals with the generation of a simple trial current density function for the bivariational analysis of an air-loaded symmetric step-in-width junction. Recent investigations of this junction have shown that the trial current density must be continuous throughout the microstrip junction. Our approach for generating such a trial current is based on the technique of conformal mapping. This method involves several steps. First, the conformal transformation for the dual electrostatic problem of a parallel-plate step in separation is solved for. This conformal transformation is then used in conjunction with a perturbation/iterational technique to compute exactly the first few static mode coefficients in both the wide-spaced and narrow-spaced parallel-plate regions. Higher mode coefficients are then derived from a simple recurrence formula, based on the edge condition. Once all of the necessary mode coefficients have been determined, we can convert them into a time-static current density using duality. The time-static current densities for the narrow and wide strip regions are now in the form of a simple Fourier series of exponential and trigonometric functions, and they are particularly suited for the bivariational analysis.

B5-3
1440

MODE-MATCHING FORMULATION FOR COMPLETE MODAL SPECTRUM OF DIELECTRIC WAVEGUIDES WITH UNIFORM SURROUND

D.P. Nyquist, E.J. Rothwell and P.F. Havala
Department of Electrical Engineering
Michigan State University
East Lansing, MI 48824

Mode-matching techniques for quantification of discrete surface-wave modes supported by dielectric waveguides of widely varying configurations have received exhaustive treatment in the recent literature. The continuous component of the complete propagation-mode spectrum has, in contrast, received relatively little attention. It is demonstrated, for the restricted class of arbitrarily-shaped, step-index guiding regions immersed in a uniform surround, that the mode-matching technique can be exploited to quantify the complete spectrum of such open-boundary waveguides. Radiation fields arising from this description may be valuable in excitation, coupling and scattering problems associated with dielectric waveguides.

Let the guiding region be designated as V_g and the surround as V_s. All analysis is performed in the axial Fourier-transform domain; all quantities, e.g., $e(\rho,\zeta)= F_z\{\mathbf{E}(\rho,z)\}$, are transforms depending upon transform variable ζ. Impressed current $j(\rho,\zeta)$ maintains impressed field $e^i(\rho,\zeta)$. The latter field interacts with the guiding region, resulting in scattered field $e^s(\rho,\zeta)$. Consequently the total field in either V_g or V_s is $e = e^i + e^s$. If $j\varepsilon V_s$ then $e^i=0$ in V_g while $e^i=0$ in V_s when $j\varepsilon V_g$, i.e., $e^i\neq 0$ in only one or the other of V_g and V_s. e^i is known, through an appropriate 2-d Green's function $g_\zeta(\rho,\rho')$, for any given j. Circular-harmonic expansions are exploited to represent e^s in the guiding (J_n Bessel series) and surround ($H_n^{(2)}$ Bessel series) regions. Total tangential e and h fields are point matched at the guiding-region/surround interface, leading to a matrix equation for the system of expansion coefficients $[a_n(\zeta)]$ as $[E_{mn}(\zeta)][a_n(\zeta)] = [f_m^i(\zeta)]$ where the forcing vector implicates known impressed field components.

The spatial field is recovered as $\mathbf{E}(\rho,z)=F_z^{-1}\{e(\rho,\zeta)\}$. Evaluation of the inversion integral by appropriate complex ζ-plane analysis leads to the complete propagation-mode spectrum excited by j. Surface-wave modes arise from simple-pole singularities at $\zeta=\zeta_p$, near which $a_n(\zeta)=\tilde{a}_n(\zeta)/(\zeta-\zeta_p)$ so the matrix equation requires $[E_{mn}(\zeta)][a_n(\zeta)]=0$ and $\det[E_{mn}(\zeta)]=0$ at $\zeta=\zeta_p$; this is the familiar mode-matching eigenvalue equation. Integration about branch points at $\zeta=\pm k_s$ leads to the radiation field as a continuous superposition of forced spectral solutions to the fundamental matrix equation. Application of this quantification scheme to the dielectric rectangular waveguide is demonstrated.

B5-4
1520

ON SOMMERFELD-INTEGRAL ELECTRIC FIELD KERNELS FOR MICROSTRIP-BASED CIRCUITS

D.P. Nyquist, M.S. Viola, M.J. Cloud and M. Havrilla
Department of Electrical Engineering
Michigan State University
East Lansing, MI 48824

Microstrip circuits are fabricated over the film/cover interface of a planar, layered conductor/film/cover surround environment. In an electric-field integral equation description of such circuits, the electric field tangential to metallic microstrip conductors, maintained by surface currents on those conductors, is required. A spectral approach through Hertz potentials leads to sommerfeld-type integral representations for required Green's function kernels.

Let the microstrip conductors reside at $y=0^+$, adjacent to the x-z film/cover interface plane. The field $\mathbf{e}(x,\zeta)$ at the conductor surface, maintained by surface current $\mathbf{k}(x,\zeta)$ on that conductor (both in the axial Fourier-transform domain; transform variable ζ), is then

$$\mathbf{e}(x,\zeta) = \lim_{y\to 0^+} (k_c^2 + \tilde{\nabla}\tilde{\nabla}\cdot) \int_{cond} \bar{\bar{g}}_\zeta(x,y|x',0)\cdot\mathbf{k}(x',\zeta)dx'$$

where $k_c=n_c k_0$ (n_c=cover index), $\tilde{\nabla} = \nabla_{xy} + \hat{z}j\zeta$ and $\bar{\bar{g}}_\zeta$ is a Hertz potential Green's dyad in Sommerfeld-integral representation. It is convenient to pass the spatial integral and the differential operator, in turn, through the spectral integral over ξ, since the former operations can all be performed in closed form. This procedure is valid provided the details (source-point singularity) are handled carefully and the $y\to 0^+$ limit is performed lastly. In much of the recent literature, the latter limit is exchanged with the spectral integral; this invalidates the differential-operator exchange and leads to a divergent spectral integration. Consequently, uncertainty has arisen in the choice of appropriate expansion and testing functions for use in MoM solutions to associated EFIE's.

In fact, pulse basis functions and point matching lead to convergent spectral integrals if the $y\to 0^+$ limit is performed appropriately. MoM matrix elements are represented by

$$I_{\alpha\beta} = \lim_{y\to 0^+} \int_0^\infty W_{\alpha\beta}(\xi) e^{-p_c y} \frac{\sin(\xi\delta)}{\xi} \begin{pmatrix}\sin\xi x_m \\ \cos\xi x_m\end{pmatrix}\begin{pmatrix}\sin\xi x_n \\ \cos\xi x_m\end{pmatrix} d\xi$$

where $W_{\alpha\beta}$ is a complicated function of ξ (carrying surface-wave poles of the surround) and $p_c=(\xi^2+\zeta^2-k_c^2)^{1/2}$. The most slowly convergent case is $\alpha=\beta=x$, where $W_{xx}(\xi)\propto\xi$ for large arguments, leading to an undamped oscillatory integrand when $y=0$. It is demonstrated, however, that the $y\to 0^+$ limit does indeed exist, and the convergence rates of the various $I_{\alpha\beta}$ are compared.

B5-5
1540 ALTERNATIVE INTEGRAL FORMULATION FOR ANALYSIS OF MICROSTRIP TRANSMISSION LINES

J. M. Grimm and J. S. Bagby
Department of Electrical Engineering
University of Texas at Arlington, Arlington, TX 76019

For natural modes of an integrated microstrip transmission line, the axially-transformed surface current $\vec{k}(\vec{\rho}';\zeta)$ satisfies the well-known homogenous dyadic integral equation:

$$\hat{t}\bullet(k_c^2 + \nabla\nabla\bullet) \int_{\ell} \ddot{g}(\vec{\rho}|\vec{\rho}';\zeta)\bullet\vec{k}(\vec{\rho}';\zeta)\, d\ell' = 0, \quad \vec{\rho} \in \ell$$

where $\ddot{g}(\vec{\rho}|\vec{\rho}';\zeta)$ is the transformed Hertzian potential Green's dyad of the background structure, k_c is the wavenumber in the cover region, ζ is the complex propagation constant of the mode, t is a unit-tangent to the transmission line, and ℓ is the cross-sectional contour of the line.

The Green's dyad components are typically given as inverse Fourier transforms with respect to ξ, the transform variable corresponding to the x direction. The inversion integrals assume the form of Sommerfeld integrals and are notoriously difficult to compute. Green's dyad component evaluation is further complicated due to surface wave singularities exhibited when the real part of ζ is less than the propagation constant of a surface wave mode in the background structure.

An alternative formulation for the Green's dyad components using complex ξ-plane analysis is presented here. In this method, Cauchy's theorem is used to represent the Green's dyad components as a sum of residues at the surface wave pole singularities plus an integration along a hyperbolic branch cut in the complex-ξ plane. This alternative formulation has the advantage of replacing slowly-convergent Sommerfeld integrals with relatively well-behaved contour integrals.

This alternative Green's dyad formulation is used in the MOM solution of the integral equation above to analyze both narrow and wide microstrip configurations. The above-described advantages are demonstrated for both cases via numerical results.

B5-6
1600

APPLICATION OF METHOD OF LINES TO MULTIPLE STRIP PLANAR PROPAGATION STRUCTURES HAVING INHOMOGENEOUS LAYERS

M.A.Thorburn and V.K.Tripathi

Department of Electrical and Computer Engineering
Oregon State University
Corvallis, Oregon 97331-3202.

This paper deals with the propagation characteristics of a class of general multiple strip structures in layered medium having inhomogeneity in both transverse directions. Such structures have found applications in electro optical devices and the techniques developed can also be applied to study other useful problems such as microstrips near the chip edge in a monolithic circuit.

The method of lines which has been used in recent years to study general propagation structures and discontinuities (Schulz, AEU, 34, 176-178, 1980.,Schulz & Pregla, Radio Science, 16, 1173-1178, 1981.,Worm & Pregla, MTT-32, 191-196, 1984.,Diestel & Worm, MTT-32, 633-638, 1984.,Sherrill & Alexopoulos, MTT-S Digest, 327-329, 1987.) is extended in this paper to apply to problems having inhomogeneity in x direction. Both quasi TEM and frequency dependent full wave solutions are considered. For the quasi TEM case the Greens function interrelating the boundary charge and potential is used to compute the capacitance matrices and the structure properties. The complete full wave problem is formulated in terms of the general impedance matrix (Green's function) of the structure which is used to solve for the eigen values (propagation constants for the normal modes), the current distribution, the line mode impedances and the field distribution of these structures. It is shown that these parameters can be used to compute all the multiport properties such as the scattering matrix elements of general coupled strip structures.

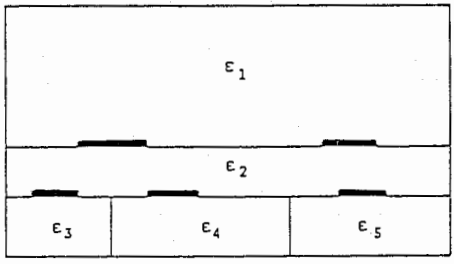

CROSS SECTION VIEW OF A GENERAL STRUCTURE

B5-7 1620 RADIATION FROM TRANSMISSION-LINE "PIGTAIL" CONNECTIONS

H. Hejase
Department of Electrical Engineering
University of Kentucky
Lexington, Kentucky 40506

A. T. Adams
R. F. Harrington
Department of Electrical and Computer Engineering
Syracuse University
Syracuse, NY 13244

The shielding effectiveness of a "pigtail" connection between a coaxial transmission line and a ground plane is treated rigorously by the method of moments, as a function of the type and number of pigtails and frequency. The type of pigtail connection is shown to be crucial with regard to radiation and shielding effectiveness, even though the pigtail itself does not radiate significantly. All pigtails are not equal, even though they may be short electrically. A short pigtail is significantly better than a longer one. A "sloppy" pigtail connection may actually enhance radiation. Multiple pigtails yield signficant improvement over the single pigtail for short pigtails.

A useful equivalent circuit representation of the pigtail problem is given. The pigtail impedance obtained by the method of moments is compared with that obtained by a quasi-static method with agreement to within a few percent for electrically short pigtails. Results have been compared with other theoretical results and with experiment, with good agreement.

C1-1
1400

Spectrum Estimation via Maximum-Likelihood Generation of Toeplitz Constrained Covariances Using the Expectation Maximization Algorithm

Michael Turmon and Michael I. Miller

Electronic Systems and Signals Research Laboratory
Department of Electrical Engineering
Washington University
Saint Louis, Missouri 63130

ABSTRACT

We consider the spectrum estimation problem in which we observe the single $G\times 1$ vector $\mathbf{y}_G$ from a zero-mean Gaussian stationary random process with unknown $G\times G$ Toeplitz covariance $\mathbf{K}_G$. The probability density function describing $\mathbf{K}_G$ is thus

$$g(\mathbf{y}_G;\mathbf{K}_G) = (2\pi)^{-\frac{G}{2}}(\det \mathbf{K}_G)^{-\frac{1}{2}}\exp(-\tfrac{1}{2}\mathbf{y}_G^\dagger \mathbf{K}_G^{-1}\mathbf{y}_G) \quad , \tag{1}$$

with † denoting hermitian transpose. The maximum likelihood problem is to maximize this function with respect to all Toeplitz $\mathbf{K}_G$.

To ensure the existence of a nonsingular estimate when given only one data vector $\mathbf{y}_G$, we perform the maximization subject to the further constraint that $\mathbf{K}_G$ be Toeplitz with a circulant extension of period $N > G$. We generate the estimates iteratively using the expectation-maximization algorithm. Within the context of this algorithm, we choose the incomplete data to be $\mathbf{y}_G$, which data are a part of the larger unobserved $N\times 1$ complete data vector $\mathbf{y}_N$. This complete data vector is from a stationary periodic process of period $N > G$ with $N\times N$ circulant covariance $\mathbf{K}_N$. It has been shown [Miller and Snyder, *Proc. IEEE*, July 1987] that the constrained MLE $\mathbf{K}_G$ in the set of $G\times G$ Toeplitz covariance matrices with N-periodic extension is the convergence point of the iteration sequence given by

$$\mathbf{K}_G^{(p+1)}(\tau) = \frac{1}{N}\sum_{m=0}^{N-1} E\{y(m)y^*(<m+\tau>_N)\,|\,\mathbf{y}_G, \mathbf{K}_G^{(p)}\} \quad , \tag{2}$$

where $<\ >_N$ denotes modulo N. It has been shown that the Toeplitz estimates defined by (2) are monotonic in the likelihood of (1) and remain in the set of positive-definite Toeplitz covariances. Furthermore, all the limit points of (2) are stable and satisfy the necessary conditions for maximizing likelihood over the constrained set of Toeplitz matrices with N-periodic extensions.

C1-2
1440

COMPONENTS OF VARIANCE INTERPRETATION OF SPECTRUM ESTIMATION

Louis L. Scharf and Li Du
Department of Electrical Engineering
University of Colorado - Campus Box 425
Boulder, CO 80309

In this paper we offer a number of alternative interpretations for D.J. Thomson's multiple window spectrum estimators. Each interpretation is coupled to the solution of a detection, estimation, or identification problem that is closely related to the problem of estimating a spectrum in a narrow band. We show that the key step in narrow band spectrum estimation is the projection of the data onto a low rank subspace where its power may be accurately estimated.

C1-3
1540

Time-frequency localization operators - a geometric phase space approach.

Ingrid Daubechies
A.T.&T. Bell Laboratories
600 Mountain Avenue
Murray Hill NJ 07974

In mathematical techniques which require good resolution in both time and frequency domains, it is customary to use the Slepian functions (prolate spheroidal wave functions) associated with the appropriate time and frequency windows, and the corresponding eigenvalues.

This paper shows how a different picture, more geometrical in nature, leads to different families of functions. In particular, if the domain of interest in time-frequency is a disk or an ellips, then the associated eigenfunctions and eigenvalues become Hermite functions and incomplete gamma-functions, respectively. These also have the virtue of being much easier to calculate than the Slepian functions and their corresponding eigenvalues.

C1-4 1620 HARMONIC ANALYSIS ON SYMMETRIC SPACES: Audrey Terras, Dept. of Mathematics, Univ. of California, San Diego, CA

E1-1
1400

VARIABILITY OF THE HIGH-ALTITUDE EMP

Conrad L. Longmire
Mission Research Corporation

ABSTRACT

Classification has severely limited the amount of information on high-altitude EMP (or HEMP) that has reached the public. A result has been the development of the misimpression that the HEMP can be well characterized by giving a single pulse shape with a maximum amplitude. A possible logical consequence is the idea that electrical and electronic equipment hardened and tested to this single pulse will, with high probability, be hard to HEMP in general. The author believes that this idea is almost certainly wrong and at least requires proof with regard to specific equipments. The author's view is prompted by the nonlinearities in the coupling of HEMP into equipments, in the processes of upset and damage, and in some hardening techniques (e.g., limiting).

Classification of HEMP environments stems from the classification of some aspects of the outputs of nuclear weapons such as the actual rise time of the gamma output pulse. We have avoided that problem by assuming a gamma pulse with zero rise time and nominal pulse width and quantum energy. The calculated HEMP as a function of azimuth and ground range for a single burst at 400 km altitude over the central U.S. is presented in this paper. The wide variability in pulse shape and amplitude in these results and the consequent difficulty in selecting a single representative pulse are discussed. The author asks for the advice from the audience as to what kind of HEMP information would be most useful in hardening of systems.

E1-2
1440

NORM LIMITERS COMBINED WITH FILTERS

C. E. Baum
Air Force Weapons Laboratory
Kirtland AFB
Albuquerque, New Mexico 87117-6008

In the general formalism of electromagnetic topology the propagation through and reflection from subshield penetrations of signals is important. This paper considers the characteristics of linear filters and nonlinear devices idealized as norm limiters which can be used at such penetrations. Both frequency-domain and time-domain concepts are employed to limit undesirable signal penetration and reflection.

E1-3
1500

EARLY TIME PERFORMANCE AT LARGE DISTANCES OF PERIODIC ARRAYS OF FLAT-PLATE CONICAL WAVE LAUNCHERS

D. V. Giri
Pro-Tech, 125 University Avenue, Berkeley, CA 94710

and

Carl E. Baum
Air Force Weapons Laboratory/NTAAB
Kirtland AFB, New Mexico 87117

Abstract

Many techniques have been investigated for the purpose of launching transient electromagnetic (EM) waves and the results have been incorporated in the design of various categories of EMP simulators. One such technique involves configuring many sources into an array. The source array synthesizes an appropriate aperture field distribution to launch a desired type of wave. The individual sources are interconnected in some series-parallel fashion, via conducting surfaces which have a significant impact on the early-time rate of rise in the distant field. Both planar and non-planar arrays have been considered in the past.

In this paper, we consider some possible geometries of unit cells in the distributed source or distributed switch wave launchers. Attention is focussed on one aspect of performance, i.e., the rate of rise in the far field (for assumed ideal step-function sources) of candidate unit cell designs. The unit cells considered are planar-conical or non-planar wave launchers. There are perhaps many module or unit-cell designs one may consider, each being associated with its own boundary value problem. Two illustrative examples are presented. Formulae for the early-time rate of rise are developed, tabulated and plotted, as a function of normalized geometrical parameters of an individual launcher and the array.

E1-4
1540

SYNTHESIS OF ANISOTROPIC LENSES FOR INHOMOGENEOUS TEM PLANE WAVES RELATED TO THE DIFFERENTIAL GEOMETRY METHOD

A. P. Stone
University of New Mexico
Department of Mathematics
Albuquerque, NM 87131
C. E. Baum
Air Force Weapons Laboratory
Kirtland AFB
Albuquerque, NM 87117

This talk is concerned with the equivalence of two methods for the design of lenses for TEM plane waves, such as might exist on certain types of transmission lines. The transition region can be used to specify lenses for transitioning TEM waves, without reflection or distortion, between these transmission lines. The desired transmission is to be frequency independent and the lens design is based on frequency independent solutions of Maxwell's equations. One approach to the design of transition regions is a differential geometric one, in which a scaling method creates an equivalence between two classes of electromagnetic problems. An alternative approach requires that differential impedances be matched at all lens-waveguide boundaries and also that a plane wave front in one region should go into a plane wave front in another region. These two methods of EM lens design may be shown to be equivalent. In the case of differential geometric scaling, one finds that for a TEM wave propagating in one of the coordinate directions that both differential-impedance matching and transit-time conservation is obtained at the lens boundaries. On the ther hand, if one starts with the impedance-matching and transit-time requirements, then arriving at the differential geometric conditions requires more effort. In order to obtain these geometric conditions, one must first consider the general case of transport of waves through a set of ducts connecting surfaces which form the boundaries for a lens. One then examines the use of these ducts to reorder positions on a wavefront and then considers two possible ways of arriving at an EM lens design, each the dual of the other.

E1-5
1600

RETURN-STROKE INITIATION

Dr. Carl E. Baum
Air Force Weapons Laboratory
Kirtland AFB
Albuquerque, New Mexico 87117-6008

The far fields from a lightning return stroke are a function of the spatio-temporal distribution of the return-stroke currents. This paper introduces a conical-transmission-line model of the return stroke immediately following leader closure. Based on this model, return-stroke speed is computed and shown to be near c at early times following leader closure. In turn the early-time far fields are also computed. This early-time speed is but one factor influencing the relationship between the return-stroke currents and the far fields. These factors are reviewed and shown to give a wide variation to this relationship, thereby making it difficult to infer return-stroke currents (with any accuracy) from the far fields.

E1-6
1620

Comparison of Lightning Models for Channel Currents and Electromagnetic Fields

Maj. R. L. Gardner
Air Force Weapons Laboratory
Kirtland AFB, NM 87117

Abstract

Many different models have been presented in the literature to predict the electromagnetic fields due to lightning. They generally fall into two categories. The first type is a model of the current in the lightning channel. These models vary from simple curve fits of current waveforms to elaborate nonlinear, nonuniform transmission line models. The second type of model is designed to predict the fields due to the currents predicted by the first type. These types of models vary from simple $1/r$ style radiating dipole models to elaborate propagation codes which include finitely conducting earth effects, scattering from discontinuities, etc.

Models presented in the literature are described and compared in this paper. The information assembled here should aid researchers as they search the literature for lightning models that contain the appropriate physics. Tradeoffs in computational expense compared to modeling detail will be apparent.

E1-7
1640

A CHANNEL ADAPTIVE HIGH THROUGHPUT METEOR SCATTER COMMUNICATION SYSTEM

A. K. Gupta and J. R. Herman
GTE Government Systems Corp.
One Research Drive
Westborough, MA 01581

The present paper discusses an adaptive high throughput meteor scatter communication system, which maintains a constant high data-rate over the trail life-time despite time-varying path losses, time-varying doppler and multipath spread during this time. The proposed system employs the coding and the interleaving in addition to the M-ary incoherent FSK signalling with waveform diversity, utilized in the earlier proposed system (A. K. Gupta and M. D. Grossi, Proc. of Ionospheric Effects Symposium, Alexandria, VA, 282-296, 1981; A. K. Gupta, National Radio Science Meeting, Houston, TX, Abstract, 1983).

A formula for varying M-ary signal alphabet, to provide a constant high data rate, is also provided for trade-off analysis with respect to specified performance, meteor burst channel parameters, data rate, code rate, code diversity, etc.

Session F-1 1355-Weds. CR2-28
SATELLITE REMOTE SENSING
A. SPECIAL SESSION ON SSM/I
Chairman: J.P. Hollinger, Space Sensing Branch, Naval Research Lab, Washington, DC 20375-5000

F1-1
1400

SSM/I POST-LAUNCH RADIOMETRIC SENSITIVITY, STABILITY AND BEAM POINTING ACCURACY

G. A. Poe and J. P. Hollinger
Space Sensing Branch
Naval Research Laboratory
Washington, DC 20375-5000

Results are presented of the radiometric sensitivity and stability and antenna beam pointing accuracy of the SSM/I instrument over the first six months of operation. Both hot load and cold reflector calibration data are analyzed to estimate the sensitivities for all seven channels and the orbital drift of the gains of the radiometers. The RMS instrument noise is well within instrument specification and the radiometer gain is very stable over all data examined.

In addition the repeatability of the SSM/I brightness temperatures is determined by examining numerous histograms of data collected over many months of selected geographical regions, the Congo Basin, the Amazon Basin, the Libyan Desert and the Sargasso Sea. These data substantiate the excellent radiometric stability of the SSM/I.

The possibility of reducing fluctuations in the radiometer calibration data due to instrument noise are presented along with a suitable calibration algorithm to perform the filtering. The reduction of the radiometer delta-G over G are presented in terms of the number of scans of calibration data averaged.

Estimates of the antenna beam pointing accuracy are presented which were derived by comparing the radiometric signatures of land/water boundaries and with well known geographical maps.

F1-2
1420

VALIDATION/CALIBRATION OF THE SSM/I ABSOLUTE CALIBRATION ACCURACY

J. P. Hollinger and G. A. Poe
Space Sensing Branch
Naval Research Laboratory
Washington, DC 20375-5000

Two approaches are being used to validate the absolute calibration of the SSM/I: 1) comparison of SSM/I brightness temperatures with those from the aircraft borne SSM/I simulator and 2) comparison with an environmental microwave radiative transfer model.

The Naval Research Laboratory RP-3A aircraft with the SSM/I simulator radiometer instrument is used to underfly the SSM/I satellite sensor. The SSM/I simulator is a non-scanning set of radiometers at the same frequencies and polarizations (19.4 Ghz H and V, 22.235 Ghz V, 37.0 Ghz H and V and 85.5 Ghz H and V) viewing the earth's surface at the same incidence angle as the conical scan angle of the SSM/I. The underflights were concentrated in the open ocean under various sky conditions since the ocean surface provides a set of significantly polarized brightness temperature signatures. Locations were chosen well away from land to avoid antenna sidelobe contamination and were at 8 km altitude above nearly all of the atmospheric absorption. Flight lines were in the form of a cross with 150 km legs to enable spatial and temporal comparison with the SSM/I footprints.

Ocean regions with very low 85.5 Ghz brightness temperatures where clear/dry atmospheric conditions were known to prevail were selected for comparison with model generated brightness temperatures. Environmental conditions used in the model were obtained from buoys and ships where possible and estimated otherwise. The estimates were based on climatology for that latitude and time of year as well as a study of other satellite weather data for the area.

F1-3
1440

STATUS REPORT ON THE SPECIAL SENSOR MICROWAVE/IMAGER CLOUD AMOUNT VALIDATION

G.W. Felde and R.W. Conant, Jr.
Air Force Geophysics Laboratory
Atmospheric Sciences Division
Satellite Meteorology Branch (AFGL/LYS)
Hanscom AFB, MA 01731

The new Special Sensor Microwave/Imager (SSM/I) is a seven channel, four frequency, linearly polarized, passive microwave radiometer which is onboard a polar-orbiting spacecraft launched in June 1987. The SSM/I provides estimates of several surface and atmospheric parameters. The Air Force Geophysics Laboratory is validating the cloud amount parameter (percent cloud coverage). Hughes Aircraft Company developed two algorithms for estimating cloud amounts from SSM/I brightness temperatures. One is applicable over snow backgrounds; the other over land backgrounds. However, it is not possible to obtain cloud amount estimates for land covered with vegetation. No cloud amount estimation algorithms for ocean or oceanic ice backgrounds were required to be developed; even though the potential over both of these backgrounds is good.

The ground truth cloud amounts used for validation are obtained from interactive computer analyses of 1.5 nautical mile resolution visible and thermal infrared meteorological satellite data. These data are from the scanning radiometer called the Operational Linescan System (OLS). The OLS is onboard the same spacecraft as the SSM/I and thus there is a good temporal match between the two data sources. Ground truth sites are located over North America and Greenland. Statistical comparisons between SSM/I and OLS cloud amount values are being generated. Two sets of validation statistics are presented, one for land backgrounds and one for snow backgrounds.

F1-4
1500

PRELIMINARY RESULTS ON THE VALIDATION OF ICE ALGORITHMS FOR THE SSM/I

Rene O. Ramseier
Atmospheric Environment Service
(AES)/Center for Research in
Experimental Space Science (CRESS)
York University
4700 Keele Street
North York, Ontario M3J 1P3

Cathryn Bjerkelund
Norland Science and Engineering LTD

Irene Rubenstein
CRESS

The validation of the SSM/I ice algorithm is part of the total validation/calibration effort being coordinated by the Naval Research Laboratory and commenced June 28,1987 with ice information (ground truth) obtained from the Beaufort and East Greenland Seas. The results to be presented will cover the melt season, (the most difficult period for ice interpretation), the onset of freezing, and the early part of the winter. The surface observations are based primarily on data obtained from Side Looking Airborne Radars (SLAR) as part of the operational ice reconnaissance activities of AES, and from ship observations (visual and 37 GHz H and V) of brightness temperatures in Baffin Bay and East Greenland Seas, respectively.

The SSM/I ice algorithm developed by Hughes Aircraft Company and coded to run operationally at the Fleet Numerical Oceanography Center and the Air Force Global Weather Center, currently employs only the 37 GHz vertically and horizontally polarized channels. Preliminary results indicate that the algorithm provides ice edge, ice concentration and ice type (age) that agree reasonably well with surface observations. Due to restrictions imposed on the creation of the Hughes algorithm in the late seventies and the scientific advances since that time efforts are underway to improve the current algorithm using the 19.35 GHz channels with the 37 GHz channels in a AES/PHD algorithm.

F1-5
1520

SSM/I WIND SPEED VALIDATION

John C. Wilkerson
NOAA/NESDIS
Washington, D.C.

Mark A. Goodberlet
Calvin T. Swift
Kuo Hua Hsush
University of Massachusetts
Amherst, Massachusetts

Abstract

The accuracy of ocean surface wind speed from the Special Sensor Microwave Imager (SSM/I), launched in June 1987, is assessed by comparing SSM/I-derived winds with coincident wind speeds measured from moored ocean buoys operated by the National Data Buoy Center, NOAA. The SSM/I environmental extraction (D-matrix) algorithm, developed by Hughes Aircraft Company, retrieves wind speed by latitude/climate zones using brightness temperatures at 19, 22 and 37 GHz as independent variables in a series of 11 linear regression equations.

Evaluation of performance is presented for 6 of these equations representing summer and fall conditions from the tropics to the arctic. Where the operational algorithm fails to retrieve winds to the accuracy goal of 2.0 m/s RMS, new sets of coefficents for the equations are derived from independent data to remove the constant and scale biases and bring the measurement within specification.

Case studies of tropical storms over the Pacific Ocean reveal the limits of sensor capability to recover winds in the presence of clouds, light rain and high gradient zones. Global maps of SSM/I-derived wind speeds are analyzed over 7-day periods to demonstrate self-consistency of the data and to show regional and seasonal characteristics of the ocean wind field. Histograms of SSM/I-derived wind speeds are compared to typical distributions of global wind observations for various latitude bands and seasons to reveal the quality and consistency of the SSM/I global data set.

F1-6
1600

SIMULATED AND ACTUAL SAR IMAGES: A COMPARISON

Robert O. Harger and Can E. Korman
Electrical Engineering Department
University of Maryland
College Park, MD 20742

The synthetic aperture radar (SAR) images obtained with the Jet Propulsion Laboratory's L-band system in the TOWARD oceanographic experiment are compared with images generated by a simulation program implementing a SAR ocean imaging model based on two-scale hydrodynamic and electromagnetic scattering approximate models. The primary means of comparison here is an estimate of the best focus parameter than uses a sub-image cross-correlation technique.

The focus parameter estimates for the actual and simulated images both show (i) a reversal in sign with reversal in dominant long wave direction relative to the SAR direction, (ii) a magnitude increase with an increase in magnitude of the angle between the dominant long wave and SAR axes, and (iii) an independence of the altitude and also the range-to-velocity ratio. These behaviors are in agreement with a related analytical prediction. All equivalent velocity estimates are of the order of the dominant long wave phase velocity, normalized by the SAR vehicle velocity. The comparisons agree well qualitatively though there are some quantitative differences.

Experimental observations over about a decade may indicate that the two-scale, or WKB, hydrodynamic model underestimates the strength of the interaction between the long and short waves. It was found that an increase in this strength by about an order of magnitude rendered much better agreement in the images and their estimated spectral densities of the simulated and actual SAR images.

F1-7
1620

ANTENNA PATTERNS FROM A CROSS ANTENNA

Andrew S. Milman
Radar Science Laboratory
Advanced Concepts Division
Environmental Research Institute of Michigan
Ann Arbor, MI 48107

Microwave radiometric imaging of the earth from space will provide important meteorological information about water in all of its forms: liquid water, water vapor, and ice. Microwave images can provide information about soil moisture and sea surface temperature, for example, in the presence of clouds and the absence of sunlight. In order to get high spatial resolution (1 to 5 km) at the low frequencies (1.4 to 18 GHz) needed for these measurements, an antenna is needed with an aperture of 20 m or more. This requirement can only be met with sparse antenna arrays.

Of the possible sparse array radiometric antennas, the most promising seems to be the cross antenna; it is two linear arrays placed at right angles to each other. Because there are two continuous arrays of antenna elements, beamforming techniques can be used to synthesize a beam of size λ / D, where λ is the wavelength and D the length of one arm of the cross, thus allowing the use of very wide rf bandwidths and therefore good radiometric sensitivity.

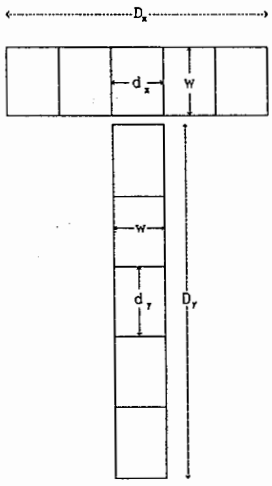

With any array antenna, there is the worry that there might be severe problems with side lobes. We can show, however, that

1) The antenna pattern can be modified either by processing the image from the radiometer; or by
2) Weighting the signals from the different antenna elements (i.e., tapering the array).

These two processes will yield equivalent results. We can also show that any antenna pattern we want can be synthesized for the cross antenna, subject only to the limitation that an aperture of finite size imposes.

F1-8
1640

SEA-BED PROPAGATION OF ELECTROMAGNETIC FIELDS FROM HARMONIC DIPOLE SOURCES LOCATED ON THE SEA FLOOR

A.C.Fraser-Smith[1], A.S.Inan[2], O.G.Villard, Jr.[1]
[1] STAR Laboratory
Stanford University
Stanford, California 94305
[2] Science and Engineering Research Center
Bilkent University
P.O.B. 8, 06572 Maltepe, Ankara, Turkey

Electromagnetic fields generated by vertical and horizontal, electric and magnetic dipoles located along the sea/sea-bed interface are considered. The interface is assumed to be a plane boundary separating two semi-infinite conducting media representing the sea and the material comprising the sea bed. All the components of the electric and magnetic fields derived previously for harmonically-varying current dipole sources are numerically evaluated and compared with those that would be produced under the same conditions in sea water of infinite extent. It is found that (1) the fields can propagate to longer distances along the sea floor because of the lower sea-bed conductivities, and (2) new field components are produced as a result of the presence of the sea/sea-bed interface. Some of these new components are larger at longer distances than the other field components; they are also more sensitive to the conductivity of the sea bed at low frequencies. The results could have applications in undersea communication and geophysical prospecting.

Session G-3 1355-Weds. CR2-26
IONOSPHERIC MODIFICATION
Chairman: Frank Djuth, The Aerospace Corp., Los Angeles, CA 90009

G3-1
1400 MEASUREMENT OF ELF FROM MODULATION OF THE POLAR ELECTROJET FROM THE HIPAS FACILITY NEAR FAIRBANKS, ALASKA

A. J. Ferraro and H. S. Lee
Communications and Space Sciences Laboratory
Department of Electrical Engineering
University Park, PA 16802
J. V. Olson
Geophysical Institute
University of Alaska at Fairbanks
Fairbanks, Alaska 99775-0800

ELF and VLF electromagnetic waves were generated from modulation of the polar electrojet in the frequency range of 200 Hz to 5000 Hz using the HIPAS heater facility near Fairbanks, Alaska. The HIPAS (High Power Auroral Stimulation) facility is operated by UCLA (Dr. A. Wong, Director) and during the period of June 10-25, 1987 extensive measurements were made at ELF and VLF for the first time using that facility. During strong electrojet conditions, locally detected magnetic field strengths up to 6×10^{-9} Gauss were obtained while during quieter current conditions, 2×10^{-10} Gauss were obtained. This compared with 1.5×10^{-11} Gauss measured in 1981 by Ferraro and Lee due to modulation of the dynamo current system near the Arecibo Observatory in Puerto Rico.

The results of ELF frequency stepping, polarization and beam swinging experiments will be described.

G3-2
1420 HIGH LATITUDE D-REGION ELECTRON DENSITIES ESTIMATED FROM STEPPED FREQUENCY ELF GENERATED FROM THE MODULATED POLAR ELECTROJET

A. J. Ferraro
Communications and Space Sciences Laboratory
Department of Electrical Engineering
University Park, PA 16802

The HIPAS (High Power Auroral Stimulation) heater facility near Fairbanks, Alaska was used for the first time in June 1987 to generate and measure ELF/VLF from modulation of the polar electrojet. ELF frequency stepping in the range of 200 Hz to 5000 Hz was performed several times with good signal-to-noise ratios. This paper explores the potential of using such data as a means of estimating D-region electron densities. Since magnitude and phase can be scanned versus frequency in a few minutes, such D-region sounder data can be interpreted with full wave solutions to estimate a model D-region for the electron densities. A sweep frequency polarimeter will be described for performing such experiments.

G3-3
1440 ILLUMINATION OF IONOSPHERIC IRREGULARITIES WITH HIGH-POWER RADIO WAVES

Paul A. Bernhardt
Naval Research Laboratory
Washington, DC 20375-5000

Lewis M. Duncan
Clemson University
Clemson, SC 29634

Craig A. Tepley
Arecibo Observatory
Arecibo, PR 00613

New observations of plasma structure were made during the January-February 1987 heating campaign at Arecibo, Puerto Rico. The airglow excited by the 400 KW HF transmitter was recorded with an intensified charge-coupled-device (CCD) camera filtered at the red-line (630.0 nm) of atomic oxygen. Images of the airglow show 1) the radiation pattern of the transmitting antenna, 2) natural field-aligned irregularities, and 3) heater induced cavities. The irregularities drift with the $\underset{\sim}{E} \times \underset{\sim}{B}$ velocity of the plasma. If the relative motion between the neutrals and plasma is large, irregularities or cavities steepen due to the E x B gradient drift instability.

G3-4
1500

LARGE F-REGION ELECTRON-TEMPERATURE ENHANCEMENTS GENERATED BY HIGH-POWER HF RADIO WAVES

F.T. Djuth[1], A.L. Newman[1], B. Thidé[2], H.M. Ierkic[3], M.P. Sulzer[3], H.C. Carlson[4], G.P. Mantas[5]

[1]Space Sciences Laboratory, The Aerospace Corporation, El Segundo, CA 90245
[2]Uppsala Ionospheric Observatory, S-755 90, Uppsala, Sweden
[3]Arecibo Observatory, P.O. Box 995, Arecibo, PR 00613
[4]Air Force Geophysics Laboratory, Hanscom Air Force Base, MA 01731
[5]University of Patras, Greece

During recent experiments conducted at Arecibo, Puerto Rico, large (1000-2000 K) enhancements in electron temperature have been observed when high-power radio waves reflect near the nighttime F-region peak. The electron temperature enhancements are accompanied by significant (50-300 K) increases in ion temperature, large (10-15%) reductions in electron density, and strong HF-induced spread F. To determine the cause of the large HF-induced temperature enhancements, we performed a theoretical study which utilized an F-region thermal response model described by (G. P. Mantas et al., J. Geophys. Res., 86, 561-574, 1981). The results indicate that low collisional cooling rates combined with strong thermal conduction along geomagnetic field lines play a key role in elevating F-region temperatures under current nighttime observing conditions at Arecibo. The observed temperature enhancements are attributable to low electron densities at the F-region peak. Because the induced temperature perturbations are so large, these experiments allow one to directly measure atmospheric cross sections and reaction rates that are difficult to determine by other techniques.

G3-5
1540

IONOSPHERIC MODIFICATIONS DUE TO LIGHTNING INDUCED ELECTROMAGNETIC WAVES

C.P. Liao, K.M. Groves, D.R.Rivas, M.C. Lee
Massachusetts Institute of Technology
Cambridge, Massachusetts 02139
S.P. Kuo
Polytechnic University
Farmingdale, New York 11735

It is generally believed that lightnings can produce significant ionospheric effects. For example, lightning induced atmospheric gravity waves have been suggested to trigger the equatorial spread F. Enhanced radar eches were constantly recorded at the equator during lightning storms by the Jicamarca radar operated at the frequency of 50 MHz. These radar echoes were detected by the radar whose beam angle is 90 with respect to the geomagnetic field in the ionospheric F region. They were seen to have fast rise time and decay time, indicating the excitation of short-lived meter-scale ionospheric irregularities. This phenomenon was termed " explosive spread F " first by Woodman and LaHoz (1976). Close correlation between the occurrence of lightning storms and the observation of explosive spread F was further confirmed by observations made by Woodman (1984) and LaHoz (1984) independently. We examine the interactions of lightning induced VLF waves with the ionospheric plasmas as a potential mechanism generating the short-lived meter-scale ionospheric irregularities. The process under consideration involves a parametric instability that can concurrently excite lower hybrid wave modes. The predicted plasma wave characteristics will be compared with observations and other mechanisms will be commented.

G3-6
1600

RADIO WAVE SCATTERING FROM ARTIFICIAL PLASMA LAYERS

M.C. Lee, D. Thurairatnam, E.R. Williams
Massachusetts Institute of Technology
Cambridge, Massachusetts 02139

Conceptualized plasma layers generated by high power radio waves in the atmosphere have been investigated theoretically by A.V. Gurevich and coworkers with intention to extend the capability of ionospheric radio communications. The required power is very high and not achievable with any existing radar facilities. However, laboratory experiments have been conducted for corroborating the concepts and the predicted plasma characteristics. We note that the plasma layers generated in the chamber experiments often have rough surfaces. It is also expected that the conceptualized plasma layers created in the atmosphere by radio waves cannot have smooth surfaces. In this paper we investigate the effect of roughness on the radio wave scattering from the artificial plasma layers. This problem has been analyzed theoretically. The results shall be compared with our recent radar observations of lightning induced plasmas. The theoretically expected wavelength dependence of power reflectivity is clearly indicated in our radar experiments though the lightning induced plasmas may have very different shapes in comparison with the electromagnetic wave produced plasmas.

G3-7
1620

STUDY OF IONIZATION OF THE LOWER IONOSPHERE BY TWO CROSSED RADIO PULSES (LABORATORY SIMULATION)

Y.S. Zhang and S.P. Kuo
Polytechnic University, Route 110, Farmingdale, N.Y. 11735

Experiments have been set up to produce a plasma in a large chamber which simulate the ionization process of the lower ionosphere by strong radio pulses. The chamber is a 2' x 2' x 2' cube of plexiglass that is filled with argon gas to a pressure range from 50m torr. to 1.8 torr. Microwave beams are fed into the cube by two s-band microwave horns placed at right angles to adjacent sides. The scheme of using two crossed high power microwave beams is employed to generate an ionized layer in the center of the cube where the beams intersect. This approach enables us to simulate how to scan the ionized layer in the atmosphere, and also to minimize beam energy loss before reaching the designated region for ionization.

The microwave power is generated by a single magnetron tube (OKH1448) driven by a soft tube modulator. The magnetron produces 1 MW peak output power at a frequency of 3.59 to 3.7 GHz. The modulator uses a pulse forming network (PFN) having a pulse width of 1.1 microseconds and a repetition rate of 60 cycles.

The detailed arrangement of the experimental set up will be described. Also, plasma has already been produced, and the experimental results which clearly demonstrate the success of this scheme will be presented.

G3-8
1640

IONOSPHERIC MODIFICATION OVER ARECIBO DURING THE SPACELAB 2 MISSION

P.A. Bernhardt
Naval Research Laboratory
Washington, DC 20375-5000

C.A. Tepley and M.P. Sulzer
Arecibo Observatory
Arecibo, PR 00613

W.E. Swartz and M.C. Kelley
Cornell University
Ithaca, NY 14853

On July 30, 1985, the Orbital Maneuvering Subsystem (OMS) of the Space Shuttle deposited 279 kg of exhaust near the peak of the night-time F-layer. The Arecibo incoherent scatter radar recorded the resulting disturbance in the plasma densities. The expanding exhaust vapors produced a plasma hole with density enhancements on the top and bottom sides. The enhancement disappeared after 30 seconds. The depletion lasted for over 300 seconds when it was convected through the bottomside F-layer. The long-lasting hole was produced by chemical reactions between the neutral exhaust and the ambient plasma. Excited states of atomic oxygen were produced during the chemical process. Measurements by photometers and intensified imagers showed that most of the ionospheric modification occurred 80 km downstream from the center of the engine burn. This was the distance required for the supersonic exhaust to come to rest in the rarefied environment of the upper atmosphere. Revised theoretical models are required to explain the results from the Spacelab 2 experiment.

H1-1
1400

DIRECTIONAL INFORMATION IN DOPPLER-BROADENED VLF WAVE SPECTRA

H.G. James
Communications Research Centre,
P.O. Box 11490, Station "H",
Ottawa, Ontario K2H 8S2
Canada

The spectrum of Doppler-broadened signals received on ionospheric spacecraft from VLF transmitters on the ground has been found to depend on the direction $\underline{L}$ of the receiving dipole antenna. The received spectrum is interpreted as corresponding to a distribution of quasi-electrostatic waves whose wave vectors lie close to the whistler-mode resonance cone. In typical observations from the ISIS-II VLF receiver, the carrier frequencies lie between 10 and 20 kHz, and the plasma and gyrofrequencies are much greater than these transmitter frequencies. The result is that the resonance cone lies within a few degrees of the perpendicular to the terrestrial magnetic field $\underline{B}_0$. When, as a consequence of satellite cartwheel spin, the angle $(\underline{L},\underline{B}_0)$ becomes small, the dipole discriminates against waves whose $\underline{E}$-vectors are in the spin plane, near the resonance cone and therefore nearly perpendicular to the dipole.

At moderately high latitudes where broadening is observed, the magnetic field direction is roughly vertical. Because the spacecraft velocity is horizontal, the discrimination against $\underline{E}$-vectors in the spin plane on one side of the resonance cone is a discrimination against Doppler components with a particular sign. As $(\underline{L},\underline{B}_0)$ passes through its minimum, the received spectrum evolves from one with enhanced positive Doppler components to one with enhanced negative Doppler components, or vice versa. The result is a characteristic downturn or upturn in the frequency-time signature of a VLF tone at constant carrier frequency. The angle between the satellite-spin and orbit-normal vectors determines uniquely whether an upturn or downturn obtains. This holds for both northbound and southbound passes in both hemispheres.

Theoretical calculations of the temporal variation of the Doppler spectrum based on the quasi-electrostatic postulate agree with observations from ISIS II. In certain cases, better fits to the observations are obtained with $\underline{k}$ vectors confined to a narrow range of azimuths about $\underline{B}_0$ rather than distributed evenly throughout all azimuths.

H1-2
1420

ULF/ELF/VLF PROPAGATION FROM A SPACEBORNE ELECTRODYNAMIC TETHER TO A SATELLITE-BORNE RECEIVING TERMINAL

Mario D.Grossi
Harvard-Smithsonian Center For Astrophysics
Cambridge, Massachusetts 02138

An electrodynamic tether, such as the forthcoming Shuttle-borne TSS-1, will generate e.m. waves at ULF, ELF , VLF, and possibly in other bands. These waves are expected to leak to the Earth surface. However, because the losses incurred in crossing the ionosphere/atmosphere boundary are substantial (at ULF/ELF only 1% of the power leaks through at night, and only 0.1 % in day time), experimenting with this propagation path requires a long integration time, and this precludes the measurement of short-time features of the e.m. waves.

We are investigating an experimental configuration that will avoid boundary-crossing, by using a satellite-borne receiver in Earth orbit. We could therefore keep the integration time very short, thus detecting rapidly-varying phenomena in the propagation path. Even more important, we would also maximize the probability of receiving above noise the e.m. waves radiated by the tether.

In the 16 hours or so that TSS-1 will radiate, a SAN MARCO satellite (designed and constructed in Italy by PSN), suitably instrumented, could be injected in orbit and perform propagation measurements with path lengths up to several thousands Kilometers, achieving various terminal-to-terminal geometries and magneto-conjugacy conditions. The instrumentation would consist of receivers and magnetic-dipole antennas in three bands : (a) 3 to 30 Hz (ULF); (b) 30 to 300 Hz (ELF); and (c) 3 to 30 KHz (VLF).

The orbital mechanics problems in performing effectively this space science mission are several and far from simple. We are helped by the fact that SAN MARCO has a choice of orbital inclinations from equatorial to polar, and a reasonably broad height range. An important requirement is that we cross at least once the tube of flux of the geomagnetic line of force where TSS-1 is located and is radiating. We would also like to explore the effect of L-conjugacy on propagation, and to measure path losses across lines and shells. This experiment would provide a thorough check of propagation theory for the ULF, ELF and VLF bands in the magneto-ionic medium of the Earth ionosphere.

The results of this experiment would be of value in assessing the ability of an electrodynamic tether to function as generator/radiator of e.m. waves, an assessment that is relevant both from a scientific and from an application standpoint.

H1-3
1440

3-DIMENSIONAL IONOSPHERIC RAY TRACING: AN APPLICATION OF SCIENTIFIC DATA VISUALIZATION

Denis J. Donohue
Space, Telecommunications and Radioscience Laboratory
Stanford University
Stanford, California 94305
James L. Green
NASA Goddard Space Flight Center, Code 630.2
Greenbelt, Maryland 20771

In this talk we describe a fully 3-dimensional computer ray tracing program which has been specially developed for ionospheric propagation studies. The program was initially written by Stan Shawhan at the University of Iowa in the mid-1960's and has been used in investigating propagation and source region characteristics of the earth's auroral kilometric radiation and Jupiter's decametric and kilometric emmisions. The program has now been modified for calculating ray paths of electromagnetic radiation in earth's ionosphere and incorporates several new developments including high resolution display graphics. The recently developed International Reference Ionosphere (IRI) model is used to describe earth's complex ionospheric plasma distribution. The IRI determines the electron density and temperature as well as the composition of 5 species of ions (H+, He+, O+, NO+ and N2+) at any point in the ionosphere.

For display of the ray path calculations, a powerful graphics package has been developed on a Silicon Graphics IRIS workstation which gives a complete 3-dimensional perspective of the ray paths and magnetic field lines and permits arbitrary rotation and spatial scaling of the image. This technique greatly facilitates the interpretation of complex 3-D ray paths in the ionosphere and will aid in the comparison of the ray path calculations to shuttle and satellite based wave observations and future wave generation experiments.

The talk will include a description of the ray tracing program, corresponding plasma and magnetic field models, and graphic displays. A videotaped demonstration of the IRIS display will also be shown.

Session G/H-1 1535-Weds. CR1-9
IONOSPHERIC-INDUCED ERRORS IN RANGING/DOPPLER SYSTEMS
Chairman: M.D. Grossi, Harvard-Smithsonian Center for Astrophysics, Cambridge, MA 02138

G/H1-1
1540

IONOSPHERIC EFFECTS ON TARGET DETECTION BY AN INTERFERENCE-CLUTTERED MULTI-CHANNEL SYSTEM

A. K. Gupta
GTE Government Systems Corp.
One Research Drive
Westborough, MA 01581

In this paper, modern detection theory principles are applied to determine the effects of a propagation channel, such as Ionosphere, on the fixed target detection in an interference environment by a multi-channel system (such as diversity, phased-array antenna, multibeam antenna system, etc.). The ionosphere is assumed to transform a deterministic signal to a Gaussian signal with Rayleigh amplitude and random phase. The interference in this paper is modelled as correlated white noise. The problem therefore reduces to that of detection of a known vector signal in correlated vector noise and to that detection of a Gaussian signal in correlated vector noise.

The determination of Ionosphere effects involves the development of optimal receivers and the analysis of probability of detection for a deterministic channel and for a random channel in an interference environment. The difference in optimal performance (by employing corresponding optimal receivers) may be attributed to Ionospheric effects. Various forms of optimal receivers are discussed in this paper, some of which may be easily adapted in real-time. The formulas for performance analysis are also useful in determining the number of channels required to counteract the ionospheric effects in the interference environment.

The approach considered in this paper can be generalized to the problems involving WSSUS ionospheric propagation channel with multipath and/or doppler spread, and phase-only ionospheric effects in various interference environments.

G/H1-2
1600

Propagation Effects on Space-based Radar

Suman Ganguly
Center for Remote Sensing
8200 Greensboro Drive, Suite 503
McLean, VA 22102

This paper describes the results of a preliminary study regarding the effects of ionosphere and atmosphere on the design of a space-based radar. Manifestation of primary concern is the severe random fluctuations of electron densities in the E and F regions of the ionosphere. These irregularities can produce scintillations in amplitude and phase of a signal propagating through the medium; they also produce radar clutter for signals that are scattered from these irregularities. Several other issues that would be of concern for the design of a SBR are addressed. We describe these relevant processes and provide recommendations for understanding them. It is stressed that the design of the SBR is intimately connected with these propagation issues, and theses issues must be an integral part of the design of the SBR architecture.

Session J-3 1355-Weds. CR0-30
IMAGE PROCESSING IN ASTRONOMY
Co-Chairmen: T.J. Cornwell and R.D. Ekers, National Radio Astronomy Observatory, Socorro, NM 87801

J3-1 1400 IMAGE RECONSTRUCTION FROM COHERENCE: J.L. Yen, Univ. of Toronto, Toronto, Ontario M4S 1A7 Canada

J3-2 1420 NOISE IN IMAGES OF VERY BRIGHT OBJECTS: R.D. Ekers, National Radio Astronomy Observatory, Socorro, NM 87801

J3-3
1440

REDUCTION OF SCANNING NOISE IN RASTER SCANNED DATA

D. T. Emerson
National Radio Astronomy Observatory
949 North Cherry Avenue
Tucson, AZ 85721

In many branches of science a 2-dimensional image of an object under study is obtained by raster-scanning a sensor across the region of interest. In general, because of unavoidable instrumental offsets and drifts, the baselevel of each individual linear scan has to be corrected. The most commonly used technique is to subtract a linear or higher order baseline derived from regions of each linear scan believed to be free from emission.

This suffers from errors resulting from:

(1) the necessary assumption of emission-free regions. This requires prior knowledge of the object, or that an unreasonably large area be sampled;
(2) random noise levels which may cause errors in the derivation of baselines, and
(3) the danger of distorting real features by an unwise choice of zero regions or by the use of higher order baseline fits.

This paper describes an alternative derivation of baseline corrections, making use of two or more data sets taken with different scanning angles. The data are treated in the Fourier domain, providing a unique, analytic, non-iterative and computationally efficient solution to the problem.

J3-4
1500 A COMPARISON BETWEEN FULLY FILLED APERTURE AND NON-REDUNDANT MASK IMAGING: T. Nakajima, California Institute of Technology, Pasadena, CA 91125

J3-5
1520

SELF-CORRECTION OF TELESCOPE SURFACE ERRORS USING A CORRELATING FOCAL PLANE ARRAY

P. J. Napier and T. J. Cornwell
National Radio Astronomy Observatory
P.O. Box 0
Socorro, New Mexico 87801

In recent years the technique of "self-calibration" has dramatically improved the quality of radio images obtained with synthesis telescopes by removing the effects of atmospheric phase fluctuations and other aberrations. In this paper we point out that self-calibration can be extended to remove the effects of various aberrations, including reflector profile errors, from images obtained in the focal plane of large single reflector telescopes. Focal plane self calibration requires that the spatial coherence function of the image be measured with a focal plane array attached to a correlator. Some of the practical difficulties to be solved in applying the technique include satisfying the focal plane spatial sampling theorem and building sufficiently large correlators.

J3-6
1540

VLA OBSERVATIONS OF SPECKLES IN INTER-PLANETARY SCINTILLATION

T. J. Cornwell, K. Anantharamaiah[1] and R. Narayan[2]
1 National Radio Astronomy Observatory
P. O. Box 0
Socorro, NM 87801
2 Steward Observatory
Tucson, AZ 85721

Historically, the scintillation patterns due to scattering in the solar wind have been studied via the fluctuations in total power received either at a single point as a function of time, or at many points simultaneously. However, extra information is available from measurements of fluctuations in the coherence function measured by an interferometric array. Snapshots of sufficiently short integration (less than 10-50 msec) should freeze the scintillation pattern on the ground. An image made by an interferometric array in that time will therefore show "speckles" similar to those seen in optical imaging through the Earth's atmosphere. The radiation from the different speckles must be coherent, and so the usual theory of interferometric imaging of incoherent objects does not apply. However, in the special case of an unresolved background scattered source, the effect of the coherence is particularly simple: for an array of N elements there are no longer $N(N-1)/2$ independent numbers per integration, but rather only N. These numbers may be thought of as the (complex) gain introduced by a scintillation pattern lying over the array. The speckles must therefore be removable by self-calibration of the observed snapshot coherences. Furthermore, given a sufficient number of telescopes, the scattering screen can be visualized directly by appropriate transformation of the array element complex gains.

We have performed this experiment using the VLA to observe the radio source 3C279 at elongations of a few degrees from the Sun. We can confirm the existence of "speckles," and their removal by self-calibration. We will show examples of both, and we will discuss the possible applications.

J3-7
1600 WIDE FIELD IMAGING: L. Baath, Onsala Space Observatory, Onsala, Sweden, and California Institute of Technology, Pasadena, CA 91125

J3-8
1620

TIME SERIES ANALYSIS WITH **CLEAN**

David H. Roberts
Astronomy Department 105-24
California Institute of Technology
Pasadena, CA 91125 USA, and
Physics Department*
Brandeis University
Waltham, MA 02254 USA

We discuss a method of time series spectral analysis which is especially useful for unequally-spaced data. Based on a complex, one-dimensional version of the **CLEAN** deconvolution algorithm widely used in two-dimensional image reconstruction, this technique provides a simple way to understand and remove the artifacts introduced by missing data. We describe the method, give several examples, and point out various analogies with the conventional use of **CLEAN.**

This work has been done in collaboration with J. W. Dreher and J. Lehár of MIT.

*Permanent address.

J3-9
1640

KALMAN FILTERING VISIBILITY AMPLITUDE OF HAT CREEK MILLIMETER-WAVELENGTH INTERFEROMETER DATA

Yong-Seon Koh, Yi Zheng, and John P. Basart
Department of Electrical and Computer Engineering
Iowa State University, Ames, IA 50011

ARIMA modeling and Kalman filtering techniques were applied to extended sources observed with the Hat Creek Millimeter Interferometer. Atmospheric fluctuations frequently prevent the dynamic range in the maps from exceeding 100. The dominating disturbance to the Hat Creek System is to the visibility amplitudes. Methods such as self-calibration cannot be used for this data since the data are recorded on only three baselines simultaneously. An alternative to self-calibration is to do model-based filtering of the signal on each baseline separately. Then models for the signal (source), the system noise, and the atmosphere must be determined. These can be complicated to find for extended sources. Models for the source are obtained from the CLEAN components after they are transformed to the spatial frequency domain. The difference between the CLEAN component time series and the data time series will be dominated by atmospheric noise. Applying time series analysis to this difference series, we get a model for the atmosphere. Finally, receiver system is modeled as white noise. After putting all three models into a state-space formalism, we filter the original data series. The results from applying our procedure to simulated data and to real data from the Hat Creek Interferometer will be discussed.

This work was partially supported by National Science Foundation Grant No. AST-8217135

J3-10
1700

KALMAN FILTERING VLA PHASE DATA WITH SOURCE MODELING

Patrick L. Anderson, Yi Zheng, and John P. Basart
Department of Electrical and Computer Engineering
Iowa State University
Ames, IA 50011

We have previously applied the Kalman filter to VLA phase data in both the spatial and spatial-frequency domains. Filtering in the frequency domain included phase models for the atmosphere, system, and a point source. This work has been continued to include modeling and filtering an extended source in the uv plane which is reported here. We model the source, atmosphere, and system as ARIMA (autoregressive integrated moving-average) processes. ARIMA processes are known to provide good short-term predictions for time-series data. The phase model is obtained for an extended source using the CLEAN components which are transformed from the spatial domain to the frequency domain in a baseline-time series. This time series is then modeled as an ARIMA process. The source phase model is subtracted from the measured phase to form residual phases. The model of the atmosphere is given by describing the residuals of the source model and the measured phase as an ARIMA process. ARIMA models of the source, atmosphere, and system are written in state-space form for application of the Kalman filter. These models provide the covariance matrices and state-transition matrices used in the Kalman filter. The phase is modeled and filtered baseline-by-baseline.

Results of the Kalman filter and self-calibration will be compared using simulations and actual data from the VLA. It is expected that the Kalman filter can be used in situations where self-calibration does not sufficiently reduce the phase noise.

Session A-4 0855-Thurs. CR1-40
MEASUREMENTS OF THE PROPERTIES OF MATERIALS
Chairman: Sedki M. Riad, Dept. of Electrical Engineering, Virginia Polytechnic Institute and State University, Blacksburg, VA 24061

A4-1
0900

DIELECTRIC SPECTROSCOPY USING A WIDEBAND DIELECTRIC FILLED CAVITY

Mohammad A. Saed and Sedki M. Riad
Department of Electrical Engineering
Virginia Polytechnic Institute and State University
Blacksburg, Virginia 24061

This paper concerns the development of a Wideband Dielectric Filled Cavity (WDFC) to be used for characterizing dielectric materials over the HF to microwave frequency region. The cavity is completely filled with the dielectric material to be characterized.

Two configurations are presented:

1. **The WDFC is adapted to the end of a transmission line. The measured reflection coefficient is used to compute the complex permittivity.**

2. **The WDFC is placed between two transmission lines. The complex permittivity is computed from the reflection coefficient or the transmission coefficient information. However, both the complex permittivity and the complex permeability can be computed if a combined reflection - transmission measurement is performed.**

The WDFC technique has several advantages over other methods which require the sample to be inserted in an air line. In those methods, the sample has to be precisely cut to fit in between the inner and outer conductors causing two problems to occur. The first problem is that samples with rough edges will result in air gaps between the sample and the conductor surfaces introducing significant errors. The second problem is the possible damage of the air line's conductor surfaces because of the sample's rough edges. Such problems are minimized in the proposed structure.

This paper presents the concept of the proposed technique. Results of computer simulation as well as experiments involving the measurement, in the time domain, of the complex permittivity and the complex permeability of some materials are also presented.

A4-2
0920

TIME DOMAIN MEASUREMENT OF ANECHOIC CHAMBER REFLECTIONS

E. N. Clouston, Dr S. Evans,
Cambridge University Engineering Department,
Trumpington St. Cambridge CB2 1PZ U.K.
Dr P. A. Langsford, Marconi Research Ltd. U.K.

Time domain techniques have been developed and demonstrated for the measurement of anechoic chamber reflectivity, and for the accurate location of the sources of reflections. They allow detailed study of any particular area of the absorber on the chamber walls.

Broadband reflectivity information is available from a single measurement of the pulse transmitted directly between two antennas and the ensuing reflections from the chamber walls. In a chamber large enough for the reflections to be delayed by more than 10ns, the trailing edge of the direct signal had dropped enough for reflectivity levels up to 50dB down to be measured above 1GHz or 43dB down above 500MHz. The noise dominated the result above 2GHz, but this can be extended to 4GHz by use of an amplifier in front of the sampling oscilloscope.

Frequency domain techniques (J. Appel-Hansen, IEEE Trans. AP-21(4), pp.490-498, 1973) rely on careful scanning to detect the worst interference between different reflections. The time domain approach can separate them from each other, so the reflectivity can be measured without moving the antennas at all; variation with antenna position can then be investigated.

The path length is available from the delay of any reflection, but the direction can only be calculated from the change in delay when one of the antennas is moved. This can be done for any reflection which can be identified in both records, and high-pass digital filtering can help. But to be sure of separating out the reflections from a particular area, the antennas must be moved close to it, and this is limited by the reflections overlapping the trailing edge of the direct signal. This was solved by rigidly fixing two antennas 2m apart on a wooden beam, and measuring the direct signal between them. This was then subtracted from subsequent records, to leave the reflections, including those which had been superimposed on the direct signal.

Although frequency domain techniques offer a better dynamic range, the time domain approach offers a simple reflectivity measurement, which gives a safe overestimate from a single measurement. It is also far more versatile in locating the sources of reflections.

A4-3 0940 LOSS CALCULATION IN SYMMETRICALLY SPHERICAL WITH CIRCULAR APERTURE UNSTABLE OPTICAL RESONATORS USING DIFFERENT TECHNIQUES

M. H. RAHNAVARD, J. ZARE MOODI
Electrical Engineering Department
Shiraz University, Shiraz, Iran
Telephone Number: Iran, Shiraz 34064-2712

Unstable Optical resonator is used in medium and high power laser. In stable resonator when Fresen number is greater than 0.5 all of the energy is not absorbed by 1st mode but energy is absorbed in higher order modes. In unstable resonator with proper gain it is possible to have mode with lowest power loss and this mode will absorbe most of the energy from the laser material and it is possible to have optical resonator with smaller length. For this reason power loss calculation is important in unstable optical resonators.

At first Fox and Li calculated power loss in infinite strip cylinderical and spherical resonators with circular aperature for Fresnel number greater than 10 by scalar theory of diffraction using iterative method (Fox, A. G. and Li, T. H. 1964. Quantum Electronic I11, 8, 1262). By using geometrical optics Siegman calculated power loss in optical resonators for large Fresnel number (Siegman, A. E. 1965. Proc. IEEE. 53, 277). Sanderson and Striefer calculated power loss by Gaussion Quadrature and Cornu spiral methods (Sanderson, R. L., and Streifer, W. 1969. Appl. Opt. 8, 2129). In the first method the integral is converted to a matrix. Using QR-method eigen value and eigen vector of the matrix is evaluated. Eigen vectors are electric field modes and power loss in each mode is equal to one minus absolute value of the eigen value of that mode. Siegman and Miller found eigen values for spherical resonator with circular aperture with Fresnel number greater than 13 using Prony's method (Siegman, A. E. and Miller, H. Y. 1970. Appl. Opt. 9, 2729). Santana and Felson calculated eigen value using waveguide theory (Santana, C. and Felsen, L. B. 1976. Appl. Opt. 9, 1470).

As Fresnel number gets larger resulting series from the integral has more elements. The number of elements in the series is usually between 6 to 10 times the Fresnel number (Siegman, A. E. and Miller, H. Y. 1970. Appl. Opt. 9, 2729). So power loss evaluation in optical resonators with Fresnel number greater than 10 takes a long time. Except Santana and Felson (Santana, C. and Felsen, L. B. 1976. Appl. Opt. 9, 1470) all of the works which is done based on scalar theory of diffraction. In this paper physical optics in exact form and with Fresnel approximation, scalar theory of diffraction without approximation, geometrical theory of diffraction and physical theory of diffraction are used in analyzing and power loss calculation of symmetrically spherical with circular apperture unstable resonators.

A4-4
1020

IMPEDANCE EFFECTS ON ELECTROMAGNETIC SUSCEPTIBILITY*

R. J. King and W. C. Ng
Lawrence Livermore National Laboratory
Livermore, California 94550

The in situ measurement of transient or cw voltage, current, or energy coupled to the input of a susceptible electronic subsystem at frequencies above a few tens of MHz cannot be measured without disturbing the coupling cable, wire, etc. Using state-of-the-art frequency domain instrumentation and signal processing techniques, means for calculating these electrical quantities is described.

From cw measurements of the self-impedance (Z_A) and received voltage across 50 ohms at the coupling terminals of a generic test object, a Thevenin equivalent circuit model is derived. Using this model, the electrical parameters are computed for several interesting load impedances. Of interest are two worst cases where the load impedance is the complex conjugate of Z_A and the conjugate pure reactance of Z_A. Another case of particular interest is where the load impedance is that of an electronic unit representing that of a typical subsystem designed for operation at much lower frequencies. These three cases are compared with the voltage, current, and energy at a 50-ohm load. It is concluded that the electrical quantities for the two conjugate cases can be one or two orders of magnitude larger than that for the 50-ohm case as might be expected. However, it is somewhat surprising that the smoothed electrical quantities at the input of the electronic units tested are comparable to those for the 50-ohm case. The spectral energy density responses are generally within a factor of two (± 3 dB), but may be as large as a factor of three (± 5 dB) over narrow frequency bands.

Examples are given showing both spectral and temporal electrical quantities at the electronic system input for assumed electromagnetic transients incident on the exterior of the coupling system.

A4-5
1040

NEAR-FIELD STATEMENT OF MONOSTATIC-BISTATIC THEOREM

David G. Falconer, Ph.D.
Remote Measurements Laboratory
SRI International
333 Ravenswood Avenue
Menlo Park, CA 94025

Over the years we have developed several enhancements and extensions of Kell's monostatic-bistatic theorem (MBT). This approximation (*Proc. IEEE*, v. 53, n. 8, p. 983, August 1965), which we use regularly in our anechoic-chamber measurements of radar cross section (RCS), states that one can estimate a target's bistatic RCS pattern at the wavenumber k by measuring its monostatic one at the bisecting angle at the reduced wavenumber $k' = k \cos(\theta/2)$, where θ is the bistatic angle. We have extended Kell's version of the MBT by introducing a phase adjustment, $\exp[i2(k - k')R]$, that allows one to estimate the phase (as well as the RCS) of the bistatic scattering amplitude. Similarly, we have developed an amplitude modification, k/k', that provides an estimate of the bistatic scattering amplitude for extended (rather than point) scatterers. Finally, we have derived a new version of the MBT that is suitable for near-field scattering conditions, i.e., for ranges $R < 2D^2/\lambda$, where D is the nominal target diameter. In the near-field case, it is necessary to measure the monostatic pattern at both the reduced wavenumber k' and the reduced range $R' = R \cos(\theta/2)$. The required phase adjustment and amplitude modification are similarly changed to $\exp[i2(kR - k'R')]$ and unity, respectively.

It is often difficult to measure the monostatic RCS pattern at both the reduced wavenumber and reduced range required under a Kell-type derivation. Accordingly, we have developed an alternate form for the near-field MBT that requires no wavenumber or range reductions during measurement of the monostatic pattern and no phase adjustments or amplitude modifications of the recorded data. This version of the MBT, however, places a slightly stricter requirement on target geometry, namely that $\theta < \sqrt{\lambda/H}$, where H is nominal thickness of the scattering body when viewed at the bisecting angle.

We have validated our work by comparing the above approximations with the RCS and phase patterns predicted by an optically oriented model for a square plate and a modal solution for a long right circular cylinder.

A4-6
1100

Millimeter Wave Transmitted Power Through Illuminated Semiconductor Panel Scanned with Strip of Shadow

M. H. RAHNAVARD, A. HABIBZADEH
Electrical Engineering Department
Shiraz University, Shiraz, Iran

One of the needs in air traffic is to know the environmental situation under any weather condition. Visble and IR radar will fail in adverse weather because of high attenuation but there are several windows in millimeter wave region with low attenuation in bad weather condition (Weibel, C. H. and Dressel, H. O. 1967, Proc. IEEE, 55, 497). One of the method to convert millimeter wave to visible light is by using illuminated semiconductor panel. Semiconductor panels are used as image convertors in both transmission and reflection mode of operation (Jacobs, H. et. al. 1967, J. Opt. Soc. 57, 913). In both cases the response of illuminated panel is important. Excess carrier in semiconductor panel under stationary illumination is obtained by Levin et. al. (Levin, B. J. 1968, IEEE letters, 56, 1230, Mavaddat, R. and Levin B. J. 1967, J. of Applied physics, 40, 5324). Using the above result reflection coefficient and attention coefficient for this case is also studied (Mavaddat, R. 1970, IEEE Trans. on Microwave Theory and Techniques, 18, 360, Mavaddat, R., 1971, IEEE Transaction on Microwave theory and Technique, 19, 555), Practically, the response of semiconductor panel to moving illumination is required. Excess carrier in moving spot illuminated semiconductor panels is studied and profiles of excess carrier for moving strip illuminated semiconductor panel vs. different parameters is obtained. (Rahnavard, M. H. et. al., 1975, Journal of Applied physics, 46, 1229). In this paper using the excess carrier results, transmitted power through illuminated semiconductor panels scanned with shadowed strip as a function of scanning velocity, position, thickness of the strip and time is studied and the resultant curves are plotted.

Session B-6 0835-Thurs. CR2-26
EM THEORY
Chairman: Akira Ishimaru, Dept. of Electrical Engineering, Univ. of Washington, Seattle, WA 98195

B6-1
0840

MAXWELLIAN AND CAVITY ELECTROMAGNETIC FIELDS WITHIN CONTINUOUS SOURCES

Arthur D. Yaghjian
Electromagnetics Directorate
Rome Air Development Center
Hanscom AFB, MA 01731-5000

The free-space operational definitions of the electric and magnetic field in terms of the forces on a test charge are inapplicable, without some modification, within continuous sources because the definitions require that the test charge be exterior to the sources producing the measured electric and magnetic fields. The free-space definitions can be modified in the source region by specifying that the test charge be placed in an infinitesimal free-space cavity formed by removing the sources within the cavity while maintaining the sources outside the cavity. These cavity-defined electric and magnetic fields depend, in general, on the geometry of the cavity (i.e. on its shape, its orientation, and the position of the test charge within the cavity) even though the size of the cavity approaches zero. In other words the cavity-defined electromagnetic fields within a continuum are not necessarily unique unless the geometry of the cavity is specified, and do not necessarily equal the Maxwellian fields, i.e., the unique fields defined mathematically by Maxwell's equations for continuous sources.

Maxwell, in Articles 395-400 and 604-605 of his treatise, used the cavity definitions of electric and magnetic fields within continuous polarized media, related the fields in cavities of various shapes to the Maxwellian fields, and specified the "narrow crevasse" cut perpendicular and parallel to the direction of magnetization as the cavities that should be used to operationally define the two magnetic field vectors (B and H, respectively) in the source region. For these particular cavities the respective cavity-defined magnetic fields equal the Maxwellian magnetic fields. Maxwell studied the subject in detail only for the magnetic fields within magnetic polarization, but stated in Article 60 that the electric field within electric polarization (and also, as we show, the time-harmonic electric field within volume current) can be treated in the same manner "to the greatest advantage."

Here, Maxwellian and cavity electromagnetic fields are derived within a continuous source distribution of volume current or electric and magnetic polarization densities by direct, rigorous differentiation of the vector potential. The derivation, which uses only operations of vector calculus, reveals naturally the contributions from interior and exterior source regions. Results are obtained for static and arbitrarily time-varying fields as well as for time-harmonic fields.

B6-2
0900

A TRANSVERSE APERTURE-INTEGRAL-EQUATION METHOD FOR NUMERICAL EVALUATION OF EDGE DIFFRACTION BY SEMI-INFINITE STRUCTURES

L. W. Pearson, McDonnell Douglas Research Laboratories, R. A. Whitaker, McDonnell Douglas Aerospace Information Services, P.O. Box 516 St. Louis, MO 63166

With a few exceptions, analytically tractable canonical problems for edge diffraction are limited to impenetrable structures. Recently Herrmann (I.E.E.E. Trans. Antennas Propagat., AP-35, 53, 1987) suggested an approach that employs signal processing methods in angular space as a means for isolating the diffraction at a single edge of an object comprising penetrable materials.

In this presentation, we propose an alternative formulation for numerical computation of diffraction at the edge of a semi-infinite section of a stratified structure. The stratified structure could comprise a number of layers of material with different electrical properties and one or more perfectly conducting sheets, the only restriction being predicated upon whether an analytic Green's function can be determined for all points in the associated infinite planar structure. It is believed that the method can be extended to structures comprising anisotropically conducting sheets, for example in some fiber composite materials (L. W. Pearson, "Reflection and Propagation Characteristics of Multiple Layers of Anisotropic Admittance Sheets," National Radio Science Meeting, Blacksburg, VA, June, 1987).

The problem is formulated as an aperture integral equation in the infinite-extent plane transverse to the structure and passing through the edge at which diffraction occurs. The aperture field at large distances from the edge can be predicted asymptotically and subtracted from the total unknown field so that one solves for a difference unknown that decays as a function of transverse distance from the edge. The asymptotic fields affect the excitation vector for the numerical system and are a function of the angle of incidence, but these fields may be represented in spectral-domain analytical forms that may be computed efficiently.

B6-3
0920

SPECTRAL DEFECTS IN THE PARAXIAL GAUSSIAN BEAM METHOD

I.T. Lu, X.J. Gao and L.B. Felsen
Dept. of Electrical Engineering/Computer Science
Polytechnic University
Route 110, Farmingdale, NY 11735

Discretization in terms of paraxial Gaussian beams, pioneered in seismology (Cerveny, J. Geophys. Res., 58, 44-72, 1985) provides an attractive numerical algorithm for tracking source-excited high frequency wavefields through complicated propagation and scattering environments. However, the algorithm is flawed by an arbitrariness in the choice of the beam and stacking parameters, and also by spectral deficiencies arising from the paraxial approximation. These deficiencies have been made evident, and explained from a spectral perspective, in a test problem involving acoustic radiation in a half space separated by a plane interface from an exterior medium with higher propagation velocity (I.T. Lu, L.B. Felsen and Y.Z. Ran, Geophys. J. R. astr. Soc., 89, 915-932, 1987). From comparison with a reference solution generated by numerical integration of an exact spectral integral, it was shown that retention of full complex spectra removes the deficiencies. These considerations are now transferred to the electromagnetic case and illustrated by additional numerical examples. They are also extended to the case of an anisotropic exterior that can support ordinary and extraordinary waves. Conclusions from these studies permit a critical assessment of the validity of the paraxial Gaussian beam method.

B6-4
0940

THREE DIMENSIONAL FIELD EXPANSION IN THE MOST GENERAL ROTATIONALLY SYMMETRIC ANISOTROPIC MEDIUM.

J. Cesar Monzon
Damaskos, Inc.
P. O. Box 469
Concordville, PA 19331

A material region characterized by tensors ε and μ and possessing general rotational symmetry is found to be specified by six parameters. A field expansion in spherical coordinates is described for the solution of three dimensional electromagnetic problems. The analysis reveals that the angular dependence is dictated by spherical harmonics whereas the radial functions satisfy a set of coupled second order ODE. A total of eight different radial functions are obtained and described in detail, including asymptotic representations.

The present field expansion is specially useful for material geometries conformal with spherical coordinates such as the one shown in the figure, but can, however, be employed for arbitrary geometries when used in combination with an alternative volumetric method. The utility of our method resides in the fact that once the tangential field components are specified on the surface, then an explicit expression for the field at any point in the interior is known.

Numerical results are presented.

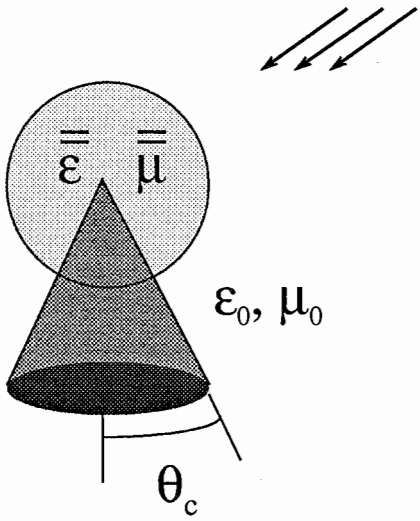

B6-5
1020

TIME DOMAIN DECONVOLUTION OF TRANSIENT RADAR DATA

E. Rothwell, K. M. Chen, D. P. Nyquist and P. Ilavarasan
Department of Electrical Engineering and Systems Science
Michigan State University
East Lansing, MI 48824

Accurate measurement of the transient response of conducting radar targets hinges on the ability to remove the effects of the transmit-receive characteristics of the measurement system. This requires deconvolving the transmitting and receiving antenna responses, as well as the response of the receiving equipment and the propagation path, from the measured data. Simple deconvolution algorithms involving matrix inversion of time-sampled data and division of Fourier spectra are known to be ill-conditioned. A new time domain technique has been developed, which is shown to be better conditioned than the simpler algorithms.

Let $c(t)$, $e(t)$, and $h(t)$ be three waveforms obeying the convolutional equation $c(t)=e(t)*h(t)$. Also, let $\{e_n\}$ and $\{c_m\}$ be measured versions of the waveforms, sampled with a time interval T_s within a truncation window $[0,T_w]$. Finally, let $C(t)$ and $E(t)$ be appropriately interpolated continuous verisons of $\{e_n\}$ and $\{c_m\}$. Then, an approximation $H(t)$ to $h(t)$ can be found by solving the convolutional integral equation $C(t)=E(t)*H(t)$, $0<t<T_w$.

A solution to the integral equation is obtained by expanding $H(t)$ in a set of basis functions and employing the method of moments. A prudent approach to chosing expansion and weighting functions is to expand $H(t)$ in a Fourier series over $[0,T_w]$ and apply Galerkin's method. Since the basis and weighting functions span $[0,T_w]$, the integrals in Galerkin's method perform a smoothing operation on the measured data, reducing the sensitivity of the resulting matrix equation to random noise. In addition, estimates of the highest frequency present in $H(t)$, from knowledge of the sample interval T_s and the highest frequency passed by the measurement system, is easily incorporated into the representation of $H(t)$ via its Fourier components.

B6-6
1040

FRESNEL EQUATIONS FOR A DIELECTRIC-CHIRAL INTERFACE

S. Bassiri, C.H. Papas
Electrical Engineering Department
California Institute of Technology
Pasadena, California 91125
and
N. Engheta
The Moore School of Electrical Engineering
University of Pennsylvania
Philadelphia, Pennsylvania 19104-6390

Propagation of plane electromagnetic waves in a lossless, reciprocal, chiral medium will be discussed in this talk. Such a medium is described electromagnetically by the constitutive relations $D = \varepsilon E + i\gamma B$ and $H = i\gamma E + (1/\mu)B$. The constants ε,μ,γ are real and have values that are fixed by the size, shape, and the spatial distribution of the elements that collectively compose the medium. In this talk the problem of reflection from, and transmission through a semi-infinite chiral medium will be addressed by obtaining the Fresnel equations. The conditions for the total internal reflection of the incident wave from the interface, and for the existence of the Brewster angle are obtained. The effects of the chirality on the polarization and intensity of the reflected wave from the chiral half-space will be shown and illustrated by employing the Stokes parameters. The propagation of electromagnetic waves through an infinite slab of chiral medium is formulated for oblique incidence and will be presented analytically for the case of normal incidence.

B6-7
1100

DYADIC GREEN'S FUNCTION AND DIPOLE RADIATION IN CHIRAL MEDIA

S. Bassiri and C. H. Papas
Electrical Engineering Department, 116-81
California Institute of Technology
Pasadena, California 91125
N. Engheta
The Moore School of Electrical Engineering
University of Pennsylvania
Philadelphia, Pennsylvania 19104

The radiation emitted by an oscillating dipole in an unbounded, lossless, chiral medium that is described electromagnetically by the constitutive relations $\mathbf{D}=\varepsilon\,\mathbf{E}+i\,\gamma\,\mathbf{B}$ and $\mathbf{H}=i\,\gamma\,\mathbf{E}+(1/\mu)\mathbf{B}$ is calculated. The constants ε, μ, γ are real and have values that are fixed by the size, shape, and spatial distribution of the elements that collectively compose the medium.

From these constitutive relations and from the time-harmonic Maxwell equations $\nabla\times\mathbf{E}=i\omega\,\mathbf{B}$ and $\nabla\times\mathbf{H}=\mathbf{J}-i\omega\,\mathbf{D}$, it is seen that the wave equation for such a medium is $\nabla\times\nabla\times\mathbf{E}-\omega^2\mu\,\varepsilon\,\mathbf{E}-2\,\omega\,\mu\,\gamma\,\nabla\times\mathbf{E}=i\,\omega\,\mu\,\mathbf{J}$ where the source term $\mathbf{J}$ is the current density of the oscillating dipole and where $\mathbf{E}$ is the electric vector of the radiated field.

The desired solution of this wave equation is found by the Green's function method, that is, by first constructing the dyadic Green's function and then evaluating the expression $\mathbf{E}(\mathbf{r})=i\omega\,\mu\int\Gamma(\mathbf{r},\mathbf{r}')\cdot\mathbf{J}(\mathbf{r}')\,dv'$. The dyadic Green's function Γ and the components of the radiated electric field $\mathbf{E}$ are obtained in closed form. The components of the radiated $\mathbf{B}$, $\mathbf{D}$, and $\mathbf{H}$ fields can be derived from knowledge of $\mathbf{E}$ by using the Maxwell equation $\mathbf{B}=(1/i\omega)\,\nabla\times\mathbf{E}$ and the constitutive relations. The wave impedance of the medium and the radiation resistance of the dipole are also obtained. The effects of the chiral medium on the polarization and intensity of the dipole radiation are discussed.

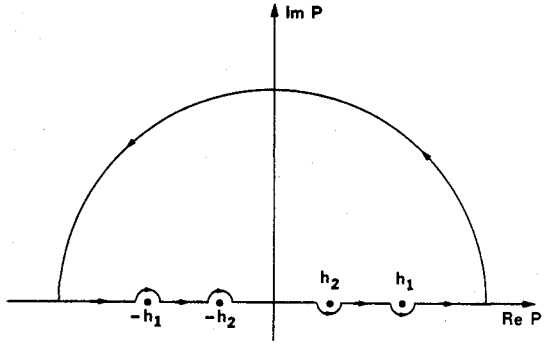

Path of integration in complex p-plane for right-handed ($\gamma > 0$) chiral medium.

B6-8
1120

ELECTRIC FIELD COMPUTATION IN A REGION OF UNIFORM CURRENT DENSITY

R. Clark Robertson
The Bradley Department of Electrical Engineering
Virginia Polytechnic Institute and State University
Blacksburg, VA 24061

The calculation of the electric field within a current-carrying region by the Green's dyadic method, given by

$$\vec{E}(\vec{r}) = \int_{V'} \vec{J}(\vec{r}') \cdot \vec{\vec{G}}(\vec{r}\,|\,\vec{r}')dV'$$

where the integration is over the volume of the current density and $\vec{\vec{G}}(\vec{r}\,|\,\vec{r}')$ is the appropriate Green's dyadic, requires that the normal Green's dyadic be modified to take into account the principal value of the Green's dyadic (J. Van Bladel, IRE Trans. on Antennas and Propagation, AP-9, 563-566,1961). This is a result of the singular nature of the portion of the Green's dyadic corresponding to an infinite homogeneous region. For the special case of a uniform current density, commonly encountered in the application of the method of moments when pulse functions are used as subsectional basis functions and Dirac delta functions are used as testing functions, the Green's dyadic method can be successfully used to evaluate the electric field inside the current density without invoking the concept of principal values or the necessity of excluding the singularity in the integrand from the volume of integration. This can be shown by comparing the expression obtained by the Green's dyadic method for the electric field at the center of a region of uniform current with that obtained by the method of retarded potentials. The use of principal values is avoided by using a volume of integration such that the singular part of the Green's dyadic is a perfect differential of the variable of integration that corresponds to the direction of current flow. If this integration is performed first, then the remaining integrations can be performed without reference to an excluded region, and the result is identical with that obtained from the retarded potential method. With reference to the moment method, integration of the Green's dyadic over the various subregions is naturally expressed in Cartesian coordinates since the subregions are usually either cubes or rectangular parallelepipeds. As a result, the expression of the singular part of the Green's dyadic as a perfect differential of one of the variables of integration is natural. Hence, the evaluation of the contribution of the singular cell can proceed without special care being taken to exclude the origin from the region of integration.

B6-9
1140

Low Frequency Response of a Current Loop in 3-D Conductive Inhomogeneity

W.C. Chew
Department of Electrical and Computer Engineering
University of Illinois
Urbana, IL 61801
R.L. Kleinberg
Schlumberger-Doll Research
Ridgefield, CT 06877

When a current loop is radiating low frequency fields in an axially symmetric, conducting inhomogeneity, a common approximation for calculating the response is the geometrical factor theory. However, when the inhomogeneity is general, and non-axially symmetric, the geometrical factor theory breaks down. Even the more general Born approximation is ineffective in such a geometry because of the Maxwell-Wagner charge build up at the interface.

In this paper, we will discuss the range of validity of the Born approximation. We will also discuss a variational solution to such a problem, which is valid beyond the range of Born approximation. The variational solution provides a calculation that is in much better agreement with experiment than the Born approximated solution, or the geometrical factor theory when compared with experiments. It can be used to ascertain the response of a current loop in the vicinity of three dimensional inhomogeneity easily.

As an illustration, we use such a theory to ascertain the response of a microinduction sensor over vertically stratified inhomogeneities.

C2-1
0840

FINE STRUCTURE IN RF SPECTRA OF LIGHTNING RETURN STROKE WAVE FORM

K. Rinnert
MPAE, Katlenberg-Lindau 3, FRG
L.J. Lanzerotti, D.J. Thomson, C.G. MacLennan
AT&T Bell Laboratories, Murray Hill, NJ 07974
E.P. Krider
University of Arizona, Tucson, Arizona
M.A. Uman
University of Florida, Gainesville, Florida

We have calculated the power spectra of the RF signals for a number of lightning return strokes measured during a thunderstorm which occurred in Lindau in August, 1984. The purpose is to quantify the periodicities recognized in the "subsidiary peaks" which have been observed to follow the onset, fast transition to peak amplitude, of return strokes. The RF data are obtained with the engineering unit of the Galileo Probe lightning experiment. The impulse signal is first removed from the data and the RF power spectra are then calculated using four prolate spheroidal data windows in the time domain and a fast Fourier transform algorithm. The RF spectra definitely show fine structure; there are two or three distinct peaks in the spectra in many of the return strokes. These peaks often occur at frequencies of ~40 and ~70 kHz, but can be quite variable in frequency in the range 0–120 kHz. We present a series of such RF spectra and show how the periodicities of the subsidiary peaks vary during the course of the thunderstorm.

C2-2
0920

THE COHERENT SIGNAL-SUBSPACE METHOD FOR THE DETECTION AND ESTIMATION OF THE DIRECTIONS OF MULTIPLE WIDEBAND SOURCES

M. Kaveh

Department of Electrical Engineering, University of Minnesota,
Minneapolis MN

This presentation addresses the problem of detecting and estimating the directions of arrival (doa) of multiple co-channel, possibly fully correlated wideband signals received by an array of sensors. The Coherent Signal-subspace Method (CSM) relies on an approximately coherent combination of spatial signal subspaces of the temporally narrowband components of the received signal vector. A two-step algorithm is described. First, initial "low-resolution" doa estimates are used to align the signal subspaces and generate an enhanced spatial covariance matrix estimate. In the second step of the algorithm, appropriate narrowband signal-subspace methods are used for detection and the estimation of the doa's. The presentation also includes a discussion of some unconventional approaches to the characterization of the performances of detectors and estimators for this class of problems.

C2-3
1020

MULTIPLE-WINDOW TRANSFER FUNCTION ANALYSIS of ELECTROMAGNETIC DATA

David J. Thomson
AT&T Bell Laboratories, Murray Hill, N.J. 07974

We discuss the estimation of transfer functions from electromagnetic data using variants of the multiple-window method. The theory upon which estimation of magnetotelluric transfer functions is founded depends on numerous statistical assumptions: *A-1* A unique solution exists and the data is temporally stationary enough for time averages to converge; *A-2* The dominant incident field is a homogeneous plane wave; *A-3* The vertical magnetic field depends linearly on the two components of the horizontal field.

Because EM data is rarely either stationary or Gaussian, robust estimation procedures have been introduced which impose additional constraints in the form of data segmentation. This implies that we can choose segment lengths so that for a majority of segments: *A-4* Features of the spectral matrix are resolved, and; *A-5* The data is essentially stationary within the segment.

In this paper we study the influence and interactions of these assumptions on the estimated transfer function and describe tests for their violation. Most of these tests are generalizations and extensions of procedures known in multivariate analysis. Such tests are sensitive to departures from normality but if A-5 is valid the transformed data will be reasonably Gaussian even if the original data is not. Induced voltage on Transatlantic cables and data from the EMSLAB array are used as examples.

C2-4
1100 ESTIMATING THE PARAMETERS OF A GENERALIZED CHIRP SIGNAL IN THE PRESENCE OF NOISE: R. Kumaresan, Electrical Engineering Dept., Univ. of Rhode Island, Kingston, RI 02881

Session F-2 0855-Thurs. CR2-6
ATMOSPHERIC SENSING
Chairman: David C. Hogg, Cooperative Institute for Research in Environmental Sciences, Univ. of Colorado, Boulder, CO 80309

F2-1
0900

ESTIMATION OF ZENITH CLEAR-AIR ABSORPTION FROM GROUND PARAMETERS FOR 10 TO 300 GHz

K.C. Allen and S.D. Hector
National Telecommunications and Information Administration
Institute for Telecommunication Sciences
Boulder, Colorado 80303

A data base of monthly mean atmospheric profiles for 37 cities was used to analyze the relationship between zenith clear-air absorption and ground level meterological parameters. The absorption rate was computed at each profile height and integrated with respect to height to estimate the zenith attenuation. A nonlinear least squares fit was then applied to the ground level parameters and zenith attenuation. Through an analysis of residuals, the functional form of a good estimator of zenith attenuation in dB from the ground parameters of pressure, P, temperature, T, and water vapor pressure, e, was found to be

$$A = \frac{a_1 P e (a_3 + T^2)}{a_2 + T} + a_4 P^2 (a_5 - T) \qquad (1)$$

where the a_i's are frequency dependent. The first and second terms in (1) give the water vapor and oxygen absorption, respectively. The RMS error of (1) for the data base is about six percent or less for most frequencies. Because the zenith attenuation was computed up to only 30 km in height, the results must be used with caution near the oxygen lines (50-70 GHz and near 118 GHz).

A second approach to estimating the zenith attenuation by multiplying the ground level attenuation rate, α_o, by an effective height, h_a,

$$A = \alpha_o h_a, \qquad (2)$$

was also investigated. A strong dependence of the effective height on the ground level attenuation rate was discovered. For the profiles in the data base, h_a ranged from 2.3 to 4.4 at 44 GHz. An effective height functionally dependent on the ground level attenuation rate or meterological parameters and frequency makes (2) a good estimator of zenith attenuation.

F2-2
0920

MILLIMETER WAVE TEMPORAL SPECTRA FOR SPHERICAL WAVE PROPAGATION THROUGH ATMOSPHERIC TURBULENCE

R.J. Lataitis, S.F. Clifford, R.J. Hill, J.T. Priestley
NOAA/ERL/Wave Propagation Laboratory
325 Broadway
Boulder, CO 80303

In atmospheric turbulence, refractive-index fluctuations produced by local small-scale variations in the temperature and humidity randomly perturb the amplitude and phase of a propagating wave. Clifford (J. Opt. Soc. Am., 61, 1285-1292, 1971) has derived the temporal frequency spectra for the amplitude, phase, and phase-difference fluctuations of a spherical wave propagating through weak refractive turbulence. At millimeter wave frequencies, humidity fluctuations can also produce small scale absorption fluctuations. We use an extended theory to include this effect. The theory is compared to results from a joint NOAA-GIT (National Oceanic and Atmospheric Administration-Georgia Institute of Technology) millimeter wave propagation experiment performed over a period of two years (1983-1985) in Flatville, Illinois. Millimeter waves of frequencies 116, 119, 142, 173, and 230 GHz were propagated over a 1.4 km path at a height of 4 m over a flat open field. The propagation path was well instrumented to provide an accurate comparison with meteorological conditions. The agreement between experiment and theory is good and indicates that small scale absorption fluctuations may dominate the low frequency portion of the amplitude spectrum while refraction fluctuations dominate at higher frequencies. The entire phase difference spectrum appears to be dominated by refraction fluctuations. Several episodes of large scale (whole path) absorption variations were also recorded. These appear to be non-stationary phenomena that can dominate the low frequency behavior of the spectra and are not explained by the theory.

F2-3
0940

USE OF DIFFERENTIAL PROPAGATION PHASE CONSTANT TO ESTIMATE LIQUID WATER IN A MIXTURE OF HAIL AND RAIN

D.S. Zrnic', N. Balakrisnan, M. Sachidananda
National Severe Storms Laboratory
1313 Halley Circle
Norman, OK 73069

The differential phase constant K_{DP} is defined as the difference between phase constants of horizontally and vertically polarized waves that propagate horizontally. This constant can be estimated with coherent polarimetric radars. K_{DP} has a unique property which allows discrimination between statistically isotropic and anisotropic scatterers. In a mixture of randomly oriented scatterers (such as hail) with aligned scatterers (such as rain drops) K_{DP} is only affected by the aligned scatterers, whereas differential reflectivity is affected by both. This is because on the average the phase shift after propagation through randomly oriented scatterers is the same for horizontally and vertically polarized electric fields, whereas horizontally-polarized electric fields propagating through rain experience relatively larger phase shifts. We show theoretically the differential phase constants expected in various mixtures of rain and hail. Also we show data consisting of reflectivity factor Z, differential reflectivity Z_{DR}, and K_{DP} which can be reconciled by the simultaneous presence of hail and rain.

Nat. Rad. Sci. Meet. Jan 1988

F2-4
1000

CLIMATOLOGICAL ANALYSIS OF RAIN AND CLOUD ATTENUATION OF MILLIMETER WAVES

E. J. Dutton
National Telecommunications and
Information Administration
Institute for Telecommunication Sciences
325 Broadway
Boulder, CO 80303-3328

Rainfall observational data are processed by least-squares curve-fitting to call attention to some of the desirable aspects of such fitting. The curve-fitting techniques are illustrated for annual rainfall and worst-month rainfall distributions, but are as readily applicable for distributions of rain-caused attenuation or scattering.

Then analysis of specific rain attenuation data observed at Huntsville, AL at 28.8, 57.7, and 96.1 GHz is discussed. These data are used to construct the third part of a CONUS-wide climatology for use in obtaining the distribution of specific attenuation at geographic locations within these zones.

Finally, the feasibility of determining zenith cloud attenuation distributions at millimeter-wave frequencies, basically using radiosonde observations as the main indictor of cloud location and occurrence, is examined. A 5 year sample for Washington, D.C. is examined and results presented.

Nat. Radio Sci. Meet. Jan. 1988

F2-5
1040

RADIOMETRIC AND RADAR MEASUREMENT OF RAIN IN HEAVY CELLS

D. C. Hogg
Colorado Institute for Research in Environmental Sciences
University of Colorado
Boulder, CO 80309

Computations of 6 GHz brightness temperatures generated by heavy rain cells embedded in an absorbing troposphere are given. It is assumed that the cell dimensions are measured by a companion radar. The radiometric measurement is made on and off the cell. The elevation angle of the radiometric beam is taken to be 2 degrees and the raindrop sizes represented by a Laws-Parsons distribution. For a 2 km diameter cell of rainrate 100 mm per hr located at a range of 75 km, the brightness is about 80 K of which only a 1.5 K correction is required for the clear-air brightness from beyond the cell. A 6 GHz measurement is also discussed.

F2-6
1100 AN ACOUSTIC SOUNDER FOR MONITORING QUALITATIVE TEMPORAL VARIATIONS IN VERTICAL RADIO REFRACTIVITY PROFILES IN THE LOWER TROPOSPHERE

S.M. Babin and J.R. Rowland
The Johns Hopkins University/Applied Physics Laboratory, Johns Hopkins Road, Laurel, Maryland 20707

Low altitude gradients in radio refractivity can have dramatic effects on radar propagation at sea. Detailed quantitative refractivity data can be gathered using helicopters and rocketsondes. A method is needed for continuously monitoring detailed qualitative changes in vertical refractivity profiles over the ocean surface so that one would know when more detailed quantitative studies were needed to predict radar propagation. One possible technique for doing this is by means of a small high frequency acoustic sounder. Since the absorption of sound in air is highly dependent on humidity, such an acoustic sounder could conceivably measure vertical humidity profiles. Assumptions about the temperature profile would allow a description of the refractive index profile. The characteristics of a small multiwavelength high frequency acoustic sounder suitable for making humidity measurements to an altitude of 200 meters are presented.

F2-7
1120

LOW COST ROCKET PROBES FOR USE IN RADAR PROPAGATION STUDIES

J. R. Rowland
The Johns Hopkins University/
Applied Physics Laboratory
Johns Hopkins Road
Laurel, Maryland 20707

Recent development of computer models that have the capability of predicting radar performance under ducting conditions at sea has produced a need for high resolution profiles of microwave refractivity. In the past, radiosondes have been used to make the types of measurements required for the radar models. Conventional radiosondes are carried by balloon and telemeter temperature, pressure and relative humidity at sampling intervals of several hundred feet altitude. In order to accurately calculate the effects of these meteorological parameters on the radar at low altitudes, however, measurements with a vertical resolution of a few feet extending all the way to the water surface are generally required. Conventional balloon carried radiosondes launched at sea from ships suffer from contaminated measurements in the vicinity of the ship due to the microclimate surrounding the ship. In addition, essential measurements at altitudes below the normal deck level at which the radiosonde is released cannot be obtained by these radiosondes. For this purpose, a simple low-cost disposable rocketsonde system has been developed. The prototype rocketsonde system was developed using mass produced off-the-shelf hobby rocket components.

Rocketsondes have been used to support several radar propagation tests. On a number of occasions they have been launched from boats at sea. Test firings have been made from boats as small as 23 feet in length. Several tests in Puerto Rico and a test at Kwajalein Atoll in the Marshall Islands have demonstrated the reliable shipboard use of the rocketsondes. This paper contains a description of the rocket system and the results of field comparisons with other sensors.

F2-8
1140

USER EXPERIENCE WITH A MODEL ROCKET RADIOSONDE:

John F. Cavanagh, Code F405, Naval Surface Warfare Center, Dahlgren, VA 22448-5000

During February of 1987, NSWC conducted sea backscatter measurements using the TRADEX, ALCOR and MMW radars at the KREMS facility on Kwajalein Atoll in the Marshall Islands. Refractive profiles were measured in support of these experiments by means of a radiosonde system launched from a research vessel located near the illuminated surface.

The rocketsonde system is under development by the Applied Physics Laboratory of Johns Hopkins University. Representative profiles will be presented showing evaporation ducts and surface ducts. Comments concerning the employment of this novel device will be offered along with suggested features for incorporation into future versions.

The ocean surface was also monitored during the radar experiments. The research vessel was used to deploy and recover a wave rider bouy. Samples of ocean wave directional spectra derived from the buoy data will be presented.

Session G-4 0855-Thurs. CR2-28
WORLD-WIDE IONOSPHERIC OBSERVING CAMPAIGNS AND STUDIES
Chairman: Sunanda Basu, Emmanuel College, Boston, MA 02115

G4-1
0900

COUPLING, ENERGETICS, AND DYNAMICS OF ATMOSPHERIC REGIONS (CEDAR) - AN NSF INITIATIVE

T. L. Killeen, Vice-Chair CEDAR Science Steering Committee
Space Physics Research Laboratory
Department of Atmospheric and Oceanic Sciences
The University of Michigan
Ann Arbor, Michigan 48109.

The Aeronomy and Upper Atmospheric Facilities Programs of the National Science Foundation's (NSF's) Atmospheric Sciences Division have jointly sponsored a new initiative aimed at providing a more detailed understanding of the physical, chemical, dynamic and radiative processes that control the Earth's upper atmosphere, ionosphere, and near-space environment. The multi-year program was designed through the efforts of many scientists from numerous institutions both within and outside the US. The CEDAR program features the development and utilization of "state-of-the-art" ground-based optical and radar instrumentation to attack a series of scientific problems associated with the vertical and global coupling between atmospheric regions. At present a series of campaigns are being undertaken using existing equipment, and these will be followed by data analysis workshops. A five year plan of equipment development and upgrading for both optical and radar diagnostic techniques has been initiated. In this talk we review the current and evolving state of the CEADR program and focus on several of the individual scientific topics that will be addressed over the next few years.

G4-2
0940

IONOSPHERIC EXPERIMENTS WITH MOTHER-SON ROCKET PAYLOADS

H.G. James
Communications Research Centre,
P.O. Box 11490, Station "H",
Ottawa, Ontario K2H 8S2
Canada

The National Research Council of Canada and NASA are studying proposals for innovative radioscientific experiments in the ionosphere. In the OEDIPUS campaign, it is proposed to launch two high-altitude sounding rockets instrumented with plasma diagnostics. Both will be flown from Andoya, Norway, during periods of auroral activity. A unique feature of each payload will be a long insulated conducting tether connecting the two subpayloads. The separation vector will be parallel to the local magnetic field direction and up to 1 km in length. This system will be deployed in flight and will be used to stimulate various plasma phenomena and to make passive observations of the ambient auroral plasma. The major scientific objectives for this program will be:

1) to measure the reponse of the long probe in the ionospheric plasma;

2) to seek new insights into plane- and sheath-wave propagation in plasmas; and

3) to make passive observations of the auroral ionosphere utilizing the long probe, in particular to measure the component of the natural dc electric field parallel to the magnetic field.

The OEDIPUS-A rocket will stress active probe and wave techniques, points 1) and 2), on a flight in winter 1989 with an apogee of about 650 km. The theme of the OEDIPUS-B rocket one year later will be the passive investigation of the parallel electric field and associated spontaneous plasma phenomena, point 3). The apogee will be 1000 km.

WISP Rocket is the name of a complementary investigation using a double payload comprising a separated transmitter and receiver (no tether), to be launched from Wallops Island in summer 1989. The characteristics of a 40-m transmitting dipole in a magnetoplasma will be investigated, including its impedance and radiation efficiency. This will be carried out at very low frequencies (VLF) on a trajectory with an an apogee of about 400 km.

All the above experiments are preparation for the Waves In Space Plasmas (WISP) investigation on Shuttle/Spacelab. All the rocket trajectories will be such that the payloads will spend a significant fraction of their operational lifetimes in the ionospheric F region, i.e., at WISP orbital altitudes. The preparatory rocket exeriments and WISP have a number of common scientific topics: plasma-wave fundamentals observed with a bistatic transmitter-receiver geometry; antennas and probes in plasmas; and natural wave-particle interactions.

G4-3
1000

WORLDWIDE ACOUSTIC GRAVITY WAVE STUDY (WAGS) - Overview of Results

Paul E. Argo
Los Alamos National Laboratory
Los Alamos, NM 87545 and
Robert Hunsucker
Geophysical Institute
University of Alaska
Fairbanks, AK 99701

The Worldwide Acoustic Gravity Wave Study (WAGS) was conducted during the month of October 1985. Some of the topics of interest were: AGW generation mechanisms, ion-neutral coupling, effects of AGW dispersive propagation, measurements of attenuation constants, and effects and conditions of wave ducting.

The days of October 14-19 were designated as high priority days, and the collection of high-time resolution data was encouraged. The geomagnetic indices for these days indicated moderate activity, and the data are in fact showing "enhanced" acoustic gravity wave activity.

Some interesting results include: (1) the periodicity measured in aurorally generated AGW's may mirror source variations rather than atmospheric filter processes; (2) in several large scale AGW's no systematic variation of period with the propagation distance were observed.

The potential for future campaigns will be discussed.

G4-4
1040

THE WORLD IONOSPHERE/THERMOSPHERE STUDY

C. H. Liu, Dept. of Electrical and Computer Engineering
University of Illinois, Urbana, IL 61801

The World Ionosphere/Thermosphere Study (WITS) is an international, interdisciplinary program of research organized by SCOSTEP for the period July 1987 to December 1989. Its aim is to increase substantially our understanding of the global dynamics of the ionosphere and thermosphere as a coupled system with coupling to the magnetosphere and middle atmosphere. Both large-scale dynamics and small-scale structures will be studied in the global sense. The current status of the program will be reported and the scientific goals and planned campaigns of WITS projects will be discussed.

G4-5
1120

THE INTERNATIONAL REFERENCE IONOSPHERE

Dieter Bilitza
Goddard Space Flight Center, code 633,
Greenbelt, MD 20771, U.S.A.

The International Reference Ionosphere (IRI) is a URSI/COSPAR sponsored project to establish reliable standard models of ionospheric density and temperature parameters based on the world-wide ionospheric data base. The IRI models are continously checked with new measurements and up-dated if necessary. We discuss the latest edition, IRI-86, with special focus on the electron density model.

Comparisons with groundbased and spacecraft data are used to show the extent of agreement between measurements and model, and to indicate areas where more work is needed.

We review the recent progress in empirical and semi-empirical modeling of the ionospheric bottomside, topside and F peak regions and its implications for the IRI.

G4-6 1140 SUNDIAL: A CONTINUING INTERNATIONAL PROGRAM IN SOLAR-TERRESTRIAL PHYSICS

E. P. Szuszczewicz, Director
Experimental Space Programs and Applications
Plasma Physics Division 157
Science Applications International Corporation
1710 Goodridge Drive
McLean, Virginia 22102

SUNDIAL is an international effort combining theoretical modelling with coordinated ground-based and satellite-borne measurement programs. The overall objective is the development of a comprehensive understanding and an associated predictive capability for the cause-effect relationships which control the quiescent and disturbed global-scale ionosphere. While the focus is the ionospheric state at any place, at any time, and under any condition, the program requires and measures solar and interplanetary inputs, and works to establish a detailed understanding of the interactive roles that the ionosphere plays with the magnetosphere and the thermosphere. The program has emphasized the importance of truly world-wide simultaneous measurements, making sure that coverage allows separation of UT and LT effects, and making possible important comparisons between Northern and Southern hemisphere observations. SUNDIAL has established the extended campaign mode as its normal operational procedure, with data collected on a minimum eight-day, around-the-clock basis. For its first three campaigns this has made it possible to observe the global-scale ionosphere transition from a stable, quiescent state to that of considerable disturbance....and then back again to a quiescent condition. This has provided a valuable data set, immensely amenable to comparisons with large scale numerical and empirical modes, and adaptable to SUNDIAL requirements which seek to quantitatively define "quiet," "average," and "progressively disturbed" ionospheric conditions for each of the seasons within a given period of the solar cycle. (Supported by NSF Grant #ATM8617560.)

Session H-2 0855-Thurs. CR1-9
ELECTRON BEAM AND MASS INJECTIONS IN SPACE PLASMAS—I
Chairman: D.A. Gurnett, Dept. of Physics and Astronomy, Univ. of Iowa, Iowa City, IA 52242

H2-1
0900

OBSERVATION OF ELF PLASMA WAVES GENERATED BY PULSED ELECTRON BEAMS

R. I. Bush, G. D. Reeves, T. Neubert, P. M. Banks
STAR Laboratory, Stanford University
Stanford, CA 94305
D. A. Gurnett
Department of Physics and Astronomy, University of Iowa
Iowa City, IA 52242
W. J. Raitt
Center for Atmospheric and Space Sciences, Utah State University
Logan, UT 84322

The Spacelab-2 payload was flown on the STS 51-F Shuttle mission in July and August of 1985, and the Vehicle Charging and Potential Experiment (VCAP) was included as part of the experiment complement. One of the VCAP investigations involved the injection of electron beams with an energy of 1 keV and a beam current of 100 milliamperes into the ionospheric plasma. The electron beam could be square wave modulated to frequencies over 30 kHz by switching the high voltage supply accelerating the electrons. Observations of plasma waves produced by the pulsed electron beams were made by the wave receiver instruments on the Plasma Diagnostic Package (PDP) which provided wide band measurments of both the electric and magnetic field fluctuations up to 30 kHz.

As part of the investigations of the Orbiter environment, the PDP was released from the Orbiter for a six hour period, and the Orbiter was maneuvered into different positions relative to the PDP. During the PDP freeflight, a VCAP sequence designed to emitted electron beams in the ELF pulsing regime was initiated a total of 8 times. In this ELF pulsing sequence, the electron beam was pulsed at 7 different frequencies between 9.5 Hz and 610 Hz. A significant difference in the measured magnitude of the electric and magnetic signatures of the pulsing frequencies was observed between ELF sequences initiated upstream (with respect to the plasma flow) of the Orbiter than for those sequences initiated downstream of the Orbiter. Comparisons of the plasma wave generation efficiency will be presented as a function of the relative positions of the electron beam source and the PDP.

H2-2
0920

AN ANALYSIS OF THE AMPLITUDE OF VLF RADIATION GENERATED BY A SQUARE WAVE MODULATED ELECTRON BEAM IN SPACE

G.D. Reeves, P.M. Banks, K.J. Harker, T. Neubert, R.I. Bush
Space, Telecommunications and Radioscience Laboratory
Stanford University, Stanford, California 94305
D.A. Gurnett
Department of Physics and Astronomy
University of Iowa, Iowa City, Iowa 52242
W.J. Raitt
Center for Atmospheric and Space Science
Utah State University, Logan, Utah 84322

During both the STS-3 and Spacelab-2 space shuttle missions a square wave modulated, 1 keV, 100 mA electron beam was injected in the ionospheric plasma and the resulting electric and magnetic fields measured with an array of plasma diagnostic instruments including a wide-band spectrum analyzer. The results of both missions showed that a square wave modulated electron beam generates narrow-band emissions at the pulsing frequencies and harmonics of those frequencies and broad band emissions throughout the 0-30 kHz frequency range.

Up to this time analysis of the wave emissions was necessarily qualitative because the recorded signals were kept within strict limits by an automatic gain control circuit. Digitization of the wide-band signals and numerical processing allows us to remove the effect of the AGC and study the amplitude of the wave emissions for both the electric and magnetic antennas.

Results of this analysis will be presented for periods of the Spacelab-2 mission during which both the fast pulsed electron generator (FPEG) and the University of Iowa Plasma Diagnostics Package (PDP) were located in the orbiter cargo bay and for periods when the FPEG was on the orbiter and the PDP was released as a free-flying satellite out to distances of several hundred meters. Results for the flux tube connection when the orbiter and the PDP were located on the same magnetic field line while the FPEG was pulsed at 1.22 kHz will be presented in detail. The amplitude of the wave emissions will be compared with the predictions from the theories of model systems [Harker and Banks, 1986., and Al'pert, 1983] and with the amplitude of emissions during a DC flux tube connection [Gurnett et al., 1986]

H2-3
0940

COHERENT CERENKOV RADIATION FROM THE SPACELAB-2 ELECTRON BEAM

W. M. Farrell, D. A. Gurnett and C. K. Goertz
Dept. of Physics and Astronomy
The University of Iowa
Iowa City, Iowa 52242

During the Spacelab-2 (SL-2) mission, the plasma wave instrument onboard the Plasma Diagnostics Package (PDP) detected intense whistler-mode radiation from a 1 keV - 50 mA D.C. electron beam. It is believed that coherent Cerenkov radiation from bunches of beam electrons is responsible for the whistler-mode radiation, where an electrostatic beam-plasma instability forms the coherently radiating bunches. In this paper, we present a detailed model of the coherent Cerenkov emission process from the SL-2 electron beam. A one-dimensional computer simulation of the beam propagating through the ionospheric plasma is used to model the expected phase space structure of the beam electrons. In the simulation, bunching of the beam by a beam-plasma instability is clearly evident. The coherent Cerenkov radiated power from the modeled beam is calculated to be ~ 10^{-8} W/Hz from a 200-meter beam segment, and is about a factor of 10 greater than those measured. It will be demonstrated that the electrostatic instability in the beam is vital to raising the wave powers above incoherent levels since it forms the highly coherent electron bunches. Increasing the radiation efficiency by pulsing the beam in the whistler-mode range of frequencies will also be discussed. Based on the results of this study, it is concluded that coherent Cerenkov radiation processes from the SL-2 electron beam can account for the detected whistler-mode power levels.

H2-4
1000

CORRELATION OF UPPER HYBRID WAVES WITH ELECTRON CONICS

J.D. Menietti, H.K. Wong, C.S. Lin, J.L. Burch
Department of Space Sciences
Southwest Research Institute
6220 Culebra Road
San Antonio, TX 78284

D.A. Gurnett
Department of Physics and Astronomy
University of Iowa
Iowa City, IA 52242

Electron conical distributions have been observed by the Dynamics Explorer 1 (DE-1) and VIKING satellites in the mid-altitude polar magnetosphere. Wong et al. (talk presented at the Fall American Geophysical Union meeting, 1987) have shown that such distributions can be generated by electrostatic upper hybrid waves. Numerical solutions of the diffusion equation, for this mechanism, have been performed and the results compared to particle data obtained by the High Altitude Plasma Instrument (HAPI) on board DE-1. Velocity-space contours of the numerical results compare favorably to the data for local plasma parameters. We have performed a survey of the data obtained by the HAPI and the Plasma Wave Instrument (also on board DE-1) that seems to indicate the presence of upper hybrid waves when electron conical distributions are present. These results support the concept of the generation of electron conics by upper hybrid waves.

H2-5
1040

ORIGIN AND THE NONLINEAR EVOLUTION OF THE ELECTROSTATIC WAVES OBSERVED DURING THE AMPTE SOLAR WIND RELEASES

N. Omidi
Institute of Geophysics and Planetary Physics
University of California, Los Angeles
Los Angeles, CA 90024-1567
K. Akimoto
Earth and Space Sciences Division and
Applied Theoretical Physics Division
Los Alamos National Laboratory
Los Alamos, NM 87545
D.A. Gurnett and R.R. Anderson
Department of Physics and Astronomy
The University of Iowa
Iowa City, IA 52242

To understand the generation and the nonlinear evolution of the electrostatic waves observed during the AMPTE (Active Magnetosphere Particle Tracer Explorers) solar wind releases a detailed investigation is conducted. Previous linear studies have suggested that two distinct sets of instabilities may be responsible for the generation of these waves. One set consists of ion-acoustic type instabilities, while the other group corresponds to the modified two stream instabilities and requires the solar wind flow to be across the ambient magnetic field. In order to establish which set of instabilities are more viable for the generation of the observed electrostatic waves, a detailed linear Vlasov theory has been conducted. In addition both the plasma wave as well as the magnetic field measurements by the IRM (Ion Release Module) spacecraft are used to correlate the frequency and the power of the observed waves with the magnitude and the direction of the solar wind magnetic field. The results of these analyses indicate that the ion-acoustic type instabilities are responsible for the generation of the observed waves. In order to investigate the nonlinear evolution of these instabilities and discern their role in the coupling of the released ions to the solar wind, one-dimensional electrostatic simulations have been performed. The results show that both the solar wind protons and the released ions may be heated and accelerated in the directions oblique to the solar wind flow velocity.

H2-6
1100

PLASMA INSTABILITIES OF A FINITE-SIZE ELECTRON BEAM-PLASMA SYSTEM

C. S. Lin and H. K. Wong
Department of Space Sciences
Southwest Research Institute
San Antonio, TX 78238

It is well known that for an infinite homogeneous electron beam-plasma system, the electron beam mode has a much larger growth rate than the whistler wave. However, for the case of a finite size beam, which is more realistic in space and laboratory experiments than homogeneous beams, it is not clear how the finite size effects will affect the growth of these waves. In this work, the elcctromagnetic dispersion equation of a bound beam-plasma system is derived by assuming that a electron beam with finite radius is imbedded in a cold uniform background plasma. The background plasma can either be bounded or unbounded, depending on the physical situations. The beam drifts along the background magnetic field line with constant velocity, and the self magnetic field by the beam is considered to be negligible. The solutions of the dispersion equation indicate that the growth rate of the beam mode is strongly suppressed around the electron cyclotron frequency if the cyclotron frequency is less than the electron plasma frequency. However, the whistler mode seems to be less affected by the finite size effects. These instabilities are examined for various frequency and plasma regimes. The relevance of these instabilities to wave emissions observed during electron beam injection experiments from the Space Shuttle will be discussed.

H2-7
1120

COMPARISON OF RADIOWAVE AND VEHICLE CHARGING PROCESSES OBSERVED WITH ROCKETS AND THE SPACE SHUTTLE

P.M. Banks, T. Neubert, P.R. Williamson,
R. Bush, G. Reeves, B. Gilchrist and W.J. Raitt
Space, Telecommunications and Radioscience Laboratory
Stanford University
Stanford, CA 94305

This paper will review a collection of interesting space plasma effects observed during the past seven years of experiments with rockets and the Space Shuttle. The question of vehicle charging in response to active electron beam emissions will be covered, showing the complexity of environmental effects. This includes unexpected responses to dramatic changes in background plasma density, hot thruster clouds, and cold nitrogen jet firings. In addition, a review will be given of ELF and VLF wave generation experimental results obtained from the CHARGE-2 rocket and, in collaboration with the University of Iowa, the PDP and VCAP experiments on Spacelab-2. These too, have strange features which are difficult to explain on the basis of present understanding of how electron beams generate waves in the ionosphere.

Session J-4 0835-Thurs. CR0-30
LOW FREQUENCY RADIO ASTRONOMY
Chairman: W.C. Erickson, Astronomy Program, Univ. of Maryland, College Park, MD 20742

J4-1
0840

NEW RESULTS ON THE PROPERTIES OF TYPE III RADIO BURSTS IN THE INTERPLANETARY MEDIUM

Robert G. Stone
Laboratory for Extraterrestrial Physics
NASA Goddard Space Flight Center
Greenbelt, MD 20771

Results are presented on two basic problems in the interpretation of kilometer type III radio observations; 1) Why trajectories in the interplanetary medium derived from type III positions disagree with expected trajectories along the spiral magnetic field. 2) New evidence that kilometer type III radio emission is more generally observed at the harmonic and less often at the fundamental of the local plasma frequency. The ISEE-3 radio experiment monitors solar radio emissions from 2 MHz to 30 kHz corresponding to radial distances from about 10 solar radii to 1 AU from the sun. Utilizing a spinning dipole parallel to the ecliptic and a dipole along the spin axis, the azimuth, elevation, and percent modulation of the radio emission at each observing frequency is determined. Because type III exciter electrons propagate along interplanetary magnetic field lines, tracking type III radio emission should provide a 3-D "snapshot" of the large scale interplanetary magnetic field configuration. But trajectories derived from the observed azimuths generally describe paths through the interplanetary medium that eventually track back to the observer at low frequencies rather than following the expected spiral field path through the interplanetary medium. It was recently demonstrated that the finite size of the source and the directivity of the radiation can account for this observed behavior. Azimuths of the radio sources at low frequencies are shown to be systematically displaced from the azimuths of the centroid of the type III exciter electron beam. A method has been developed that derives the source locations using observed characteristics of the radio burst This yields trajectories that are consistent with the interplanetary magnetic field configuration.

The most recent considerations of whether type III bursts are observed at the fundamental of the plasma frequency, at the harmonic or at both, was presented by Dulk et. al.(G. A. Dulk, J.L. Steinberg, and S. Hoang, Astron. Astrophys., 141, 30-38, 1984). They believe "the evidence for harmonic emission is not as strong as that for fundamental emission in at least some bursts." We studied Type III events whose trajectories crossed 1 AU (observed azimuth passed through 90 degrees) less than one day to the west of the observer . The observing frequency for 1AU is compared with ISEE-3 *in-situ* density measurements assumed to be the same as at the time of the type III event. For 50 events analyzed, *only* harmonic emission is seen. We suggest that harmonic emission is the rule, and that the fundamental is so directive that it is seen only when the observer is looking along the direction of the electron beam.

J4-2
0900

KILOMETER WAVE RADIO BURSTS FROM BEHIND THE SUN

George A. Dulk
Department of Astrophysical, Planetary and Atmospheric Sciences
University of Colorado
Boulder, CO 80309–0391

One of the common types of radio radiation at kilometer wavelengths occurs when streams of multi-keV electrons originate near the Sun's surface and propagate out through the corona and interplanetary space. The flux densities attain values as high as 100 GJy, making the bursts easy to detect with receivers such as were on the Voyager and ISEE–3 spacecraft. A newly-found characteristic of these "type III" bursts is that they are visible to sensitive radio instruments irrespective of the locations of the radiating sources, be they in front of or behind the Sun.

Explanations of the radio emissions will be described in terms of recent ideas of the generation of plasma waves and the emission and propagation of radio waves in a severely inhomogeneous medium.

This work is in collaboration with Drs. A. Lecacheux, J.L. Steinberg and S. Hoang of the Observatoire de Paris, Meudon, France.

J4-3
0920

STUDIES OF LARGE SCALE STRUCTURE OF THE SUN's UPPER CORONA FROM LOW FREQUENCY IMAGING OBSERVATIONS

M. R. Kundu
Astronomy Program
University of Maryland
College Park, MD 20742

We discuss the use of Clark Lake multifrequency radioheliograph for several studies of the large scale structure of the Sun's upper corona. The radioheliograph is used as a coronagraph to study coronal streamers. In particular, we compare our streamer data with similar data obtained in white light from satellite experiments, P78-1 solwind and SMM-C/P. We study the rotation of streamers as they move across the disk and show that they can be used to study 3-D structure of coronal structures. We study the propagation of type III-burst producing electrons in coronal streamers and deduce electron density distribution above streamers. Using daily quiet sun images, we produce synoptic charts and compare them with white light synoptic charts, which reveal the existence of streamers and coronal holes as bright features and voids. Finally, we show that slow ($\lesssim$ 100 km/s) coronal mass ejections events (CME's) can have radio signatures associated with them.

J4-4
0940

IMPORTANCE OF RADIO OBSERVATIONS TOWARDS THE UNDERSTANDING OF CORONAL MASS EJECTIONS

N. Gopalswamy
Astronomy Program
University of Maryland
College Park, MD 20742

We present the analysis of low frequency imaging observations of coronal mass ejection events. The observations of nonthermal radio emission generally reveal the dynamics of energetic particles and their inter-action with the associated coronal mass ejection (CME) and the ambient corona. "Precursor" type III bursts indicate the presence of particle acceleration and heating during the onset phase of CME's. Positional analysis of the II bursts provides information about the origin of the shocks - whether created by the CME or by the flare explosion. The moving type IV burst associated with a CME can be used to study the nature of the plasmoid associated with the CME and the characteristics of the nonthermal particles trapped in the plasmoids. Thus radio emissions at various stages of the CME could be used to study the evolution of the CME's.

J4-5
1000

URANUS RADIO EMISSIONS

M.L. Kaiser
Goddard Space Flight Center, Code 695
Greenbelt, MD 20771

Uranus was very slow in revealing direct evidence of its magnetosphere. For both Jupiter and Saturn, polarized emissions of magnetospheric origin were detected by the Voyager Planetary Radio Astronomy instruments when the spacecraft were still several A.U. from their respective encounters. In contrast, the first Uranian emissions were not detected until just a few days before the Voyager-2 fly-by which occurred on January 24, 1986.

Radio observations in the immediate vicinity of Uranus showed that although the Uranian emissions were generally weaker than their Jovian and Saturnian counterparts, the were by no means simpler. Uranus' radio spectrum appears to consist of perhaps as many as six separate radio components originating from separate magnetospheric source regions and with a variety of emission mechanisms. These radio components are all in the band from a few kHz to about 850 kHz. In addition to the megnetospheric radio components, some signals above 1 MHz were detected which may originate in atmospheric discharges (lightning). The observational characteristics of each component will be described and the ongoing analysis effort aimed toward localizing the individual source regions will be reviewed.

J4-6
1020 THE MAIN SOURCE OF RADIO EMISSION FROM THE MAGNETOSPHERE OF URANUS

Thomas D. Carr, Department of Astronomy, University of Florida, Gainesville, FL 32611.

Samuel Gulkis, Space Science Division, Jet Propulsion Laboratory, Pasadena, CA 91103.

We developed a geometrical model to account for the main component of the modulated radio emission, which was left elliptically polarized, observed from about 20 to 900 kHz as Voyager 2 passed near Uranus. We assumed cyclotron maser emission by electrons descending within the L=17 magnetic shell toward the boundary of the UV auroral region seen on the dark side of the planet. In the model, X-Mode radiation is emitted in a thick-walled hollow-cone beam from each point within a sector of the so-called auroral radio ring. The axis of each hollow cone is tangent to the magnetic field at the emission point. The radio ring at each observed frequency is located just above the intersection of the L=17 shell with the contour surface on which the electron cyclotron frequency equals that observed. The overall emission beam at a given frequency is thus the sum of the hollow-cone beams from all source points lying in the active sector of the ring. With optimized sets of the adjustable parameters, reasonably good fits to the main features of the observed modulation patterns were obtained. The Uranian radio emission, the Auroral Kilometric Radiation (AKR) from Earth, the emission from Saturn, and that from Jupiter are compared in this frequency range. An electron density profile model based on the similarity of the Uranian emission to AKR was obtained.

J4-7
1040

INTERFEROMETRIC PHASE SCINTILLATION IN THE IPM

B. Dennison[1,2], S. Ananthakrishnan[3], R. S. Simon[2], R. L. Fiedler[2]

1 Virginia Polytechnic Institute & State University
Blacksburg, VA 24061

2 E. O. Hulburt Center for Space Research
Naval Research Laboratory
Washington, DC 20375

3 Tata Institute of Fundamental Research
Ooctacamund 643 001, India

Using a global VLBI array operating at 327 MHz, we find strongly correlated scintillations in the fringe phase obtained on various baselines. The magnitude of the fringe phase scintillations is approximately proportional to baseline length. Cross correlation of the fringe phase on different baselines reveals maximum correlation at some small lag, whose value is dependent upon baseline pair. We find that the lags of maximum correlation (for different baseline pairs) are fit very well by a model in which the phase fluctuation pattern is moving across the array with fixed velocity. Since the fit velocity is 410 km/s, almost radially outwards from the sun, we confirm that the interplanetary medium is responsible. The implied phase power spectrum is in good agreement with other observations.

These results have important implications for VLBI, particularly at low frequencies. These implications will be discussed for existing arrays, as well as planned extensions into space.

J4-8
1100

THE GALACTIC PLANE AT 30.9 MHz

Namir E. Kassim
Astronomy Program
University of Maryland
College Park, MD 20742

The Galactic plane has been mapped with the Clark Lake TPT telescope at a frequency of 30.9 MHz with unprecedented resolution. The synthesized beam at the zenith is 13.0 × 11.1 arc–minutes. Contour maps have been produced for the region $350° < l < 250°$ with $|b| \leq 2° - 3°$, and a source list of nearly 700 discrete emission sources accompanies them. The survey has permitted the study of the interaction between small–scale Galactic nonthermal emission processes and their absorption by intervening ionized gas which was not possible with earlier lower resolution surveys.

Results from this study which will be presented include:

1. New SNRS. More than 60 discrete nonthermal sources which have been catalogued are probably either previously unidentified or missidentified Galactic SNRs. If so, these candidates could significantly increase the number of catalogued SNRs.
2. Known SNRs. The survey has permitted the construction of the accurate low frequency spectra of known Galactic SNRs. From these, low frequency optical depths towards 51 SNRs have been derived and used to determine the distribution of ionized gas in the ISM. Patchiness in the absorption towards distant SNRs places an upper limit on the density of any hot (T $\sim$ 8000K), widely distributed ionized component of the ISM at 0.25 cm^{-3}. Taken together with 325 MHz recombination line observations, they indicate the presence of hot (T $\sim 3000 - 8000$K), low density ($n_e \sim 1 - 10$ cm^{-3}) ionized gas, probably associated with the outer envelopes of 'traditional' HII regions.
3. Numerous foreground HII regions were detected in absorption against the Galactic background. Combined with lower resolution observations these measurements have permitted a determination of the strength of the Galactic background and foreground emission towards the HII regions.
4. Patchiness in the distribution of extragalactic source counts at higher longitudes has been used to infer the presence of a low density ionized halo associated with a known HII region in the outer Galaxy.
5. No prominent new sources with steep spectra similar to the millisecond pulsars PSR 1937+21 and PSR 1821−24 have been found. This indicates that any such similar sources located along the Galactic plane must be at significantly lower flux densities.

Composite maps of the entire survey will be shown and a qualitative discussion of their morphology as a function of Galactic longitude will be given.

J4-9
1120

THE LOW FREQUENCY SPACE ARRAY

K.W. Weiler[1], B.K. Dennison[1,2], W.C. Erickson[3], K.J. Johnston[1], M.L. Kaiser[4], R.S. Simon[1], and J.H. Spencer[1]
[1]E.O. Hulburt Center for Space Research, Naval Research Laboratory, Washington, DC, 20375-5000
[2]Virginia Polytechnic Institute and State University, Blacksburg, VA, 24061
[3]University of Maryland, College Park, MD, 20742
[4]NASA Goddard Space Flt. Ctr., Greenbelt,MD 20771

At the lowest radio frequencies (≤30 MHz), the Earth's ionosphere transmits poorly or not at all. This relatively unexplored region of the spectrum is thus an area where high resolution, high sensitivity observations can open a new window for astronomy. Also, extending observations down to such very low frequencies approaches a fundamental physical limit where the Milky Way becomes optically thick due to diffuse free-free absorption.

To obtain data at these frequencies requires the difficulty and expense of placing radio telescopes into Earth orbit, but the scientific rewards of a space mission are likely to be great. Even without considering the serendipitous discoveries which have always accompanied the opening of a new realm of frequency, resolution, or sensitivity in astronomy, a low frequency telescope in space can:

1. map the entire sky, particularly the galactic background non-thermal emission;
2. survey the galactic diffuse ionized hydrogen absorption;
3. study of the interstellar plasma scattering and refraction;
4. study individual source spectra for energy production and absorption/loss mechanisms;
5. study the correlation between steep spectrum galaxy clusters and enhanced x-ray emission;
6. search for "fossil" radio sources;
7. image individual sources with high resolution;
8. study the impulsive emission from Jupiter and the Sun; and
9. search for cosmic coherent radiation.

A scientific justification and technical description is developed for a Low Frequency Space Array (LFSA) operating at deka-hectometer wavelengths to carry out high resolution, high sensitivity full sky mapping and individual source imaging at frequencies between 1.5 and 26.3 MHz.

J4-10
1140

LOW-FREQUENCY RADIO ASTRONOMY WITH SMALL SATELLITES

D.L. Jones, T.B.H. Kuiper, M.J. Mahoney, and R.A. Preston
Mail Code 238-700
Jet Propulsion Laboratory
4800 Oak Grove Drive
Pasadena, CA. 91109

There are many important astrophysical questions which could be answered with observations at frequencies of a few MHz and angular resolution of an arcminute or better. Such data can be obtained with an interferometer array composed of several small satellites in Earth orbit.

A workshop was held at JPL in May 1987 to consider how small and simple the individual satellites for such a mission could be. Since then two spacecraft designs have been studied: 1. cylindrical, gravity gradient stabilized, with two orthogonal dipoles in the horizontal plane, and 2. spherical, unstabilized, with three orthogonal dipoles. In either design the satellites contain uncooled receivers for frequencies below $\approx$ 15 MHz, nearly omnidirectional antennas, a high quality crystal oscillator, and a low power telemetry transmitter. There are no gyros, thrusters, data recorders, or other moving parts, and no expendables. The weight of each satellite could be as low as 35-45 kg. This is important because the performance of the array depends strongly on the number of satellites.

For satellites without thrusters, careful deployment with velocities $\approx$ 1 cm/s is essential. Deployment is particularly simple in the case of spherical satellites, which can be dispersed spherically from the launch bus. This requires no special orientation of the bus. The array would then slowly disperse under the influence of the deployment velocities and various differential drag forces. In a 30000 km altitude circular orbit it should take at least a year for the size of the array to exceed 200-300 km, the maximum useful baseline length at a few MHz. For orbital heights $\geq$ 10000 km, a single small ground antenna could receive data simultaneously from all satellites in the array.

A number of specific areas are still being studied, including the optimal orbital parameters, radiation hardening (if a $\approx$ 10000 km orbit is chosen), methods for accurately determining the three-dimensional configuration of the array as a function of time, sensitivity limits, and the effects of man-made interference on data calibration.

This work was carried out by the Jet Propulsion Laboratory, California Institute of Technology, under contract with the National Aeronautics and Space Administration.

Session A-5 1355-Thurs. CR1-42
EMI MEASUREMENTS AND STANDARDS
Chairman: Edward K. Miller, Rockwell Science Center, Thousand Oaks, CA 91360

A5-1
1400

NBS CALIBRATION PROCEDURES FOR HORIZONTAL DIPOLE ANTENNAS (25 to 1000 MHz)

Dennis Camell and Ezra Larsen
Electromagnetic Fields Division, 723.03
National Bureau of Standards
Boulder,CO 80303

The theoretical basis and test procedures for horizontally polarized dipole calibrations at the National Bureau of Standards will be described. Two different techniques and two different test sites are used for these measurements. The standard antenna method uses the calculation of a field strength level, from the response of a simple half-wave dipole, to calibrate an antenna. This method is used at an open field site in the frequency range of 125 to 1000 MHz. The standard field method applies the theoretical gain equations of waveguides to determine the field strength level. This latter method is used in an anechoic chamber in the frequency range of 200 to 1000 MHz. Procedures for both techniques are explained and measurement setups are illustrated. Measurement uncertainties are discussed.

A5-2
1420 ELECTROMAGNETIC SUSCEPTIBILITY TESTING OF ELECTRONIC SUBSYSTEMS BY DIRECT INJECTION*

R. J. King and W. Ng
Lawrence Livermore National Laboratory
Livermore, California 94550

The lack of realistic threat-level transient electromagnetic simulators in the HF through the microwave frequency range mandates the development of clever techniques for evaluating the susceptibility of electronic subsystems. Even if such pulsed simulators existed, cost and size would limit the range of threat environment parameters, such as spectral frequency components which can be generated, threat engagement angles, polarization, and peak fluence levels. Therefore, there is strong motivation to:

(a) measure coupling down to the input terminals of a subsystem using low level (linear) cw techniques, and then
(b) use this information to properly inject high power pulses directly into the subsystem to achieve burnout or upset, and thereby establish susceptibility threshold levels. Having established such thresholds, there is a need to verify that the electronic subsystems can survive a real threat for full system analysis.

Accomplishing step (a) is now relatively routine. Step (b) is a new challenge which this paper addresses.

A proposed direct injection technique for testing the electromagnetic susceptibility of electronic subsystems is outlined. This technique accounts for the highly complex structure of the threat signal appearing at the terminals of the subsystem, and permits the susceptibility level to be precisely and continuously measured over a wide frequency spectrum. It takes advantage of the high precision attainable from modern frequency domain instruments, as well as time domain pulsing to account for heat build-up within susceptible electronic components. The technique uses linear cw coupling measurements made at the cable terminals which feed the subsystem. It therefore includes the effects of the external EM threat parameters, e.g., spectral intensity of frequency components, polarization, and incidence direction. Besides being useful for establishing electronic breakdown thresholds, the technique can be used for full system analysis to verify that the electronics can survive an assumed threat.

The instrumentation system is fully automated for data acquisition and control of test parameters. Testing up to 200 W peak power has been done over the 1 to 18 GHz range, but the technique is sufficiently general that it can be adapted to any frequency range.

A5-3
1440

ALTERNATIVE TECHNIQUES FOR SOME TYPICAL ELECTRIC FIELD MEASUREMENTS IN A SCREENROOM

J. E. Cruz and E. B. Larsen
Electromagnetic Fields Division
National Bureau of Standards
Boulder, Colorado 80303

This report deals with alternative techniques for several types of screenroom measurements to be considered by the U.S. Army for more accurate electromagnetic compatibility (EMC) testing. Most testing is performed in a shielded enclosure (screenroom) which leads to uncertainty in the measurement of emissions from electronic equipment, or the susceptibility of equipment to electromagnetic (EM) radiation. Possible alternative techniques for improved measurements in a screenroom have been developed by the National Bureau of Standards (NBS). These techniques are covered in this talk.

We present antenna factors determined in a screenroom which was partially loaded with radio frequency (rf) absorbing material, using the two-antenna insertion-loss technique. These antenna factors are compared with the antenna factors obtained in an unloaded screenroom, a fully loaded screenroom (anechoic chamber), and at an open field site. In addition, measurements at the eight corners of a cube were made in the partially loaded and fully loaded screenroom to determine the field deviation at the eight corners of the cube with respect to its center. Also, measurment improvements are quantified for electric field strength beneath a single-wire transmission line, in a partially loaded screenroom. Finally, electric field measurements were made on top of the grounded table in a partially loaded screenroom to determine the field strength variation above the table.

A5-4
1520

ANALYSIS OF MODE STIRRED CHAMBERS USING GEOMETRICAL OPTICS

John M. Dunn

Department of Electrical and Computer Engineering
University of Colorado
Box 425
Boulder, Colorado, 80309

Mode stirred chambers are presently under consideration at a number of research laboratories as an attractive alternative to the more conventional anechoic chambers for use in the testing of systems in various electromagnetic environments (M.T. Ma et. al., Proc. of IEEE, 73(3), 388–411, 1978), (P.C. Corona et al., IEEE Trans. EMC, 18(2), 54–59, 1976). The mode stirred chamber typically consist of a rectangular test chamber with metal walls, and a stirrer, usually in the form of a large paddle or fan blade, near the ceiling of the chamber. The object under test is placed in the chamber and exposed to an electromagnetic field, during which time the stirrer slowly revolves. The average response of the object to the field is found by integrating the response over the time period of one revolution of the stirrer. The metal walls of the cavity allow a large field to be built up inside the cavity. At the same time the stirrer smooths out the sharp nulls of the field, usually present in such a resonant structure. The object under test can therefore be exposed to a high field level consisting of several different polarizations. It is therefore possible to test the object in a matter of hours instead of days.

The conventional thinking in the study of such chambers has been to decompose the field into a series of modes without the stirrer present, and to then regard the stirrer as coupling or mixing the various modes together, thus the name mode stirred chamber. It is shown that there are a large number of modes present in the chamber for reasonably high frequencies, typically several hundred. It is then not possible to carry the analysis much farther, and a random field is assumed. It is then possible to derive an approximate value for the Q of the chamber (B.Liu, et. al., NBS tech. note 1066, 1983).

The same formulas for the Q of the chamber can be derived in an alternative way using geometrical optics. This method has two advantages over the more conventional method of analysis using modes. The first is that the technique can be extended to chamber shapes other than rectangular. The second it that the posssibility of a better physical understanding of the fields in the chamber can be reached, leading to the possiblility of better chamber design.

In this talk, I will first explain the geometrical optical method of calculating the chamber Q, and will then go on to explain how a number of better designs are suggested.

A5-5
1540

THE EFFECT OF A LARGE ROTATING SCATTERER IN A RECTANGULAR CAVITY

D. I. Wu
Electromagnetic Fields Division 723.03
National Bureau of Standards
Boulder, CO 80303
D. C. Chang
Department of Electrical and Computer Engineering
University of Colorado
Boulder, CO 80309

In a mode-stirred chamber, the field in the cavity is perturbed with a stirrer, i.e. a rotating scatterer, in such a way that it is uniformly random. This uniformity feature is the governing characteristic of the mode-stirred (or reverberating) chamber widely used in the area of electromagnetic interference testing. To establish a design guideline for the stirrer, it is essential that we understand the key mechanism which produces this uniform randomness. Since it has been shown that a small resonating stirrer of dimension less than a wavelength can not produce a statistically uniform field (D. I. Wu and D. C. Chang, URSI/AP Symposium, URSI Abstracts, p.55, June 1986), in this analysis we focus on the effect of a large body stirrer.

In treating a large body scatterer, we begin by examining the fundamental properties associated with a perturbing body in a cavity. Using the concept of perturbation, we find that the key to effective perturbation lies not so much in resonance but in the shifting of eigenmode frequencies. When the size of the perturbing body becomes large, the shifting may be large enough that the new perturbed modes no longer resemble the original unperturbed modes. In effect, as the stirrer rotates, different perturbed modes may be excited, thus introducing randomness into the system. To capture the essence of effective field perturbation as well as to minimize numerical complexity, we revert to a two-dimensional case for illustrative purposes. The numerical complexity is further simplified by the use of a 2D Transmission-Line-Matrix (TLM) method. The TLM method is a time domain numerical method where the propagation of plane wave in any medium or structure is modeled by a Cartesian mesh of transmission lines. Plane wave propagation is manipulated by monitoring the voltage and current at every node throughout the mesh as time progresses. The response in the frequency domain is obtained by performing the discrete Fourier transform on the output function. Using the TLM method, the shifting of eigenfrequencies and the variation on the magnitude of the fields for different stirrer sizes are examined. From this analysis, useful insights are drawn which include an analogy between the action of a large rotating scatterer and a frequency modulator.

A5-6
1600

AIRCRAFT FIELD DEGRADATION AND ELECTROMAGNETIC COMPATIBILITY

Kenneth H. Cavcey and
Dennis S. Friday
Electromagnetic Fields Division
National Bureau of Standards
Boulder, Colorado 80303

This paper discusses the first tests undertaken to study the problem of field degradation in army aircraft (helicopters and one fixed wing airplane) due to the deterioration of electronic and electrical systems. The electromagnetic compatibility (EMC) of such systems were investigated by considering the aircraft as a collection of radio frequency sources. Methods to detect these sources were developed including the non-stationary noise that existed.

Next the collected data was studied to see if there existed any obvious factors derived from the data that one could use to correct potential problems that might affect flight safety. Emphasis was placed upon making such test methods appropriate, inexpensive, and easily performed by army field personnel. In addition applications to quality control or acceptance testing, as related to the Environmental Stress Screening (ESS) program, are examined.

Session B/F-1 1355-Thurs. CR2-6
RANDOM MEDIA
Chairman: David Chang, Dept. of Electrical and Computer Engineering,
Univ. of Colorado, Boulder, CO 80309-0425

B/F1-1
1400

AN EXAMINATION OF THE "FULL-WAVE" METHOD FOR ROUGH SURFACE SCATTERING

Eric. I. Thorsos
Applied Physics Laboratory
College of Ocean and Fishery Sciences
University of Washington
Seattle, WA 98195

Akira Ishimaru
Department of Electrical Engineering
University of Washington
Seattle, WA 98195

The accuracy of Bahar's "full-wave" solution for scattering from rough surfaces (E. Bahar, IEEE Trans. Antennas. Propagat., AP-28, 11-21, 1980; Eqs. 4.10 and 6.5b) is examined for the case of the Dirichlet (zero field) boundary condition using one dimensional surfaces with a Gaussian roughness spectrum. This corresponds to scattering of horizontally polarized electromagnetic waves from perfectly conducting rough surfaces. The field quantity calculated is the bistatic scattering cross section, which is obtained with a Monte Carlo technique. The full-wave solution is compared to that obtained with the Kirchhoff approximation, with first order perturbation theory, and with exact numerical results obtained by solving an integral equation. The full-wave solution is found to agree closely with the Kirchhoff solution, except for grazing incident and scattered angles. The full-wave solution does not reduce to the first order perturbation solution as the rms surface height and slope become small. Also, exact numerical results begin to diverge from the Kirchhoff results as the surface correlation length is reduced below the radiation wavelength; in this region the full-wave solution continues to agree closely with the Kirchhoff solution, except for grazing incident and scattered angles. In summary, we find that the full-wave method is not an improvement over the Kirchhoff approximation for this case.

B/F1-2
1420

A SIMPLE MODEL OF THE BACKSCATTER ENHANCEMENT EFFECT FOR RANDOM ROUGH SURFACES

F. K. Schwering
US Army CECOM, ATTN: AMSEL-RD-C3-TA-1
Fort Monmouth, NJ 07703

The backscatter enhancement effect is analytically demonstrated for a simple model of a random rough surface. The model consists of a planar metal surface with a random distribution of scatter centers in the form of vertical dipoles (Fakir's bed). For simplicity, the two-dimensional problem is treated where the dipoles are replaced by parallel, vertical ridges as indicated in Fig. 1; the incident plane wave is TM-polarized with regard to the ground plane. The dipoles or ridges are assumed to be loss-less passive scatterers; the dipole moment per unit length of the n^{th} ridge is $p_n = \alpha E_{zn}$ where α is a constant, which is the same for each ridge, and E_{zn} is the vertical electric fieldstrength at the locaton of the n^{th} ridge generated by the sum of the incident plane wave, the specular wave reflected by the ground plane, and the scatterfields of all other ridges.

The scatter problem for this surface is solved by an iterative procedure where the first term represents single scattering, the second term double scattering, etc. These terms and the associated power patterns are obtained in the form of multiple sums which, however, can be substantially simplified on careful inspection. In particular, the second order theory has been reduced to closed form analytical expressions. The backscatter enhancement appears quite natural in this representation and no special effort is needed to extract it from the formulas.

The theory shows that, as expected, the backscatter enhancement is caused by second and higher order scattering, and that the maximum enhancement is limited to 3 dB which occurs when multiple scattering dominates over single scattering. The theory shows, furthermore, that the backscatter enhancement will be clearly visible only if the average spacing d of the scatter centers is in the order of a wavelength or more while it becomes obscured as d is reduced. Also, the backscatter lobe is much broader than the forward scatter lobe (which is caused by single scattering). For given overall size of the scatter surface, the width of the forward lobe is independent of d, while the width of the backscatter lobe increases with $\sqrt{\lambda/d}$ as the number of scatter centers is increased and d is reduced.

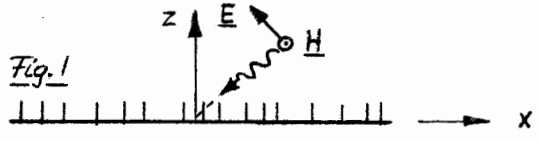

Fig. 1

B/F1-3
1440

EMISSIVITY OF A HALF SPACE ANISOTROPIC RANDOM MEDIUM

Jay K. Lee and Saba Mudaliar
Department of Electrical and Computer Engineering
Syracuse University
Syracuse, NY 13244-1240

A model for calculating the emissivity of a half space anisotropic random medium is presented here. We follow the multiple scattering approach using the Dyson equation for the mean field along with the Bethe-Salpeter equation for the covariance of the electric field. The modified radiative transfer (MRT) equations thus constructed are solved under a first order approximation to obtain the upward- and downward-travelling incoherent intensities. The procedure is the same as followed by the authors for calculating backscattering coefficients for the above-mentioned medium (URSI Meeting, Blacksburg, VA, 1987). We provide analytic expressions for bistatic scattering coefficients and compare them with those obtained by the Born or single scattering approximation (Lee and Kong, IEEE Trans., GE-23, 924-932, 1985). The structure is exactly the same except for two changes. The single most striking feature observed due to a multiple scattering approach is that the propagation constants which appeared in the Born approximation results are replaced by "effective" propagation constants. This is exactly what one would expect under the first-order approximation to the MRT equations.

Secondly, we notice that there are some modifications in the terms which contribute to backscattering. We observe that these are due to "backscattering enhancement," which is a unique result of the wave theory as compared to the phenomenological radiative transfer theory.

Using these expressions for bistatic scattering coefficients we proceed to compute the emissivity through $e = 1 - r_c - r_i$ where r_c is the coherent reflectivity and r_i is the incoherent reflectivity obtained by integrating the bistatic scattering coefficients over the upper hemisphere. A number of numerical results are presented to facilitate comparison with the corresponding single scattering approximation results. Finally the theoretical results will be used to explain a set of measured emissivity data of terrain media which are electrically anisotropic and highly scattering.

B/F1-4
1500

BACKSCATTERING ENHANCEMENT BY RANDOMLY DISTRIBUTED LARGE PARTICLES

Yasuo Kuga and Akira Ishimaru
Department of Electrical Engineering
University of Washington
Seattle, Washington 98195

The experimental evidence of the backscattering enhancement due to randomly distributed particles was first reported by Kuga and Ishimaru (J. Opt. Soc. Am. A, 1, 831, 1984) and later by other groups. This enhancement was caused by the constructive interference of two waves traveling through identical multiple scattering paths in opposite directions. It is also known as the weak Anderson localization effect in solid state physics. We call this backscattering enhancement type I. The characteristics of enhancement type I are (1) it is most visible when the particle size is comparable to the wavelength, (2) the peak is observable only in densely distributed particles, and (3) the angular width of the peak is less than 0.1 - 0.2 degrees and it is related to the transport cross section. When the particle sizes become much larger than the wavelength, backscattering enhancement type I is not observable. However, it has been indicated previously that the backscattering enhancement can be caused by large particles and turbulences (Kravtsov and Saichev, Sov. Phys., 25, 1982). This enhancement is also known as the double-passage effect and focusing effect. It has been indicated that this enhancement may occur in sparsely distributed random media, and therefore, it may be important for remote-sensing applications. We call this backscattering enhancement type II. In this paper we will show the experimental evidence of backscattering enhancement type II. The experiment was conducted using large particles (45 μm) and a HeNe laser (λ = 0.475 μm in water). Both the co-polarized and cross-polarized components were measured for optical distances of 0.5 to more than 100. Unlike enhancement type I, type II is most visible around a particle concentration of 1% and an optical distance of 15. It disappears in a dense concentration of particles. The shape of the peak in the cross-polarized components is substantially different from the one in the co-polarized components. The differences between enhancement types I and II will be discussed.

Session B-7 1535-Thurs. CR2-6
RESONANCES
Chairman: David Chang, Dept. of Electrical and Computer Engineering, Univ. of Colorado, Boulder, CO 80309-0425

B7-1
1540

USING THE EFIE IN THE PRESENCE OF CAVITY RESONANCES

Francis X. Canning
Rockwell International Science Center
Thousand Oaks, CA 91360

Hollow, perfectly conducting bodies support internal resonances at discrete frequencies, at which the total current flowing on the surface cannot be determined by the EFIE and the incident external field. The undeterminable component of the surface current, i.e., that associated with the cavity mode, does not radiate, so the scattered fields are determined by the EFIE. However, it has been widely reported that Method of Moments (MoM) calculations based on the EFIE have severe numerical problems at such resonant frequencies. One may ask if a different numerical procedure, based on the EFIE, would circumvent these problems. We will demonstrate such a procedure. In addition, we will gain insight into the mechanisms by which moment method calculations based on the EFIE often fail near these resonant frequencies.

A matrix algebra technique called the Singular Value Decomposition (SVD) is used. While the algorithms implementing this technique have existed for decades, this author's literature search found no references to its application to moment method problems. One purpose of this paper, therefore, is to describe how SVD applies to moment method problems, and to describe the information it provides about the MoM matrix.

We begin by describing what is known theoretically about the matrices used in the moment method. We find that close to the resonant frequencies the numerical problem comes from a term that can be isolated. This term is the product of three numbers, two of which are close to zero and one which is very large. Numerical calculations are performed on a trivial test case, that of scattering by a conducting circular cylinder. The SVD is applied to these calculations, showing the cause of the numerical problems. This detailed information suggests possible solutions, which we explore.

B7-2
1600

A HYBRID E-PULSE/LEAST SQUARES TECHNIQUE FOR NATURAL RESONANCE EXTRACTION

E. Rothwell, K. M. Chen, D. P. Nyquist and W. Sun
Department of Electrical Engineering and Systems Science
Michigan State University
East Lansing, MI 48824

Interest in using natural resonances in the discrimination of radar targets has prompted the need for an efficient, automated technique for extracting the complex resonance frequencies of a target from a measurement of its transient response. A new scheme based on the E-pulse technique has been developed, and is found to have the additional benefits of random noise and mode content insensitivity.

An E-pulse waveform is defined to be a finite duration signal which when convolved with a sum of damped sinusoids produces a null result in the late-time. If m(t) represents the measured transient response of a target (assumed to be a finite sum of damped sinusoids in the late-time), then the E-pulse waveform e(t) is the solution to the convolutional integral equation $m(t)*e(t)=0$, $t>T_L$, where T_L is the beginning of late-time. The natural frequencies contained in m(t) are then the solutions to E(s)=0, where E(s) is the Laplace transform of e(t). By an appropriate representation of e(t), E(s)=0 becomes a polynomial equation.

As there are many possible solutions for e(t), it becomes prudent to define the "best" solution as that which minimizes the squared difference between the measured waveform and a waveform constructed using the natural frequencies found from solving E(s)=0. This criterion becomes the basis for an automated method for determining the natural frequencies which is insensitive to the presence of random noise and to estimates of modal content.

Examples using the measured responses of various radar targets are considered.

B7-3
1620

The Calculation and Identification of the Complex Natural Resonances of a Circular Strip

Jeffery T. Williams

Applied Electromagnetics Laboratory
Department of Electrical Engineering
University of Houston
Houston, TX 77004, USA

Donald G. Dudley

Electromagnetics Laboratory
Department of Electrical and Computer Engineering
University of Arizona
Tucson, AZ 85721, USA

The circular strip is an ideal canonical scattering structure for use in system and target identification studies and in transient antenna range experiments. It offers a tractable theoretical solution, and it is relatively easy to model experimentally. In addition, the circular strip supports two distinct species of natural resonances: exterior resonances and interior resonances. The interior resonances suffer little radiation damping, whereas, the exterior resonances are more highly damped. Therefore, the circular strip provides an excellent model in which to compare the relative contributions of strong natural resonances and weak, highly damped resonances.

An electric field integral equation is formulated in terms of the current induced on the surface of the strip and solved using the method of moments (MOM). Using the MOM formulation, we determine the natural resonances of the circular strip. We show the pole trajectories for the first layer of exterior resonances for a wide range of strip height-to-radius ratios. In addition, we locate the strong interior resonances and relate them to the TM_{0pq} modes of the circularly cylindrical cavity. We find that the interior resonances which correspond to the TM_{0p0} cavity modes are weakly damped, dominating the scattered field response.

Using the transient scattered fields calculated from the MOM formulation as input and output data for a single input, single output identification algorithm, we identify the dominant poles in the scattered fields. We show that these dominant poles are those associated with the TM_{0p0} interior resonances of the circular strip. We also show that by using intelligent filtering and source selection, resonances with higher damping can be identified.

B7-4
1640

NATURAL RESONANCE EXTRACTION USING THE FINITE ELEMENT METHOD-DIELECTRIC PROLATE SPHEROIDS

Philip J. Moser
AVTEC Systems, Inc.
3025 Hamaker Court
Fairfax, VA 22031-2217

Michael A. Morgan
Naval Postgraduate School
Monterey, CA 93943

Anton Nagl and Herbert Uberall
The Catholic University of America
Washington, D.C. 20064

The Finite Element Code for Electromagnetic Scattering (M.A. Morgan and K.K. Mei, IEEE Transactions AP-27, pp. 202-214, 1979) has been adapted for finding resonances of axisymmetric penetrable bodies and applied to solid dielectric spheroids. These resonances are created by creeping waves both in the dielectric material and along its exterior surface and are distinctive to the material composition and body shape (H. Uberall, et al., J. of Applied Physics, September 15, 1985). Because of the flexibility inherent in the Finite Element Method, it is now possible to extend the research for resonances to penetrable bodies and is applicable to both homogeneous and non-homogeneous materials with both real and complex dielectric constants. This method has been applied to homogeneous real dielectric prolate spheroids and resonances found. From the resonances a scheme has been applied using phase matching techniques to obtain phase velocity dispersion curves and attenuation curves. The effects of the resonances on the body's radar cross-section can now be evaluated and their importance in target identification noted.

Session G-5 1355-Thurs. CR2-26
HIGH LATITUDE IONOSPHERIC PHENOMENA
Chairman: Herbert Carlson, Ionospheric Physics Lab, Hanscom AFB, MA 01731

G5-1
1400 SMALL SCALE ELECTRODYNAMIC STRUCTURE OF THE HIGH LATITUDE IONOSPHERE

James F. Vickrey
Geoscience and Engineering Center
SRI International
333 Ravenswood Avenue
Menlo Park, CA 94025

Traditionally, the study of ionospheric irregularities at high latitudes has concentrated on fluctuations in electron number density and/or integrated electron content. This emphasis was driven largely by the fact that readily available experimental diagnostics were limited to scintillation measurements and occasional in-situ langmuir probe observations. Over the past several years, our knowledge of the processes that control the formation and dissipation of plasma structure have increased greatly. This is a result of improved theoretical modeling and more comprehensive diagnostics. We now know that the evolution of F-region plasma structure is strongly affected by electrodynamic coupling to the E-layer below and to the magnetosphere above. Information about the conditions in these various altitude regimes is conveyed via electric fields perpendicular to the geomagnetic field B and by magnetically field-aligned currents. Thus the spectral characteristics of density fluctuations are intimately associated with those of the electric and magnetic fields. In this review we will emphasize the electrodynamic coupling processes along the magnetic field and their consequences for the evolution of plasma structure. We will also present examples of the spectral forms of electric and magnetic field fluctuations and discuss the exchange of Poynting flux between the magnetosphere and the ionosphere as a function of scale size.

G5-2
1440

NIGHTSIDE UV AURORAL IMAGES AND VHF/UHF SCINTILLATION

Santimay Basu, R.W. Eastes, F.P. DelGreco, and R.E. Huffman
Air Force Geophysics Laboratory
Hanscom AFB, MA 01731
Sunanda Basu
Emmanuel College
Boston, MA 02115

The ultraviolet (UV) images and VHF/UHF beacon transmissions obtained with the Polar Bear satellite at Tromso and Sondrestrom Fjord were utilized to study the relationship of UV emissions from the nightside aurora and phase/amplitude scintillations on magnetically quiet days. Preliminary results indicate that UV images of auroral structure present near the local magnetic L-shell of the observing station are associated with moderate enhancement of scintillations. This result probably indicates that the quiet aurora creates weak F-region irregularities. Under such magnetic conditions, more intense scintillations are often associated with increases in total electron content (TEC). Closely spaced transits of the HiLat satellite are utilized to determine the nature of the energetic electron precipitation. Spectral characteristics of phase scintillations associated with UV images are compared with those observed in conjunction with TEC enhancements.

G5-3
1500

IONOSPHERIC IMAGING USING COMPUTERIZED TOMOGRAPHY

J. R. Austen, S. J. Franke, and C. H. Liu
Department of Electrical and Computer Engineering, University of Illinois at Urbana-Champaign, Urbana IL 61801-2991

A two-dimensional image of the electron density in the ionosphere can be produced from TEC data by using computerized tomography (CT) techniques. The imaging of large-scale structures such as the ionospheric trough and equatorial bubble should be possible. Different reconstruction algorithms will be compared and the effects of noise on the reconstruction will be discussed Several geometries will be compared using a set of ionospheric models, and factors affecting the ultimate resolution of this technique will be investigated. Images produced from simulated TEC data as well as from actual data will be presented.

G5-4
1540

Conjugate Radar Studies of High Latitude Ionospheric Irregularities

R.A. Greenwald, K.B. Baker
Johns Hopkins University/Applied Physics Laboratory
Johns Hopkins Road
Laurel, MD 20707

J.R. Dudeney, M.J. Pinnock
British Antarctic Survey
High Cross Madingly Road
Cambridge, CB3 OET, U.K.

At the present time all authors of this paper except the speaker are in Halley Bay, Antarctica where they are assembling the southern half of the Polar Anglo-American Conjugate Experiment (PACE). The experiment consists of two broadband HF phased-array radars, the Halley radar, which is under construction, and the Goose Bay radar, which has been operating in Labrador, Canada since 1983. These radars have very large magnetically-conjugate fields-of-view from which they are sensitive to ionospheric irregularities with wavelengths ranging from 8-17 m. The goals of the experiment are to examine the conjugate aspects of the irregularity formation, transport and dispersal processses. When it is possible, the conjugate observations of irregularity Doppler motions will also be used to examime the conjugacy of high latitude plasma motions in the ionosphere. In this presentation we will present an overview of the initial research program for the PACE radars and discuss opportunities for collaboration.

G5-5
1600

HIGH LATITUDE HF IONOSPHERIC MODE STRUCTURE STUDY

**Nikhil Dave' , Naval Ocean Systems Center,
Ocean and Atmospheric Sciences Division,
Code 542
San Diego, CA 92152-5000**

For specified temporal conditions, improvement of HF propagation prediction for frequency management requires knowledge of which ground ranges are accessible to which frequencies for transmissions on a given bearing from a point on the earth's surface. Also of interest is information regarding reflecting layers, number of hops, and path losses for all of the modes reaching a specified ground range for these conditions. The results of such a study can be displayed as plots of frequency versus ground range for each time and bearing. Mode structure is highlighted in terms of 1-hop, 2-hop, and higher modes; path losses are shown by shading. Much information which would not otherwise be obvious is conveyed by such a display, thus simplifying the reaching of conclusions regarding the best use of the ionosphere for communication.

As an example, such a study is done based on a HF propagation prediction program (AMBCOM) for HF transmission originating in Andoya, Norway using a representative set of frequencies in the HF spectrum. The study is performed for a selected number of hours, months, and bearings around the transmitter so as to gain knowledge of propagation patterns as a function of these variables. Since Andoya is a high-latitude station, it has the property that comparison between results for north and south bearings can indicate differences between high-latitude and mid-latitude propagation. Another advantage of studying propagation around Andoya is that there is some published data of observed maximum usable frequencies for this station (Folkestad, K., in Folkestad, K., editor, "Ionospheric Radio Communications" Finse, Norway, April 13-19, 1967, pp. 279-288), which can be used for comparison.

Some of the more interesting mode structure diagrams resulting from this study are presented with discussion regarding implications for usable frequencies. Comparison is made with predictions of less accurate programs such as HFBC84.

G5-6
1620

NEED FOR AN ANTARCTIC INCOHERENT SCATTER RADAR TO EXPLOIT HEMISPHERIC DIFFERENCES TO STUDY HIGH-LATITUDE PHENOMENA

Vincent B. Wickwar
Geoscience and Engineering Center
SRI International
Menlo Park, CA 94025

To understand the upper atmosphere, particularly the very complex high-latitude phenomena, requires observations made under different conditions, e.g., levels of magnetic activity, season, and so on. However, one important set of differences has not been exploited sufficiently in the quest to understand the upper atmosphere. These are hemispheric differences, including insolation, separation between geographic and geomagnetic poles, magnetospheric inputs, and the upward propagation of tides and gravity waves from the mesosphere. A strong network of instruments, particularly incoherent-scatter radars, in the northern hemisphere. To take advantage of hemispheric differences will require significant additional observational capability at high latitudes in the southern hemisphere, i.e., in Antarctica. The instrument that can add the greatest number of appropriate measurements and complement the present capabilities is an incoherent-scatter radar.

Session H-3 1355-Thurs. CR1-9
ELECTRON BEAM AND MASS INJECTIONS IN SPACE PLASMAS—II
Chairman: D.A. Gurnett, Dept. of Physics and Astronomy, Univ. of Iowa, Iowa City, IA 52242

H3-1
1400

SIMULATION STUDIES OF ELECTRON BEAM INJECTION FROM SPACECRAFT: OPTIMUM CONDITIONS FOR BEAM PROPAGATION

R. M. Winglee
Department of Astrophysical, Planetary and Atmospheric Sciences,
University of Colorado,
Boulder, CO 80309-0391

P.L. Pritchett
Department of Physics,
University of California, Los Angeles
Los Angeles, CA 90024-1547

Electron beams injected from spacecraft have been used over the last ten years to probe the ionosphere and magnetosphere and to investigate beam-plasma interactions. During such beam injections, spacecraft charging can become appreciable and the properties of the beam can become significantly modified as the beam propagates away from the spacecraft. Two-dimensional (three velocity component) electrostatic simulations are used to investigate the optimum conditions for which the beam can most easily propagate away from the spacecraft and maintain a coherent structure. Important factors in determining the spacecraft charging are the ratio of the beam to background density, the beam energy, and the spacecraft size. Even with small spacecraft charging the beam can be subject to disruption due to beam-plasma interactions. Disruption can be partially suppressed if the beam injection is rapidly pulsed. The spatial extent of the plasma perturbations and induced electrostatic wave emissions is discussed.

H3-2
1420

PLASMA OBSERVATIONS IN THE VICINITY OF THE SHUTTLE

L. A. Frank and W. R. Paterson
Department of Physics and Astronomy
The University of Iowa
Iowa City, IA 52242

P. M. Banks and R. I. Bush
STAR Laboratory
Stanford University
Stanford, CA 94305

W. J. Raitt
Center for Atmospheric and Space Sciences
Utah State University
Logan, UT 84322

Outgassing by the Shuttle-Orbiter and electron beams emitted from the Orbiter's bay alter the ionospheric plasma environment. These phenomena have been observed with a plasma analyzer on board the free-flying Plasma Diagnostics Package. This instrument sampled the velocity distributions of electrons and positive ions with energy-per-unit charge between 2 V and 36 kV at distances up to 400 m from the Orbiter. Electron beams emitted from the Orbiter's bay are observed to result in a narrow sheet of energy-degraded electrons on magnetic field lines directly behind the Orbiter. This sheet is oriented parallel to the direction of motion of the spacecraft and to the direction of Earth's magnetic field. The width of the sheet perpendicular to those vectors is approximately 20 m. Outgassing of neutral molecules results in a cloud of gases that surrounds the Orbiter and moves through the ionosphere with an orbital speed of 8 km s^{-1}. These gases are subject to collisions with atmospheric gases and to ionization by charge exchange with ambient ionospheric ions. This latter process is responsible for distributions of hot ions, mostly H_2O^+, observed during the free flight. These ions are entrained in a long tail, $\gtrsim$ 10 km in length, behind the Orbiter. This population of hot ions may be a source of free energy for plasma waves, e.g., broadband electrostatic noise.

H3-3
1440 QUASI-STATIC ELECTRIC FIELD MEASUREMENTS NEAR THE SPACE SHUTTLE AT TIMES OF SHUTTLE THRUSTER OPERATION

John T. Steinberg, Donald A. Gurnett and Christoph K. Goertz
Dept. of Physics and Astronomy
The University of Iowa
Iowa City, IA 52242

During the Spacelab-2 mission of the space shuttle, the ionospheric plasma surrounding the orbiter was investigated with the University of Iowa Plasma Diagnostics Package (PDP). Quasi-static electric fields were measured using a double floating probe. The electric field measurements reported here are all made when the PDP was over 80 meters away from the shuttle. Generally, the measured electric field was approximately equal to the motional electric field $\vec{V} \times \vec{B}$, where $\vec{V}$ is the velocity of the spacecraft relative to the ionosphere. However, at certain times when the shuttle's Reaction Control System (RCS) thrusters were operated, the measured field was reduced in magnitude from $\vec{V} \times \vec{B}$ by up to 20%. The observed screening of the motional electric field can be explained in the following manner. Charge exchange reactions between ambient O^+ ions and the neutral molecules from the thruster plume will produce pickup ions. The pickup ions are displaced in the direction of the motional electric field, producing a pickup current, which screens the motional field. The pickup current is closed by field-aligned currents which are carried by a propagating Alfven wave.

H3-4
1520

DISTRIBUTION OF RADIATED VLF ENERGY FROM A PULSED ELECTRON BEAM IN THE IONOSPHERE

D. J. Donohue, K. J. Harker, and P. M. Banks
Space, Telecommunications and Radioscience Laboratory
Stanford University
Stanford, California 94305

This talk addresses one of the primary objectives of the CHARGE-3 rocket electron beam experiment, an analysis of VLF wave generation and propagation from pulsed electron beams in space plasmas. Spatial and frequency distributions of the radiated VLF energy will be discussed and a prediction of the optimal locations for ground-based receiving antennas will also be presented.

For the radiated energy calculation, two important tools have been developed. The first is a mathematical treatment of the radiation source characteristics of a coherent electron beam. The solution to a single charged particle orbiting a magnetic field line in a homogenous medium is summed coherently over all electrons in the beam to give the far-field distribution. To examine wave propagtion away from the beam, this field distribution is then treated as a radiation source in a 3-dimensional computer ray tracing program which has been developed for special application to VLF ionospheric propagation. Details of the beam wave generation theory will be presented here while the 3-D ray tracing program will be described in a separate session. Results of the research will be shown in the form of 3-D ray paths and a prediction of the VLF radiation "footprint" and corresponding distribution of electric field intensity.

H3-5
1540

ELECTRON BEAM EMISSIONS FROM A MOTHER-DAUGHTER SOUNDING ROCKET

B.E. Gilchrist, P. M. Banks, P.R. Williamson, T. Neubert
Space,Telecommunications, and Radioscience Laboratory
Stanford University, Stanford, CA 94305
S. Noble, J. Jost
SRS International, Dickinson, TX 77539
F.T. Djuth
The Aerospace Corporation, El Segundo, CA 90245
W. J. Raitt, N.B. Myers
Center for Atmospheric and Space Sciences
Utah State University, Logan, UT 84322
S. Sasaki
Institute of Space and Astronautical Science
4-6-1 Komaba, Meguro, Tokyo, Japan

During the Charge-2 sounding rocket experiment at White Sands in December, 1985, electron beams with energies of 1 keV and currents from 1 to 40 mA were injected downwards from a mother payload. The tethered daughter payload was propelled out to a distance of 426 m perpendicular to the Earth's magnetic field using a nitrogen thruster source. In addition to electron beam emissions, sequences were performed in which the potential between the mother and the daughter were varied up to 500 V. A 50 MHz pulsed doppler radar was simultaneously operated at Presidio, TX. It viewed the expected 170 - 190 km altitude ionization region perpendicular to B. Results from simultaneous vehicle potential/charging measurements, ground radar observations, and wave-fields monitored from the daughter payload are presented.

Near the mid-point of a long DC beam emission, occurring at 250 km altitude, a 3 second thruster firing was observed to cause unusual and pronounced mother/daughter charging and tether current flow. At the same moment, a radar event was observed from the ground occurring near the range expected for ionization in the 170 - 190 km altitude regime. The sense and magnitude of the change in vehicle potential and current flow indicates that substantially higher electron current was flowing to the mother during this interval. The radar observation indicates a substantial beam escape occurred only in conjunction with thruster firing. It was also observed that the VLF waves stimulated during DC beam emissions were almost identical in spectral shape and intensity to waves observed during potential bias sweep sequences without beam emission. This points to the importance of the return current relative to an electron beam for generation of VLF wave emissions.

H3-6
1600

MODEL OF THE INTERACTION OF A HOLLOW CATHODE WITH THE IONOSPHERE

M. Dobrowolny and L. Iess
Istituto Fisica Spazio Interplanetario
CNR
00044 Frascati, Italy

We present self consistent calculations of the expansion of a plasma source of the hollow cathode type into an ambient plasma. The source is polarized with respect to the surrounding medium. The model considered is a fluid model with inclusion of anomalous friction arising from plasma instabilities. The potential profiles which are calculated show a very large extent of the interaction region. Correspondingly we obtain quite substantial current enhancements with respect to the operation of the plasma source in vacum.

Session J-5 1355-Thurs. CRO-30

COSMOLOGY

Chairman: J.M. Ulson, National Radio Astronomy Observatory, Socorro, NM 87801

J5-1 1400 EXCESS IR FLUX IN THE MICROWAVE BACKGROUND: P.L. Richards, Dept. of Physics, Univ. of California, Berkeley, CA 94720

J5-2
1420

RADIO OBSERVATIONS OF QUASAR ABSORPTION SYSTEMS

F.H. Briggs
Department of Physics and Astronomy
University of Pittsburgh
Pittsburgh, PA 15260

The light emitted by high redshift quasars often passes through intervening material that chances to lie along our lines of sight to the quasars. Distinctive patterns of absorption are created which can be discovered and classified through inspection of the quasars' optical spectrum. The absorbers are too distant to be detected photographically, but, in fact, normal galaxies at these redshifts are also undetectable.

The class of absorber that is typified by large column densities of neutral gas is suitable for study at radio wavelengths by observation of the 21cm line of neutral hydrogen (HI). Radio techniques provide unique information that complements the studies performed at optical wavelengths: Autocorrelation spectrometers can obtain high resolution of the velocity structure of the absorber. Very Long Baseline Interferometers (VLBI) can resolve the absorber spatially with fine angular resolution. Combination of radio and optical results produces a measure of the HI spin temperature, which is generally an indicator of the kinetic temperature of the absorbing gas.

The radio source PKS 0458-020 provides a good example of the capabilities of the radio techniques. The background quasar has an emission redshift $z = 2.286$. An intervening absorber has $z = 2.04$ which places the frequency of observation of the 21cm line at 467 MHz. Detailed VLBI and VLA study of the radio continuum of the background source shows structure on a wide range of scales from 10 milliarcseconds to 2 arcseconds. Therefore VLBI experiments performed in the absorption line can probe the absorber on these angular scales, which tranlate into distances of 50 pc to 10 kpc at $z = 2.04$. The observation finds that the absorber extends more than 5 kpc across the line of sight and that the spin temperature is less than 500 K. These properties resemble those of the spiral galaxies that are observed nearby at the present, and support the conclusion that this class of absorber contains gas-rich disk galaxies that are the progenitors of spiral galaxies.

OBSERVATIONS OF QUANTIZATION IN GALAXY REDSHIFTS

J5-3 W.G.TIFFT and W.J.COCKE
1440 Steward Observatory
University of Arizona
Tucson, Arizona 85721

The Hubble law, whereby galaxy redshifts are observed to increase for fainter galaxies, is central to modern cosmology. The assumption that the redshift is a Doppler shift converts the Hubble law into a velocity-distance relationship which couples with gravitational theory to provide the framework of expanding universe cosmologies. The assumption of a Doppler basis for the redshift also leads to well known problems, excess motion in clusters and in various other situations requires large amounts of invisible mass. Rarely discussed alternatives are that the redshift might not be entirely Doppler in origin or that the extrapolation of gravitational theory to the scale of galaxies is incorrect or incomplete. Basic tests of the velocity interpretation of the redshift are possible and there is clear evidence that something is indeed wrong.

Among the possible tests, one addresses the question of continuity. Velocity is a continuous variable, is the redshift? The answer to this very basic question appears to be no, the redshift appears to have quantum properties. Evidence for this conclusion comes from studies of absolute and differential redshifts in dynamical systems and globally. 21-cm radio data plays a prominent role in the work. Several studies of accurate redshift differences in isolated double galaxies indicate that the distribution of differences is quantized in steps near 72 km/s. Reproduced below is the cumulative distribution of redshift differences within the three best samples of pairs available. Conventional dynamics predicts a smooth monotonic distribution peaking at zero. Observations yield a quantized distribution and suggests that an exclusion principle could be operating which prevents identical redshifts (zero differences). Analysis of clusters also yields a characteristic 72 km/s periodic pattern. The quantization can be traced to the global level as well, suggesting that the phenomenon is not limited to individual gravitational potential domaines.

The current status of the principal tests will be reviewed. A broad introductory review of the subject is available in Sky and Telescope (January 1987).

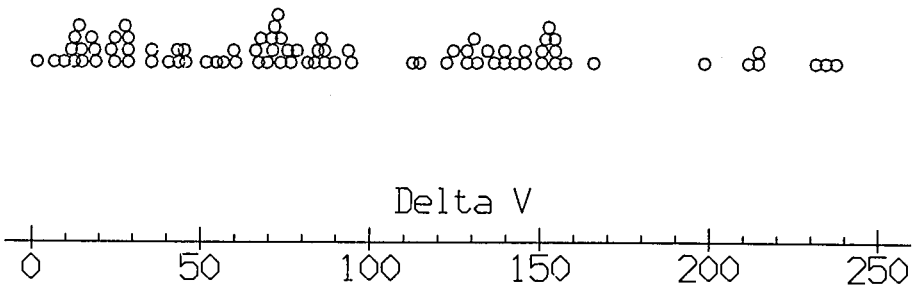

J5-4
1520

A SEARCH FOR MEDIUM-SCALE STRUCTURE IN THE MICROWAVE BACKGROUND

Peter Meinhold and Philip Lubin
Department of Physics
University of California at Santa Barbara
Santa Barbara CA 93106

We have built and are testing a stabilized balloon gondola with a one meter microwave telescope to make measurements of the Cosmic Background Radiation (CBR) anisotropy on medium angular scales (1 to 10 degrees).

Our radiometer is a liquid Helium cooled Superconductor-Insulator-Superconductor mixer, operated at 90 GHz (3mm wavelength), which could optimally give us a sensitivity of approximately 0.03 mk for temperature fluctuations on our scale in a 15 hour flight.

Stabilization and tracking are accomplished with an active servo, controlled by an on-board computer. Orientation information comes from an inertial gyro system and a magnetometer, with real time adjustment capability from the ground. A star camera is used for absolute reference.

Results of testing of the various systems will be presented, along with an overview of the experiment and our flight status.

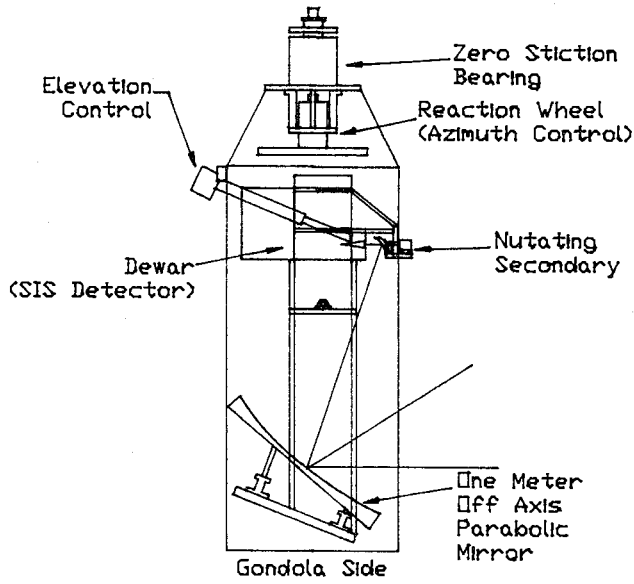

J5-5
1540 OBSERVATIONS OF THE SUNYAEV-ZEL'DOVICH EFFECT: M. Birkinshaw, Dept. of Astronomy, Harvard Univ., Cambridge, MA 02138

J5-6
1600

MICROJANSKY RADIO SOURCE SURVEYS

K. I. Kellermann
National Radio Astronomy Observatory
Edgemont Road
Charlottesville, VA 22903

The VLA has been used at 5 GHz to survey small regions of the sky to determine the density of microjansky radio sources. The most sensitive survey was made in the D configuration to synthesize a 16.5 arc second beam corresponding to an effective aperture of 700 meters. After 80 hours of integration time, the rms noise level was only 5 μJy which is close to the value expected from thermal noise fluctuations.

We detected a total of 28 sources above our completeness level of 25 μJy corresponding to a source density of about 3×10^6 sources per sr. We have also analyzed the P(D) distribution to estimate the source density down to one microJy where we estimate that there are about 10^9 sources per sr. This is only 0.1 percent of the number predicted from an extrapolation of the strong source count based on a uniformly filled static Euclidean model.

At the 25 μJy limit of our survey there are about 24 sources per synthesized beam, so the data are clearly confusion limited. Further, even more sensitive surveys are planned using higher resolution to both to reduce the confusion level and to obtain better information on the angular size and structure of the microjansky radio sources.

J5-7
1620

VERY SMALL-SCALE STRUCTURE IN THE MICROWAVE BACKGROUND

E. B. Fomalont
National Radio Astronomy Observatory
Charlottesville, VA 22903-2475

Deviations from isotropy of the Cosmic Background Radiation provide a source of information about the early universe. At an angular scale of an arcminute or less primeval galaxy and cluster formation may produce fluctuations which can be measured with sensitive instruments. Even upper limits to such fluctuations can place significant constraints on models of the interaction of matter and energy at early epochs.

The sensitive VLA observations at 5 GHz, described by Kellermann in a companion paper, to determine the density of weak radio sources has been used to determine limits to the structure of the sky emission between 10" to 60" angular scales. Because of the high density of weak sources, sophisticated modeling methods were needed to distinguish between blends of point sources and possible sky fluctuations.

We find the 2-sigma limit of fluctuations of 0.12 mK on a scale of 60" and a limit of 0.5 mK on a scale of 18". Recently, another small region of sky has been observed with nearly the same sensitivity. Limits to the possible sky fluctuations from the new observations are consistent with the above values.

J5-8
1640

OBSERVATIONS OF HIGH REDSHIFT HYDROGEN

Juan M. Uson, K. Anantharamaiah and Durgadas Bagri
National Radio Astronomy Observatory
Socorro, NM 87801

We have used the NRAO–VLA telescope in the P–band to search for the redshifted "21–cm" emission of proto–clusters of galaxies. At the observed frequency of 333.1 ± 1.6 MHz the redshift probed is 3.26 ± 0.02 .

If baryons are the main massive component of the Universe, the most natural path for the evolution of large–scale structures is the "Top–down" scenario proposed by Sunyaev and Zel'dovich (Astron. Astrophys., 20, 189–200, 1972). In this theory, the first structures to develop as the Universe expands will have masses of the order of $3 \cdot 10^{14}$ $M_\odot$ with an average diameter of 2 Mpc and a line–of–sight velocity dispersion of about 600 km$\cdot$ s^{-1}. At a redshift of 3.3, the predicted structures would be between 4' and 7' in diameter, depending on the value of Ω, the density parameter of the Universe and emit a "21–cm" line that should have an observed width of about 500 kHz, with a peak flux between 4 mJy and 15 mJy, again depending on the value of Ω.

We have used the VLA in its "D" configuration. The field of view is determined by the primary beam of the antennas (HPBW = 156') and the "D–array" gives a resolution of about 3'. We observed a "blank" field centered at R. A. = 10^h50^m ; Dec. = 68^o. We used 127 channels with a channel–width of 24.414 kHz, centered at 333.125 MHz. The main source of systematic errors was interference, which determined the observing and data reduction techniques as well as the frequency and band used. We will discuss our choices in some detail.

After subtraction of the continuum (about 11 Jy from many point sources with fluxes up to 1.2 Jy) the channel images have (rms) fluctuations as low as 5.7 mJy, only about 20% above the theoretical sensitivity expected from the useful data collected in 34 hours of observation. At the writing of this *Abstract* the images are still being analyzed. The results will be presented at the meeting.

Session B-8 0835-Fri. CR2-6
SCATTERING—II
Chairman: Professor D.P. Nyquist, Dept. of Electrical Engineering, Michigan State Univ., East Lansing, MI

B8-1 0840 **SCATTERING FROM A CONDUCTING STRIP USING THE BIVARIATIONAL TECHNIQUE WITH PHYSICAL OPTICS TRIAL CURRENTS**

R. G. Olsen and G. Ellis
Electrical and Computer Engineering Department
Washington State University
Pullman, WA 99164-2752

E. F. Kuester
Electrical Engineering Department
University of Colorado
Boulder, CO 80302

A number of methods have been used to study electromagnetic scattering from a perfectly conducting strip. These include an infinite series of Mathieu functions, numerical solutions of integral equations, physical optics and the geometric theory of diffraction. Until recently, the variational method has been used almost exclusively to develop low frequency scattering formulas.

The purpose of this work was to determine if the bivariational technique could be used to develop as simple formula for the high frequency scattering problem which is significantly more accurate than the physical optics formula. To do this, physical optics trial functions for the induced current were chosen because they can be determined a priori with a minimum amount of effort. Since these trial functions often have components of current normal to the boundary which are discontinuous, they lead to non-convergent integrals in the standard bivariational formula. Thus, a new formula was developed in which the non-convergent term was subtracted but the variational property was retained.

Using this formula, a very simple expression for the radar cross section of a strip was derived. Numerical results were generated and compared to numerical solutions of the exact integral equation and the physical optics solution. It can be concluded that the bivariational formula is no better than physical optics and that it suffers from innacuracies at grazing angles of incidence typical of the physical optics solution since edge diffraction currents are neglected in both cases.

B8-2
0900

Analytic Element Method for EM Scattering from a Metallic Plate

by A. Q. Howard, Jr.
and J. W. Miles

SCHLUMBERGER WELL SERVICES
HOUSTON, TEXAS 77252-2175

Abstract

We give a new technique for solving a class of three dimensional electromagnetic scattering problems. This technique, the analytic element method (AEM), is developed to compute the scattered electromagnetic field from a thin planar perfectly conducting plate, with an irregular perimeter and holes. General sources can be easily described, but for numerical examples, plane wave sources are used. In common with finite element methods, scatterer dimensions are required to be no more than a few wavelengths. The numerical method is based upon an **E** field integral equation, which is solved using a generalization of the volume current method where the plate surface current is expanded in raised Bessel functions defined on disc shaped subdomains, or patches. This approach produces a representation of the vector potential which is a continuous function, with continuous derivatives of the observation point coordinates. Consequently, both the integration and differentiation operations occurring in the integral equation are performed analytically. The resulting matrix equation for the plate current amplitudes is full, complex symmetric. Each matrix element I_{nm} contains a monopole and quadrupole current interaction term between the n^{th} and m^{th} surface elements. This interaction factors into a product of radial and angular functions. The angular behavior of the patch interactions is isotropic for the monopole and varies as $\cos 2\phi_{nm}$ for the quadrupole, where ϕ_{nm} is the angle between the centers of the n^{th} and m^{th} patches. Such a representation is ideally suited for table look up. The matrix elements are Fourier Bessel numerical integrals which are evaluated on the real axis. Numerical results for the two independent components of the plate current are in agreement with established results.

B8-3
0920

DISCRIMINATION OF CONDUCTING PLATES BY E-PULSE TECHNIQUE

W.M.Sun, K.M.Chen, D.P.Nyquist and E.Rothwell
Department of Electrical Engineering & Systems Science
Michigan State University, East Lansing, MI 48824

Rectangular conducting plates of various dimensions have been illuminated by Gaussian pulses at various aspect angles in a time-domain scattering range which was built on a ground plane. Transient responses of the plates were measured and from them the natural frequencies of the targets were extracted by using a hybrid E-pulse / least square technique recently developed at Michigan State University. Invariance of the target's natural frequencies with respect to the aspect angle was studied.

The E-pulses of the plates were synthesized on the basis of their natural resonant frequencies. These E-pulses were then used to convolve with the transient responses of the plates to discriminate among them.

A study is being conducted to study the transient behavior of a conducting plate coated by a layer of lossy material. The effects of the lossy coating on the target's natural frequencies and on the effectiveness of the E-pulse technique to discriminate such targets are investigated.

B8-4
0940

HIGH FREQUENCY SCATTERING BY A THIN MATERIAL HALF-PLANE AND STRIP

John L. Volakis
Radiation Laboratory
Department of Electrical Engineering and Computer Science
The University of Michigan
Ann Arbor, MI 48109-2122

Diffraction coefficients will be presented for a thin dielectric half plane and strip having arbitrary permittivity and permeability. These were derived by modeling the thin material layer with a pair of modified resistive and conductive sheets (Senior and Volakis, Radio Sci, 22, 1987). The resulting integral equations were then solved via the dual integral equation approach. Using the half plane solution up to third order multiple diffraction coefficients were also generated for the case of a strip. The latter were obtained via the extended spectral ray method (Herman and Volakis, Radio Sci, 22, 335-349, 1987) and include the surface wave diffraction effects in a uniform manner. Numerical and measured results will also be presented to validate the accuracy of the model and that of the derived diffraction coefficients.

B8-5
1020

COLLECTIVE RAY AND HYBRID RAY-MODE METHOD FOR SOURCE EXCITED PROPAGATION IN A MULTI-LAYERED MEDIA- I. FORMULATION

I.T. Lu
Department of Electrical Engineering/Computer Science
Polytechnic University
Route 110, Farmingdale, NY 11735 USA

When source-excited wave phenomena in a layered medium are resolved into travelling wave (ray) constituents, wave coupling at boundaries and interfaces generates a proliferation of wavefields that makes successive tracking impractical for all but a few such encounters. When wave processes are modelled alternatively by composite layer reflection and transmission matrices, one loses the possibility of tracking some travelling wave constituents individually, as may be desirable. These observations apply to wave phenomena that emphasize propagation vertically across the layer boundaries as well as to those that emphasize propagation along the layers, as is the case when source and receiver are widely separated in range; in that event, the composite effects may also be presented in terms of the normal modes. By a more flexible arrangement, one may attempt to retain some ray fields and account for the remaining ones collectively through use of modified collective layer reflection and transmission matrices or through use of some guided modes subject to a remainder field that accounts for truncation effects. Such a hybrid format can actually be constructed self-consistently by utilization of a new and very general Green's function formulation (I.T. Lu and L.B.Felsen, Geophys. J. R. astr. Soc., 84, 31-48,1986). This formulation is structured so as to permit access to all "interesting" layers (e.g. those containing a source or receiver, or causing significant change of ray phases) but to treat the remaining "uninteresting" ones in "hidden" form. The general theory is applied here to multilayer dielectrics, with emphasis on the physical interpretation of the various wave processes. Computational aspects are discussed as well.

B8-6
1040

COLLECTIVE RAY AND HYBRID RAY-MODE METHOD FOR SOURCE EXCITED PROPAGATION IN MULTI-LAYERED MEDIA - II. APPLICATION TO GAUSSIAN BEAM INPUT

I.T. Lu and L.B. Felsen
Department of Electrical Engineering/Computer Science
Polytechnic University
Route 110, Farmingdale, NY 11735 USA

Gaussian beams, either individually or as synthesizing basis fields, provide useful models for the response due to Gaussian or more generally shaped high frequency source inputs, respectively. When propagating into a layered environment, an initially well collimated beam undergoes diffusion after successive reflections and refractions, and is converted eventually into the oscillatory pattern of one or more guided modes. Multiple layering accelerates the diffusion process. Utilizing a general matrix Green's function method (Lu, this meeting), this phenomenology is examined here for a plane parallel waveguide filled with a two-layer dielectric, and excited by a sheet beam source in one of the layers. The beam is modeled via the complex source point method whereby a Gaussian-waisted input is generated from a line current by assigning complex values to the source coordinates. This scheme avoids the need for plane wave spectral decomposition and synthesis, but the analytic continuation to complex source coordinates requires precautions which are discussed. Algorithms based on beam tracking, mode summation and a hybrid beam-mode format are presented, and their role in explaining the beam-to-mode transition is emphasized. Numerical implementation illustrates these aspects.

B8-7
1100 COMPUTERIZED RAY-OPTICAL ANALYSIS OF RADIATION THROUGH THREE-DIMENSIONAL LAYERED RADOMES

J. S. Bagby, Dept. of Electrical Engineering
Univ. of Texas at Arlington, Arlington, TX 76019

A fully-automated, ray-optical technique for calculating the far-field produced by a phased-array aperture antenna enclosed in an arbitrary three-dimensional layered dielectric radome is presented. This technique utilizes the high-frequency Geometrical Optics Approximation, and accounts for direct and singlely-reflected rays in the far-field of the antenna system.

The radome surface shape is described by the user-supplied, multi-valued function $z = F(x,y)$, and the aperture antenna array is modeled as a collection of sources with arbitrary pattern, excitation, and location within the radome.

Points of transmission and reflection for direct and singlely-reflected rays are determined numerically. At these points the fields associated with the rays are decomposed into parallel and perpendicular polarized components, and the appropriate planar Fresnel-type layer transmission or reflection coefficient is applied. The resultant fields are then summed in the far-field of the radome to form the radiation pattern.

This technique is applied to analysis of the far-fields of the nose radar system of the General Dynamics F-16 aircraft, and numerical results generated on an IBM PC-XT computer are presented and compared to measured radiation patterns.

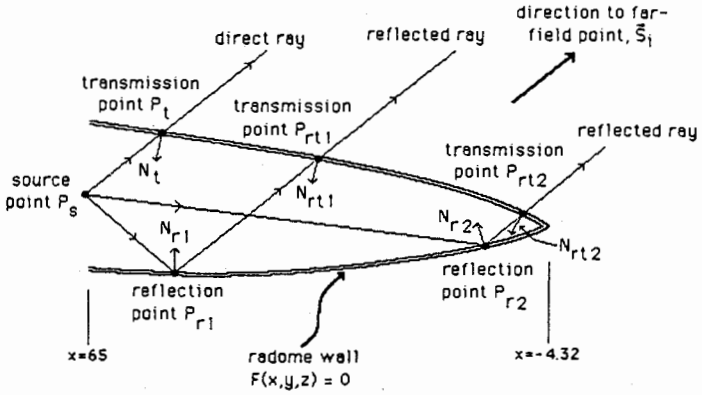

B8-8
1120

A HYBRID METHOD FOR SOLVING TIME-DOMAIN INTEGRAL EQUATIONS IN TRANSIENT SCATTERING

Anton G. Tijhuis*
Laboratory of Electromagnetic Research
Department of Electrical Engineering
Delft University of Technology
P.O. Box 5031, 2600 GA Delft
The Netherlands

In global techniques for solving transient-scattering problems, the unknown field is to be found from space-time-domain source-type integral equations. Conventionally, two types of techniques have been employed for solving such equations. In frequency-domain techniques, the transient response of the scatterer is represented as a Laplace or Fourier inversion integral, the integrand of which is obtained by solving the corresponding frequency-domain equations. The main advantage of such techniques is that they produce stable and accurate results; their main disadvantage is that the computation time consumed in determining the frequency-domain response typically increases with some integer power of $|\omega|$. In the marching-on-in-time method, one utilizes the property in the time-domain integral equations that the scattered field at each space-time point is expressed in terms of field values at previous instants. Its principal advantage is its numerical efficiency, which is achieved by using the same discretization at all instants; its main disadvantage is that the accumulation of discretization errors may give rise to instabilities.

In this paper, we propose a hybrid method that combines the advantages of both approaches, while avoiding their disadvantages. In this method, we discretize in space only. As in the marching-on-in-time method, we use the same space discretization at all instants. This results in a finite, time-invariant, linear system of equations for the discretized field quantities. From this system, the field is resolved by transforming to the time-Laplace domain, as outlined above. Compared with the marching-on-in-time method, this approach has the advantage that instabilities are inherently avoided; compared with frequency-domain techniques, the advantage is the fixed computational effort required in determing each Fourier component.

Numerical results obtained for some simple scattering geometries will be presented and discussed.

*Presently on leave at the University of Colorado at Boulder, with the financial support of the Netherlands Organization for the Advancement of Pure Research (Z.W.O.).

B8-9
1140

COMPUTATION OF A BRANCH-CUT INTEGRAL ARISING IN TRANSIENT SCATTERING BY A PERFECTLY CONDUCTING CYLINDER

K. Naishadham and A. Arnett
Department of Electrical Engineering
453 Anderson Hall
University of Kentucky
Lexington, KY 40506-0046

The time-domain Green's function due to a magnetic line source residing on the surface of a perfectly conducting cylinder has been presented by E. Heyman and L. B. Felsen (*I.E.E.E. Trans. Ant. and Propag.*, AP-31, 426, 1983). The Singularity Expansion Method (SEM) representation of the Green's function involves a branch-cut integral in the complex spectral plane, manifested by the infinite extent of the cylinder. In this paper we discuss an algorithm to compute this integral. The algorithm can easily be modified to compute the branch-cut integral in the SEM representation of the transient field due to a line source, located off the cylinder surface, or due to plane wave excitation.

Numerical computation of the integrand requires determination of the complex zeros of Hankel function of the second kind in the order-plane. These zeros are determined using a complex-order Bessel function subroutine (A.G. Tijhuis, private communication) and a zero-search procedure (B. K. Singaraju, et. al., AFWL Mathematics Note 42) consisting of successive numerical integration of the function along the periphery of rectangular cells into which the search area is divided. The accuracy of the zeros thus determined is checked by comparison with published results. These zeros occur frequently in electromagnetic scattering by circular cylinders, as poles of the amplitudes of creeping waves in the angular wavenumber plane.

The branch cut integral for the problem being considered is evaluated numerically by dividing the integration interval into three subintervals according to the suitability of the appropriate small and large-argument approximations of the integrand. The expontential decay of the integrand for large values of the integration variable ka, where k is the wavenumber and a is the cylinder radius, facilitates truncation of the seminfinite integration interval at $|ka| = 10$. For $|ka| \leq 0.01$, the small argument approximations of the Hankel functions and the order-plane zeros are employed to simplify the integrand. For $0.01 < |ka| \leq 2$, the integrand is computed numerically and for $|ka| > 2$, the large-argument approximations are utilized. The branch point at $ka = 0$ is a removable singularity, as can be shown by approximating the integrand over a small circle centered around the branch point, and taking the limit of the integrand as $|ka| \rightarrow 0$. The branch-cut integral is computed for several observation times for an observer location on the cylinder, and the influence of the branch-cut contribution on the early-time response is evaluated.

Session G-6 0855-Fri. CR2-26
IONOSPHERIC SCATTER PHENOMENA
Chairman: Dr. Kenneth Davies, U.S. Dept. of Commerce, NOAA/SEL, Boulder, CO 80303

G6-1
0900

Effects of Multiple Refractive Scattering on Trans-ionospheric Propagation

Richard A. Sprague
Ocean and Atmospheric Sciences Division
Naval Ocean Systems Center
San Diego, CA 92152-5000

Henry G. Booker
Department of Electrical and Computer Engineering
University of California, San Diego
LaJolla, CA 92037

When the fluctuations of relative electron density within the ionosphere become large, multiple refractive scattering by large scale (greater than the Fresnel scale) irregularities begins to dominate diffractive scattering by smaller scale (Fresnel scale) irregularities. A theory based on the deeply modulated phase changing screen which describes this transition from weak to strong scattering has been presented by Booker and MajidiAhi (Booker and MajidiAhi,J.Atmos.Terr.Phys.,43,1199,1981). Previously, it has been used to predict the effects on HF signals which are below the penetration frequency and are returned to the earth by ionospheric reflection (Booker and Tao,J.Atmos.Terr.Phys.,49,915,1987;Booker,Tao and Behroozi-Toosi,J.Atmos. Terr.Phys.,49,939,1987).

In this paper the theory of multiple refractive scattering is applied to trans-ionospheric propagation of signals from the penetration frequency up to the gigahertz range. The model currently assumes transmission from a satellite in geo-stationary orbit to an earth-bound receiver and assumes a constant representative irregularity drift velocity of 200 m/s. We also assume isotropic irregularity structure. Plots and tables illustrating the effects of scattering on system performance (correlation bandwidth, spatial scale of intensity correlation, etc.) as a function of the strength of the density fluctuations and length of line-of-sight path from receiver to satellite are presented.

G6-2
0920

ASPECT SENSITIVITY MEASUREMENTS OF EQUATORIAL SPREAD-F IRREGULARITIES AT JICAMARCA

Erhan Kudeki and Elaine Chapin
Department of Electrical and Computer Engineering
1406 W. Green Street, University of Illinois, Urbana, IL 61801
Donald T. Farley
School of Electrical Engineering
Cornell University, Ithaca, NY 14853
Ronald F. Woodman
Jicamarca Radio Observatory, Aptd. 3747, Lima, Peru

The first central moments of the angular spectra of 50 MHz equatorial spread F radar returns were measured at Jicamarca with a multiple baseline radar interferometer. The measurements show to what extent the naturally occurring 3 meter plasma irregularities are aligned in the ambient geomagnetic field direction in the equatorial F region, and how the alignment strength varies as a function of Doppler shift, irregularity lifetimes, turbulence strength, and other background conditions. Typical values for the angular half width of the bottomside spread F irregularities vary between 0.1^{o} and 0.025^{o}, close to the resolution limit of the measurement technique. The smallest angular half width observations correspond to instances with strongest signal levels and broadest Doppler spectra. When broad and frequency aliased Doppler spectra are observed, half width values are often independent of Doppler shift.

G6-3
0940

RADAR INTERFEROMETER OBSERVATIONS OF MESOSPHERIC ECHOING LAYERS AT JICAMARCA

Erhan Kudeki and Gary R. Stitt
Department of Electrical and Computer Engineering
1406 W. Green Street, University of Illinois, Urbana, IL 61801

VHF radar observations at Jicamarca show that the most intense mesospheric echoes at the equator are returned from thin horizontal layers of relatively long lifetimes (tens of minutes to hours). A few such layers may be present at a time, and they are typically separated in altitude by a few kilometers. Interferometric studies of radar returns from these layers indicate that the width of Doppler spectra are usually determined by the spatial integration effect of finite size scattering volumes. Returns from lower mesospheric layers appear to be due to randomly distributed scatterers being convected through the observation volume by an essentially non-turbulent wind field. The scatterers in question may possibly be specularity points on corrugated refractive index surfaces. Higher mesospheric layer echoes, however, imply the existence of turbulent flow fields in the vertical plane, with strong eddy motions at scale sizes comparable with the scattering volume dimensions of about a kilometer.

G6-4
1020

SIMULATION AND ANALYSIS OF THE EFFECTS OF SCINTILLATION PM TRANSIONOSPHERIC COMMUNICATIONS SYSTEMS

N. R. Lo, S. J. Franke, and C. H. Liu, Dept. of Electrical and Computer Engineering, University of Illinois, Urbana, IL 61801

Simulations of transionospheric communication have been carried out. The simulation consists of two phases. First, transionospheric communication channels under different propagation conditions are generated using a phase screen model with power-law irregularities. The second phase involves the evaluation of the performance of a phase modulated digital system in those channels. This second phase is carried out using COMSIM, a communication simulation software package provided by Lockheed. A systematic study has been carried out for different carrier frequencies, phase variances and power-law indices. Comparisons will be made for the performance of several types of modulations.

G6-5
1040 PHASE AND AMPLITUDE FLUCTUATIONS OF A PROPAGATING ELECTROMAGNETIC WAVE IN THE IONOSPHERE AS A RESULT OF SCATTERING AND LOSS MECHANISMS

G. R. Akers
E-Systems, Greenville Division
P. O. Box 1056
Greenville, TX 75401

Electromagnetic wave propagating in an ionospheric attenuative medium are derived. The classical electromagnetic wave equation is modified to account for damping and a perturbation technique for small ionic inhomogenieties is utilized. The effect of these ionic loss mechanisms is apparent in the integral solution as illustrated in the amplitude and phase fluctuations decaying spatially.

G6-6
1100

A METEOR ECHO PROCESSING SYSTEM FOR ST/MST RADARS

R. L. Obert
S. K. Avery
J. P. Avery
University of Colorado
Department of Electrical and Computer Engineering and
Cooperative Institute for Research in Environmental Sciences
Campus Box 425
Boulder, Colorado 80309-0425

ABSTRACT

MEDAC (Meteor Echo Detection And Collection) is a radar processing system designed to run in parallel with the normal operation of an ST/MST radar. While normal ST/MST radars use turbulence scatter to determine wind profiles in the lower to middle atmosphere, MEDAC uses scatter from meteor trails to determine atmospheric tidal components from the upper atmosphere.

A brief description of MEDAC's hardware and its interaction with the radar will be given. Results obtained during a campaign at the Poker Flat, Alaska MST radar installation, in which MEDAC was tested and compared with turbulence methods of tidal observations, will also be presented.

Session H-4 0855-Fri. CR1-9
SPACE PLASMA HEATING BY NATURAL AND MAN-MADE WAVE SOURCES
Chairman: M.J. Keskinen, Plasma Physics Division, Naval Research Lab, Washington, DC 20375

H4-1
0900

LABORATORY STUDIES OF ION ENERGIZATION BY ELECTROSTATIC ION CYCLOTRON WAVES

R. L. Merlino
Dept. Physics & Astronomy
University of Iowa
Iowa City, IA 52242-1479

High latitude satellite observations at ~ 1 R_E have indicated two kinds of energetic ion distributions: "conics," with peak fluxes between the directions perpendicular and parallel to the geomagnetic field, and highly collimated distributions with peak fluxes along the magnetic field (e.g., Shelley et al., GRL 3, 654, 1976). Both distributions provide a strong source of O^+ ions for the magnetotail. The ion "conic" distributions are usually attributed to perpendicular ion heating at low altitudes and subsequent magnetic focusing as the energized ions move up the magnetic field lines.

We report here a laboratory study of ion-conic formation by electrostatic ion-cyclotron (EIC) waves. The experiments were carried out in a single-ended cesium Q-machine with a region of non-uniform (diverging) magnetic field. The EIC waves are excited by drawing a supercritical electron current in a small current filament along the axis of the device. Using gridded ion-energy analyzers, we followed the evolution of the ion-velocity distribution as the ions passed through the heating region and subsequently flowed out along the diverging $\underline{B}$ field. As expected, the ions (heated in the perpendicular direction by the EIC waves) transfer their energy from perpendicular to parallel motion as they travel along the diverging field lines while conserving their magnetic moment.

H4-2
0920

TRANSVERSE ION ENERGIZATION AND LOW FREQUENCY PLASMA WAVES IN THE MID-ALTITUDE AURORAL ZONE

W.K. Peterson and E.G. Shelley
Lockheed Palo Alto Research Laboratory
S.A. Boardsen and D.A. Gurnett
The University of Iowa
B.G. Ledley
NASA Goddard Space Flight Center
M. Sugiura
Koyoto University
T.E. Moore and J.H. Waite, Jr.
NASA Marshall Space Flight Center

The transport of ions from the ionosphere to the magnetosphere requires that ions acquire significant energy in directions both transverse and parallel to the magnetic field. There is a considerable body of experimental evidence that shows that transverse energization occurs over a wide range of altitudes on auroral field lines. Many recent analytical and simulation studies have addressed the micro-physics involved in transverse ion energization. There are however remarkably few published high resolution plasma and plasma wave observations obtained in the mid-altitude auroral region available to compare with the analytical and simulation studies.

Several hundred hours of high resolution plasma data were surveyed and a wide variety of plasma environments that are difficult to simply characterize were found. We present a comprehensive set of high-sensitivity, high-resolution plasma wave, ion, and magnetometer data obtained from an evening auroral zone crossing at r/Re ~ 2.5 by the Dynamics Explorer -1 Satellite. The total density, thermal structure, and composition of the plasma in this representative interval varied rapidly, as did the the character (mode) of low frequency plasma waves observed. We did not find an unambiguous particle and wave signature of local transverse ion energization, but we did frequently find intervals where local transverse ion heating was consistent with the observations.

H4-3
0940

HEATING OF IONS ON AURORAL FIELD LINES IN THE PRESENCE OF A LARGE AMPLITUDE CYCLOTRON WAVE

K.-I. Nishikawa
Department of Physics and Astronomy
The University of Iowa
Iowa City, Iowa 5242

Heating of oxygen ions has been investigated in the presence of a large amplitude hydrogen cyclotron wave which is commonly observed on auroral field lines. A three wave decay process, in which a large amplitude pump hydrogen cyclotron wave decays into a daughter hydrogen cyclotron wave and a low frequency oxygen cyclotron wave, is studied theoretically and by means of particle simulations. Both one- and two-dimensional simulations showed a decay instability resulting in strong heating of both the oxygen ions and the hydrogen ions. In particular, the high energy tails of the oxygen ions are observed in the perpendicular distribution.

On the other hand, heating of hydrogen ions is also studied by means of simulations in the presence of an electrostatic oxygen cyclotron (EOC) wave which is commonly observed on auroral field lines at low altitudes (400-600 km). Two types of instabilities have been found which can be driven by an EOC wave. One of them is an oscillating current-driven electrostatic hydrogen cyclotron instability whose frequency is near the hydrogen cyclotron frequency. The other is an oscillating lower hybrid two-streaming instability whose frequency is near the lower hybrid frequency, $\omega \approx \omega_{pH}$. The simulations with the use of two-dimensional codes confirmed the presence of both instabilities resulting in strong heating of hydrogen ions. High energy tails of the hydrogen ions are observed in the perpendicular distribution.

H4-4
1000

GENERATION OF BROADBAND ELECTROSTATIC NOISE AND PLASMA HEATING IN THE MAGNETOTAIL

M. Ashour-Abdalla[1,2] and D. Schriver[2]
[1]Institute of Geophysics and Planetary Physics
[2]Department of Physics
University of California
Los Angeles, CA 90024

The earth's plasma sheet boundary layer in the magnetotail is a very active area of space and is the primary region of plasma transport and heating in the tail. Two of the main features of the boundary layer are its high-speed ion beams that flow both earthward and tailward along magnetic field lines and the intense broadbanded electrostatic noise found in the boundary layer. We have used linear theory and computer simulations to examine the various wave modes that can be driven unstable by an ion beam free energy source and how the wave energy is then transferred back to the plasma. We have done this for various intitial plasma configurations determined from observations; for example, we added cold ionospheric plasma to the predominantly hot plasma to simulate lobe plasma convecting into the boundary layer as well as the effects of counterstreaming ion beams. Our results show that ion beams can generate broadband electrostatic noise and that the heating resulting from wave-particle interactions is consistent with plasma observations in the central plasma sheet.

H4-5
1040

REAL MODIFICATION

Suman Ganguly
Center for Remote Sensing
8200 Greensboro Drive, Suite 503
McLean, VA 22102

Controlled ground based ionospheric modification is a well established technique. However, all the experimental facilities here have fallen by at least two decades behind the current technology of high power transmitters. After briefly describing the results achieved with the present day facilities, we present a scenario for the generation of strong ionospheric modification and the impact of such a situation to the society.

H4-6
1100

ELECTROMAGNETIC TORNADOES IN SPACE

Tom Chang
Center for Theoretical Geoplasma Physics
MIT Center for Space Research
Cambridge, MA 02139

Imagine tornadoes the size of earth or larger containing whirlwinds of charged particles reaching speeds of tens of thousands of kilometers per hour. Such are the exotic phenomena recently detected by polar orbiting satellites. Space physicists have measured positive ions at altitudes from one to several earth radii at the auroral and polar cusp latitudes. These ions gyrate around the earth's magnetic field lines at extremely high speeds with energies ranging from tens of eV to several keV; and populations of these ions have been christened "ion conics".

A recent theory (Chang et al., Geophys. Res. Lett. 13, 636-639, 1986) suggests that the charged particles are merely tracers of an extended region of turbulent states of low frequency, electromagnetic waves. These turbulent waves rotate about the earth's magnetic field in a manner not very different from that of a funnel-like tornado which commonly descends upon the midwestern plains during a hot, humid, summer day.

Since charged particles also gyrate around the magnetic field, the rotating electric fields can push the ions along and energize them to very high energies and speeds. Using a mathematical tool commonly known as the "Monte Carlo" technique, we have calculated the effects of the electromagnetic turbulence on the charged particles (Retterer et al., Phys. Rev. Lett., 59, 148-151, 1987). This result is the very first successful quantitative prediction of an observed conic. For the special case considered, it was possible to determine that the conic was oxygen-dominated, a result verified recently by the EICS instrument on board the Dynamics Explorer 1 satellite. (Peterson et al., private communication).

H4-7
1120

QUASILINEAR ION HEATING BY ELECTROSTATIC ION CYCLOTRON WAVES IN THE HIGH LATITUDE IONOSPHERE

P. Satyanarayana
Science Applications International Corporation
McLean, VA 22102

M.J. Keskinen, P.K. Chaturvedi, S.L. Ossakow
Plasma Physics Division
Naval Research Laboratory
Washington, DC 20375-5000

Recently, much attention, both theoretical and experimental, has been given to the problem of ion energization and conics in the terrestrial ionosphere and magnetosphere. Some observations indicate ion conic formation in the high latitude ionosphere as low in altitude as 400-600 km. Various mechanisms, both AC and DC, have been proposed to account for this energization with considerable quantitative progress being made using wavelike sources, e.g., ion cyclotron waves. However, the problem of ion heating and acceleration by low frequency waves in the collisional ionospheric environment has not been resolved. In this study we develop a simple model of quasilinear ion heating by current-driven electrostatic ion cyclotron waves in the presence of ion-ion collisions including multi species effects. We find both analytically and numerically ion-ion collisional effects (1) reduce the absolute magnitude of heating predicted by quasilinear theory and (2) lead to temperature isotropization ($T_\perp \simeq T_{||}$) on the order of several tens of ion cyclotron periods where $T_\perp (T_{||})$ is the average ion temperature perpendicular (parallel) to the ambient geomagnetic field.

H4-8
1140

ELECTROMAGNETIC WAVES FROM ANTENNA-PLASMA NONLINEARITIES OBSERVED IN A BISTATIC PROPAGATION EXPERIMENT

H.G. James
Communications Research Centre,
P.O. Box 11490, Station "H",
Ottawa, Ontario K2H 8S2
Canada

On 21 Jan. 1976, the ISIS-I and ISIS-II topside sounder spacecraft participated in a recorded rendezvous during which the minimal separation was 58 km. The ISIS-II sounder was commanded to operate as a transmitter and the ISIS-I sounder as a receiver for a bistatic propagation experiment. The rendezvous occurred at high latitudes and at a height of about 1400 km. During the observations in question, the angle between the separation vector and the magnetic field varied from about 100° to about 80°.

The close encounter revealed the existence of anomalous signal enhancements at certain frequencies in the range 0.5 to 3.5 MHz, the plasma frequency being about 0.25 MHz and the gyrofrequency about 0.97 MHz. These signals propagated in the normal cold-plasma upper-branch O and X modes. Using conventional theories of transmitting and receiving antennas to define reference intensities, two types of enhancement were identified: signals near twice the gyrofrequency $2f_c$ and above the transmitter carrier frequency were 10 - 20 dB above the reference intensity, and a component at a separation of about f_c below the carrier was amplified by up to 50 dB.

Cyclotron convective amplification and three-plane-wave decay nonlinearity have been examined as possible explanations. Neither postulate accounts satisfactorily for the observations. Nonlinear electron motion in the intense near field of the transmitting dipole is thought responsible for both types of spectral anomaly.

Index

Condensed Technical Program
(Continued from inside front cover)

1700-1800

Commission B Business Meeting		CR2-6
Commission C Business Meeting		CR0-36
Commission E Business Meeting		CR1-46
Commission F Business Meeting		CR2-28
Commission H Business Meeting		CR1-9

THURSDAY, 7 JANUARY

0835-1200

B-6	EM Theory	CR2-26
C-2	Spectrum Estimation Applications	CR0-36
J-4	Low Frequency Radio Astronomy	CR0-30

0855-1200

A-4	Measurements of the Properties of Materials	CR1-40
F-2	Atmospheric Sensing	CR2-6
G-4	World-Wide Ionospheric Observing Campaigns and Studies	CR2-28
H-2	Electron Beam and Mass Injections in Space Plasmas - I	CR1-9

1355-1700

A-5	EMI Measurements and Standards	CR1-42
B/F-1	Random Media	CR2-6
G-5	High Latitude Ionospheric Phenomena	CR2-26
H-3	Electron Beam and Mass Injections in Space Plasmas - II	CR1-9
J-5	Cosmology	CR0-30

1535-1700

B-7	Resonances	CR2-6

FRIDAY, 8 JANUARY

0835-1200

B-8	Scattering - II	CR2-6

0855-1200

G-6	Ionospheric Scatter Phenomena	CR2-26
H-4	Space Plasma Heating by Natural and Man-Made Wave Sources	CR1-9